Microbioreactors for Bioprocess Development

by

ZHIYU ZHANG

Master of Science, Chemical Engineering Practice, MIT, 2002
Master of Engineering, Biochemical Engineering, Tsinghua University, 2000
Bachelor of Engineering, Chemical Engineering & Technology, Tsinghua University, 1998
Bachelor of Engineering, Computer and Applications, Tsinghua University, 1998

Submitted to the Department of Chemical Engineering
in partial fulfillment of the requirements for the degree of

DOCTOR OF PHILOSOPHY IN CHEMICAL ENGINEERING

at the

MASSACHUSETTS INSTITUTE OF TECHNOLOGY
[June 2006]
May 2006

Signature of Author: _____
Department of Chemical Engineering
April 18, 2006

Certified by: _____
Klavs F. Jensen
Lammot du Pont Professor of Chemical Engineering and
Professor of Materials Science and Engineering
Thesis Advisor

Accepted by: _____
William M. Deen
Professor of Chemical Engineering
Chair, Committee for Graduate Students

Microbioreactors for Bioprocess Development

by

Zhiyu Zhang

Submitted to the Department of Chemical Engineering on April 18, 2006,
in partial fulfillment of the requirements for the degree of
Doctor of Philosophy in Chemical Engineering

Abstract

This thesis presents the design, fabrication, and characterization of a microbioreactor integrated with automated sensors and actuators as a step towards high-throughput bioprocess development. In particular, this thesis demonstrates the feasibility of culturing microbial cells in microliter-volume reactors in batch, continuous, fed-batch operations.

The microbioreactor is fabricated out of poly(methylmethacrylate) and poly(dimethylsiloxane). Active mixing is made possible by a miniature magnetic stir bar. On-line optical measurements for optical density, pH, and dissolved oxygen are integrated. Oxygenation in the microbioreactor is characterized and reproducible batch fermentation of *Escherichia coli* and *Saccharomyces cerevisiae* are demonstrated and benchmarked with bench-scale bioreactors. Global gene expression analysis of *S. cerevisiae* exhibits physiological and molecular characteristics which parallel those of large-scales.

A microchemostat, continuous culture of microbial cells, is realized in the microbioreactor. *E. coli* cells are fed by pressure-driven single phase flow of fresh medium through a microchannel. Chemotaxis, the back growth of bacterial cells into the medium feed channel, is prevented by local heating. Using poly(ethylene glycol) -grafted poly(acrylic acid) copolymer films, PMMA and PDMS surfaces are modified to generate bio-inert surfaces resistant to non-specific protein adsorption and cell adhesion. These advances enable cell growth kinetics and stoichoimetry to be obtained in the microchemostat consistent with reported phenomena from conventional stirred-tank bioreactors, as indicated by the time profiles of OD_{600nm}, pH, and DO measurements at steady states.

Water evaporation from the microbioreactor allows feeding of base and glucose solutions into the small reactor to realize fed-batch operations. Commercial microvalves are integrated to obtain closed-loop pH control. pH value in the microbioreactor is successfully maintained within a physiological scale during the time course of *E. coli* cell cultivation in rich media.

One key issue for high-throughput bioprocessing is the parallel operation of multiple microbial fermentations while keeping each single microbioreactor disposable. Plug-in-and-flow microfluidic connectors and fabricated polymer micro-optical lenses/connectors are integrated in the microbioreactor "cassettes" for fast set-up and easy operation. A protocol multiplexed system for the parallel operation of four microbioreactors is demonstrated. The demonstrated functionality of the microbioreactor with integrated measurements and flexible operations could potentially have a large impact in bioprocess developments.

Thesis Supervisor: Klavs F. Jensen
Title: Lammot du Pont Professor of Chemical Engineering and Professor of Materials and Engineering

Acknowledgements

First and foremost, I would like to extend my gratitude to my thesis advisor, Klavs Jensen, for his guidance, wisdom, insights, and professional supports during the thesis work. I truly appreciate the opportunities for creative thinking and problem-solving, and this thesis would never have come together without the direction, training, and continuous encouragement Klavs has provided throughout my time at MIT. Many thanks to my committee members: Professors Anthony Sinskey, Martin Schmidt, and Patrick Doyle, for their invaluable inputs and suggestions. In particular, Prof. Sinskey's deep insight and unfailing support has helped so much in terms of strategy and details.

I would like to thank my collaborators for their contributions to the work in this thesis. Thanks to Nicolas Szita, in particular, for working closely together and for teaching me a lot about optics and mechanics, as well as scientific presentations and writings. Many thanks to Paolo Boccazzi, for his patience and supports, for always backing me up and trouble-shooting together with me. Other past and present members of the team are, Gerardo Perozziello, whose support and knowledge are essential for the thermal bonding and the reactor cassette work; Hyun-Goo Choi, whose ready and indispensable help on surface chemistry and patience in exploring many novel ideas with me; Ruben Kolfschoten, for working together on the pH control system; Andrea Zanzotto, whose early work in DMA was of great help to this thesis. Thanks also go to Jamil El Ali, who helped me a lot on CFD simulation and temperature control, and to Hang Lu, for her much-needed advices.

I would also like to thank my UROP students: Patrick Boyle for his help with pH control, Labview programs, and multiplexed system. His involvements and contributions are as important as from a collaborator. Thanks also go to Yelena Gorlina, Cynthia Wilson, Morgan Mills, Minyoung Jiang for their help with the thesis, and Kinfai(Max) Au, who was a visiting undergraduate student from Tsinghua University and was one of the most hard-working students. I would like to thank Fred Cote from MIT Edgerton Student Machine Shop for his tutoring and training. I also thank the Dupont-MIT Alliance for the research funding and the DuPont team for their intellectual inputs.

I have to admit that being a graduate student life is not always as sweet as honey and raisin cake. I feel a deep appreciation for the friendships from the group that have contributed to my survival at MIT: Hang, for being a good listener with sympathy and great wisdom; Axel for sharing so many fascinating new ideas; Jamil for willing to help even when he is busy; Thomas and Jacob, for helping with the computer when I punch the keyboard; Andrea, for kindly lending me her dog to pull me up the hill during group hiking; Kishori, for her company every time I work on weekends. I feel grateful for so many things from the group, from exchanging ideas and technical details to borrowing lab supplies, from enjoying coffee breaks to sharing information about free foods.

Finally, I would like to thank my family for their love and support, and Lili for everything.

Table of Contents

List of Figures

Chapter 1. Introduction

1.1. Bottlenecks in Bioprocess Development

Bioprocess engineers are faced with a bottleneck in the transition from screening discovery to bioprocess developments. In standard screening processes using simple assays such as shake flasks, test tubes, and microtiter plates, a large number of experiments are performed with little process information obtained during each individual fermentation experiment. Bioprocess developments are normally performed in expensive stir tank bioreactors instrumented with online measurements. Optimization of operating conditions is complicated by the limited number of experiments possible.

In various conventional bioreactors, instrumented stirred-tank bioreactors effectively control temperature, pH, and dissolved oxygen (DO) levels by controlling mixing and gas sparging rate, thus yielding valuable physiological and metabolic information at different stages of the fermentation. However, fermentation experiments using conventional stirred-tank bioreactors are typically expensive and labor-intensive for screening purposes. Improvements have been made in lab-scale stirred-tank bioreactors including reducing the reactor volume and increasing the number of reactors operating in parallel (Weuster-Botz *et al.*, 2002), but many of these solutions require efforts, such as sterilization, assembly, cleaning, and calibration of sensors in reactors, which scale with the number of bioreactors. Thus, the need remains for developing bioreactor systems that will enable parallel experimentation with only minimum increase in handling and operational efforts.

Test tubes, shake flasks, and microtiter plates are widely used as simple bioreactors for fermentation and cell culture experiments. Fast developments in lab automation technologies

allow these bioreactors, especially microtiter plates, to be easily operated in parallel and with small volumes. There is little control over bioprocess conditions in these reactors, and the data obtained are often limited to endpoint measurements. Thus applications of these simple bioreactors are typically limited to screening. Efforts have been made to implement on-line pH or DO measurements units in microtiter plates (Weiss *et al.*, 2002; John *et al.*, 2003a and b) or shake flasks (Weuster-Botz *et al.*, 2001; Tolosa *et al.*, 2002; Wittmann *et al.*, 2003; Gupta and Rao, 2003) to obtain continuous process information during fermentation.

1.2. Microbioreactors

Microbioreactors with integrated sensors combine the small volumes of microtiter plates with the monitoring and control features found in bench-scale systems to form promising tools for rapid, high-throughput, and cost-effective screening. Kumar *et al.* (2004) have reviewed recent progress in the area of minibioreactors as well as small-scale conventional bioreactors.

One fundamental requirement for mL- or μL-scale bioreactors is the ability to obtain optical density (OD), pH, and DO data in real time and thereby avoid the need for sample removal. Recent developments in electrochemical and optical sensor technologies have made such measurements possible in microbioreactors. Walther *et al.* (1994) first realized a microreactor for yeast cell culture. Kim and Lee (1998) proposed a microfermentor chip that uses microelectrodes to measure biomass, pH, DO, and glucose concentration. Van der Weide and Blattner (2002) correlated capacitance and resistance to the biomass in microbial growth assay wells with a liquid content of up to 30 μL. The microbioreactor developed by Maharbiz *et al.* (2003) is a hybrid of plastic microplate reactors combined with silicon technology; in the reactor oxygen is generated and delivered by hydrolysis of water. Most recently, Maharbiz *et al.* (2004) have integrated 250 μL microbioreactor arrays with OD measurement and pH ISFET sensors on

a commercial printed circuit board.

Rao and co-authors (Kostov *et al.* 2001; Rao, 2002; Harms *et al.*, 2002, Kermis *et al.*, 2003) pioneered optical measurements of OD, pH, and DO, which are non-invasive, easily integrated, and reliable - advantageous features for high-throughput bioprocess development. In the minibioreactor by Kostov *et al.* (2001), fermentation parameters were measured on-line continuously; cell growth was compared with a bench-scale 1 L fermentor. Optical sensors were also used in the 6 mL miniature bioreactor reported by Lamping *et al.* (2003), as well as in the microbioreactor described by Zanzotto *et al.* (2004), in which stable signals were obtained in a 5 μL microbioreactor. Commercialized applications of the optical sensors include the Cellstation® bioreactors developed by Fluorometrix Corp. (Stow, MA, USA), in which 12 miniature stirred-tank bioreactors are operated in parallel. Most recently, Puskeiler *et al.* (2005) reported parallel operation of 48 magnetically-mixed milliliter scale bioreactors arrays. In these bioreactors, OD and pH were monitored on-line; automation of fed-batch operation and pH control were implemented by using commercially available liquid-handling systems. These efforts in miniaturization and parallelization of microbioreactors, as well as automation of measurements and controls, demonstrate the potential for obtaining valuable growth kinetics data from microbioreactors and indicate the promise of high-throughput technologies for bioprocessing.

Most of the reported microbioreactors to date operate in batch and fed-batch modes. In batch and fed-batch cultures, the properties of microorganisms, such as size, composition, and functional characteristics vary considerably during the growth of the culture. Steady state cell growth, in the state of which cell biomass, substrates and products concentrations remain constant, can only be realized in continuous culture experiments. Kinetic parameters and yield coefficients can be determined more accurately using continuous culture. Continuous culture

also permits a degree of control and flexibility that are not available for batch processes: chemical environmental conditions can be defined and maintained independently of growth rate (chemostat). The cause/effect relationships are more easily determined (Akgün *et al.*, 2004). These features make a chemostat a unique and powerful tool for biological and physiological research. However, continuous culture experiments in conventional stirred-tank bioreactors are often time- and labor- intensive. The rational for research in miniaturized chemostat bioreactors is to increase the throughput and make microchemostat a widely applicable routine for screening and bioprocess optimization. Efforts have been made in miniaturization as well as in parallel operation. Gu *et al.* (1999) used a miniature stirred-tank bioreactor with working volume of 58 mL in a two-stage continuous culture experiment and further applied it in a multi-channel system (2001). Akgün *et al.* (2004) realized continuous culture in shaken Erlenmeyer flasks and demonstrated the potential for parallel operations. Walther *et al.* (1994, 1999, and 2000) developed a 3 mL continuous bioreactor with integrated biomass, pH, and temperature microelectronic sensors to investigate physiological and morphological properties of yeast cells in microgravity environments (in space lab). This microbioreactor was a self-sustained and controlled system: medium flow rate measured by a microsensor was controlled by a piezo-electric silicon membrane pump; pH was measured by a miniaturized ion-selective field effect transistor (ISFET) sensor (Walther, 1996) and controlled by coulometric generation of hydroxyl ions at a titanium electrode. Aeration was through gas-permeable cylindrical silicone tubes in the bioreactor, and mixing was realized by a magnetic stir bar (Walther, 1999). A novel microchemostat system was recently reported by Balagaddé *et al.* (2005) by integration of poly(dimethylsiloxane) (PDMS) peristaltic pumps and valves using soft lithography technology; small population of *E. coli* cells ($\sim 10^4$) were cultured in liquid segments (with volume of 15 nL)

that flow in a microfluidic loop for periodical flushing and medium feeding. Most recently, a perfusion-type microfluidic device was used by Groisman *et al.* (2005) by physically trapping cells in nL-volume chambers. Although cells were cultivated in a batch process in absence of active mixing, "chemostat" operation was claimed by Balaban (2005) with the reasoning of constant growth conditions observed with the expression of a fluorescent protein.

Oxygenation is an important aspect in bioreactor design and performance. In most stirred-tank bioreactors, air or oxygen gas bubbles are sparged into the culture medium to provide microbial cells with the oxygen necessary for growth or maintenance of cellular functions. For example, the miniature bioreactor by Lamping *et al.* (2003) machined in Plexiglass and outfitted with air spargers and stirring baffles, can be seen as a scaled-down version of conventional bench-scale stirred-tank bioreactors. Sparging of air/oxygen, such as the oxygen bubbles created electrochemically in the microbioreactor by Maharbiz *et al.* (2004), also contributes to mixing. Shaking is another way to improve gas-liquid oxygen transportation in bioreactors (Duetz *et al.*, 2000; Wittmann *et al.*, 2003). Zanzotto *et al.* (2004) provided oxygenation to cells growing in the microbioreactor by diffusion through a thin, gas-permeable PDMS membrane. In this reactor, PDMS membrane separates gas and liquid phases thereby eliminating the risk of contamination from air and cross-talk between adjacent microbioreactors. Oxygen diffusion in PDMS is sufficiently fast so that mass transfer is not limited by the PDMS membrane, but by diffusion into the broth so that an oxygen concentration gradient develops through the depth of the reactor (Zanzotto *et al.*, 2004). As a result, such reactors must have shallow depth (e.g., a few hundred microns) and the volume can only be increased by enlarging the diameter, which creates potential difficulties for the membrane design.

1.3. Thesis Objective

There is great interest in the development of new microbial cell cultivation technologies for high-throughput screening as well as for bioprocess development with less mechanical manipulations and cost than standard fermentation technology. The aim of this thesis is to develop miniaturized, automated microbioreactors with integrated bioanalytical devices, including non-invasive monitoring and/or control of temperature, pH, dissolved oxygen (DO), and biomass. Microfluidics technologies are integrated in the microbioreactors to allow effective control over environmental conditions thus physiological conditions for microbial cells. Such a microbioreactor system will address packaging and multiplexing issues to allow a high-throughput process. The microbioreactor will potentially address the continuing demand in bioprocess science and engineering for obtaining fast and accurate analytical information to rapidly evaluate the interactions between biological systems and bioprocess operations. Potentially, the microbioreactors will provide the platforms for efficiently incorporating modern tools of biology (genetics, enzymology, bioinformatics) to improve bioprocesses.

1.4. Thesis Outline

The work in this thesis covers four major topics: (1) design and fabrication of a well-mixed and integrated microbioreactor for batch cell cultivation, (2) construction of a microchemostat system – continuous culture in the microbioreactor, (3) implementation of an evaporation-driven fed-batch microbioreactor, and (4) integration of a reactor cassette and design of a multiplexed system.

Chapter Two addresses the fundamental issues in constructing a well-mixed, polymer-based, and instrumented batch microbioreactor as an extension of the membrane-aerated

microbioreactor by Zanzotto *et al.* (2004). Active mixing is achieved by using a mini magnetic stir bar driven by an external rotating magnetic field. A volume of 150 μL in the microbioreactor makes sampling possible for bioanalysis, such as HPLC or global gene expression analysis (Boccazzi *et al.*, 2006). Construction of the microbioreactor in layers of poly(methylmethacrylate) (PMMA) and PDMS makes the reactor transparent for optical measurements and rigid for handling while preserving the aeration and septic properties of the PDMS membrane. Optical sensors for on-line monitoring OD_{600nm}, pH, and DO measurements are integrated into the microbioreactor. Water evaporation during operation, a critical issue particular for small reactors and for fermentation with slow-growing microorganisms (Kumar *et al.*, 2004), is compensated by connecting the microbioreactor to a pressurized water reservoir maintaining the reactor volume constant during experiments. *Escherichia coli* and *Saccharomyces cerevisiae* are used as model systems. The oxygenation and performance of the microbioreactor is characterized and benchmarked against conventional bench-scale cell culture systems (e.g. test tubes, shaking flasks, and 500-mL stirred-tank bioreactors). Comparative global gene expression analysis of *Saccharomyces cerevisiae* cultivated in two different media is used to demonstrate the potential applications of the microbioreactor.

Based on the work on the microreactor for batch culture, Chapter Three addresses issues for continuous culture of microorganism in microbioreactors by integration of more functionality. A microchemostat requires a dynamic balance of medium feeding and cell growth to avoid "wash-out" or overpopulation of cells in the microbioreactor. Additional challenges for chemostat in microdevices include avoiding cell growth on the reactor walls and avoiding chemotaxis of bacteria into microfluidic channels. The long culturing time in chemostats means that cell adhesion and wall growth on the surfaces of bioreactor can become significant issues unless

reactor surfaces are modified to provide resistance to non-specific cell adhesion. Cells growing on surfaces have different physiological properties to those growing in suspension (Pilyugin and Waltman, 1999) and thus cell wall growth kinetics deviates from the chemostat model (Topiwala and G. Hamer, 1971). This problem is further accentuated by the high surface-to-volume ratio of micro-scale devices. Surface modification with poly(ethylene glycol) (PEG) –grafted poly (acrylic acid) (PAA) copolymer coatings on PDMS and PMMA are used to effectively reduce *Escherichia coli* cell adhesion and cell wall-growth. Chemotaxis, the bias random walk of motile bacterial cells towards nutrients, presents a major challenge for implementing microchemostat. A single cell migrating back through the feed line to the medium reservoir would rapidly contaminate the medium and ruin the chemostat experiment. The microbioreactor is implemented with local heating to prevent cell chemotaxis.

Chapter Four addresses issues in fed-batch operation and pH control in the microbioreactor. Different to the microchemostat, in which cells and liquid continuously flow out of the system, in a fed-batch system one major challenge for the microbioreactor, is to find an exit for the additional liquid feed and keep the reactor at a constant volume. The implemented solution is to apply water evaporation from the microbioreactor through the PDMS membrane as the driving force for liquid flow. Buffer titration experiments are designed to characterize evaporation rates at different air moisture and air convection conditions. Experimental results from passive feeding and active delivery systems are compared and discussed, and closed-loop pH control using commercial microvalves are implemented. During the time course of *E. coli* cell cultivation the pH value in the microbioreactor is effectively controlled within a physiological scale, which extend cell growth and improve the biomass yield during experiments. Furthermore, a glucose fed-batch system is designed and controlled based on DO level during

cell cultivation. The feed-back control system in the microbioreactor demonstrates the potential for high density cell culture at small scale.

Having demonstrated the batch, continuous, and fed-batch operations in the microbioreactor, Chapter Five discusses the integrated microreactor as a "cassette" for ease of setup and operation. "Plug-in-and-play" silastomer fluidic connectors are designed and integrated as the aseptic fluidic interface between reactor cassette and external facilities. Thermal bonding of multilayer PMMA device is used to embed PDMS membrane and fluidic connectors to make the device as a single body. Micromachined PDMS microlenses are designed and implemented as the optical interface for the reactor cassette. These microlenses increase the signal-to-noise ratio for optical measurements. Their self-alignment function also facilitates the setup process. Finally, this chapter also describes the construction of a multiplexed system for parallel operation of microbioreactors as proof of concept for high-throughput process. The system includes miniature motors for magnetic mixing in the microbioreactors and a motor-controlled optics system with cost not scaled with number of reactors. Reproducibility of the system is demonstrated by results from four independent batch bioreactors.

Chapter Six summarizes the work presented in this thesis and gives recommendations for future work.

Chapter 2. Instrumented, Well-Mixed, and Membrane-Aerated Microbioreactor for Batch Culture

2.1. Abstract

This chapter addresses the fundamental issues in constructing a microbioreactor for batch culture experiments. A newly designed 150 μL microbioreactor fabricated with poly(methylmethacrylate) (PMMA) and poly(dimethylsiloxane) (PDMS) is used for batch cultures of microorganisms. Mixing is achieved by a small magnetic stir bar. Fluorescent sensors are integrated for on-line measurement of pH and dissolved oxygen, as well as optical transmission measurement of cell density. The body of the reactor is made out of PMMA with a thin layer of PDMS for aeration purposes; oxygen diffuses through this gas-permeable membrane into the microbioreactor to support metabolism of bacterial cells. The K_La of the microbioreactor ranges from 20 hr^{-1} to 75 hr^{-1} under different mixing conditions. *Escherichia coli* cell growth in the microbioreactor is demonstrated and the growth behavior is benchmarked with conventional lab-scale bioreactors. Batch culture experiments with *Saccharomyces cerevisiae* further demonstrate the reproducibility and flexibility in the microbioreactor system, and the potential biological applications using the microbioreactor, as exemplified by the global gene analysis of cells cultivated in different media.

2.2. Materials and Methods

2.2.1. Microbioreactor design

The microbioreactor body consists of two PMMA layers with two PDMS layers sandwiched

in between them (see Figure 2-1). The bottom PMMA layer, made by using a computer-numerical-controlled (CNC) milling machine, includes the microbioreactor chamber (diameter 10 mm, depth 1 mm) and three connecting channels (depth 500 μm, width 500 μm), used for inoculation and replenishment of water. A thin layer (100 μm) of spin-coated PDMS (Sylgard 184, Dow Corning Corp., Midland, MI, USA; mixing ratio of silicone to curing agent 10:1; baked at 70 °C for 2 hours) covers the chamber and serves as the aeration membrane. The thin PDMS layer is held by a 5 mm-thick PDMS gasket layer to facilitate device assembly, hermetical sealing, and connection of microfluidic channels.

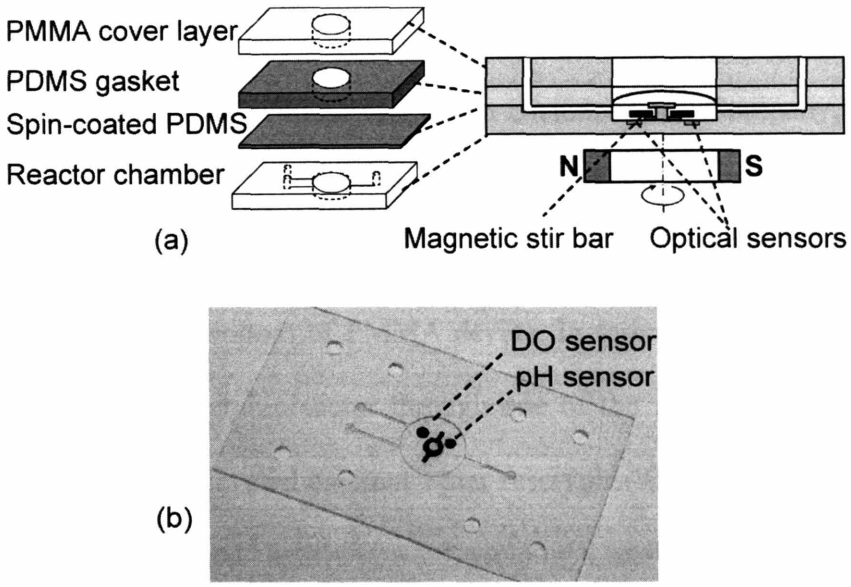

Figure 2-1. (a) Schematic view of the longitudinal section of the microbioreactor; (b) Photograph of the empty PMMA chamber of the reactor with the magnetic stir bar in the center and DO and pH fluorescent sensors at the bottom of the chamber.

Two recesses (diameter 2 mm, depth 250 μm, 2.7 mm radial distance from the center) at the bottom of the bioreactor chamber accommodated pH and DO fluorescence lifetime sensors (DO sensor foil PSt3, and pH sensor solution HP2A, PreSens - Precision Sensing GmbH, Regensburg, Germany). For mixing, a ring-shape magnetic stir bar with an arm length of 6 mm and a thickness of 0.5 mm (custom-made by Engineered Concepts, Vestavia Hills, AL, USA) rotated

in the center of the reactor chamber. The rotation axis was defined by a vertical post (height of 800 μm, diameter of 1.35 mm) machined out of PMMA in the center of the reactor chamber. A piece of PMMA of 250 μm thick and 3 mm in diameter is attached on top of the PMMA post by using acrylic solvent (Weld-On 4, IPS Corp., Gardena, CA, USA) to keep the magnetic stir bar in position (Figure 2-1). By residing the stir bar on a shallow shoulder (height of 200 μm, diameter of 2.2 mm) machined out of bulk PMMA at the bottom of the reactor, the friction between the stir bar and PMMA surface was minimized. The placement of the stir bar relative to the bottom of the reactor chamber had important effects on the quality of mixing, which will be explained through simulation.

Polyethylene tubes (1/32" outer diameter, Becton Dickinson and Company, Franklin Lakes, NJ, USA) were inserted into small holes punctuated through the 5 mm PDMS layer by using fluidic needle adapters (20 gauge, Becton Dickinson and Company) to connect to the channels (two inlets, one outlet) in the bottom of PMMA device. In fermentation experiments, syringes were used to inoculate the microbioreactor through one of the inlet channels. The other inlet channel was connected to an elevated external water reservoir. Water pressure of 300mm keeps the thin PDMS membrane bulged slightly upward, yielding a total volume of approximately 150 μL. Water was passively replenished into the microbioreactor at the same rate as water evaporated through the highly permeable PDMS thin membrane, thus keeping the volume of the microbioreactor constant during fermentation. By measuring the weight increase of anhydrous calcium sulfate pellets (W.A. Hammond Drierite, Xenia, OH, USA) placed in a closed chamber with the microbioreactor, the water evaporation rate from the microbioreactor was determined to be 4.3 ± 0.4 μL/hr at 37 °C. Thus, there would be a significant loss in fluids in the bioreactor if water had not been replenished. The use of passive feeding of water makes it possible to run the

150 μL bioreactor for long period of time without an observable volume change.

The device shown in Figure 2-1 was used for *E. coli* fermentations. For *S. cerevisiae* cell culture experiments, in which oxygen requirement is less demanding due to longer generation time, we used a bioreactor covered with an additional layer of stainless steel grid (B-PMX-062, Small Parts Inc., Miami, FL, USA) to provide a rigid top perforated membrane structure.

2.2.2. Optical measurement setup

The experimental set-up is shown in Figure 2-2. Dissolved oxygen (DO), pH, and optical density (OD_{600nm}) were measured by the optical sensing methods described in detail in Zanzotto *et al.* (2004), so only a brief summary is included here. Fermentations were carried out by placing the microbioreactor in an aluminum chamber maintained at 37 °C by flowing heated water through the chamber base. An external magnetic stirrer (Thermolyne, SP72725, Barnstead International, Dubuque, USA; placed directly below the aluminum chamber) controlled the stir bar in the microbioreactor. Bifurcated optical fibers (custom-made by RoMack Fiber Optics, Williamsburg, VA, USA) led into the chamber from both the top and the bottom and connected to LEDs and photodetectors (PDA-55, Thorlabs, Newton, NJ, USA) to perform the optical measurements. Biomass was followed by OD_{600nm} data obtained from a transmission measurement using an orange LED (Epitex L600-10V, 600 nm, Kyoto, Japan). The bifurcated branch provided a reference signal to compensate for any intensity fluctuations of the orange LED. Both dissolved oxygen and pH were measured using phase modulation lifetime fluorimetry. The DO and pH sensors were excited with a blue-green LED (505 nm, NSPE590S, Nichia America Corporation, Mountville, PA, USA) and a blue LED (465 nm, NSPB500S, Nichia), respectively. Excitation bandpass filters (Omega Optical XF1016 and XF1014) and emission long pass filters (Omega Optical XF 3016 and XF 3018) separated the respective

excitation and emission signals to minimize cross-excitation. Data switches (8037, Electro Standard Laboratories, Cranston, RI, USA) multiplexed the output signal and the input signal of the function generator (33220A, Agilent Technologies, Palo Alto, CA, USA) and the lock-in amplifier (SR 830, Stanford Research Systems, Sunnyvale, CA, USA). All instruments were computer controlled under LabVIEW® (National Instruments Corp., Austin, TX, USA), which enabled automated and real-time measurement of the parameters.

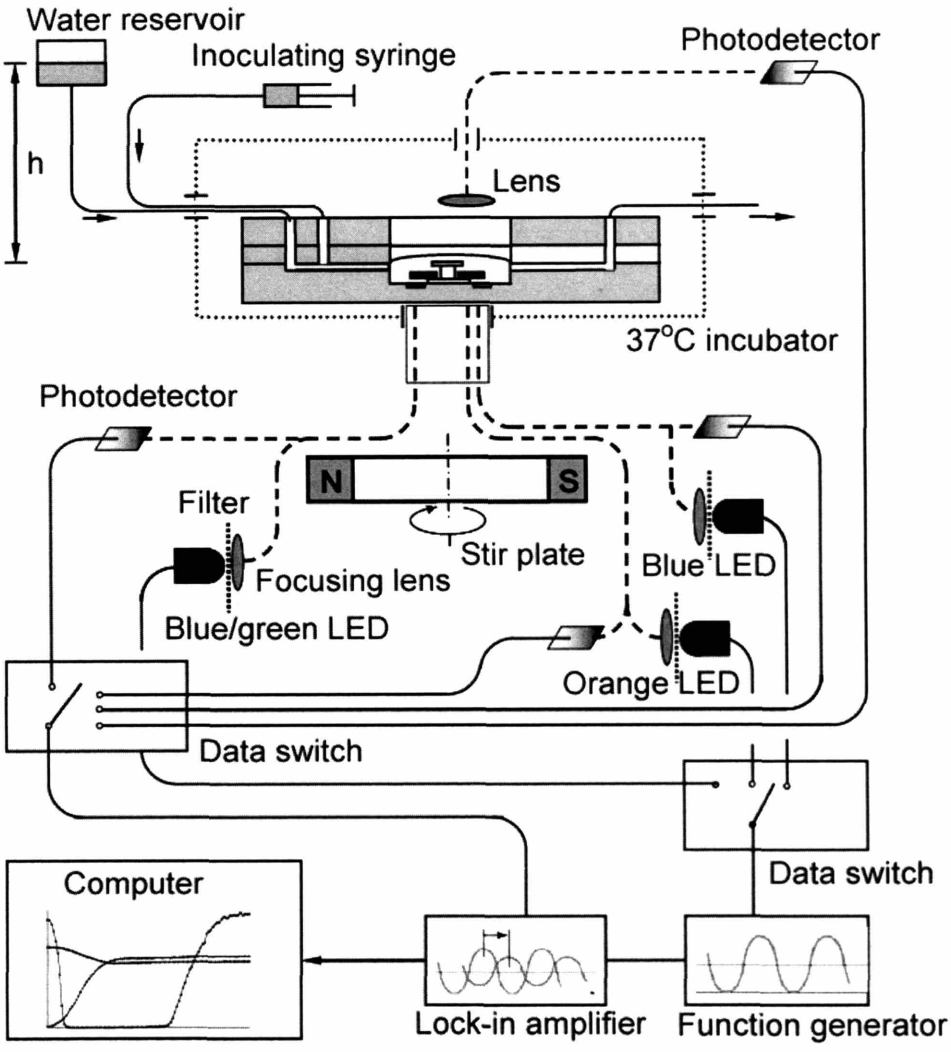

Figure 2-2. Experimental setup for the microbioreactor (h = 30 cm). The microbioreactor is kept at 37 °C in an aluminum chamber; three optical fibers carry different wavelengths of light to the bottom of the microbioreactor for OD, DO, and pH measurements, respectively. A computer collects and analyzes the transmitted or emitted light through photodetectors and a lock-in amplifier.

2.2.3. Microbioreactor experimental setup

Experiments were carried out in an airtight, aluminum chamber (Figure 2-2). The chamber provided a means for controlling the humidity and the composition of the gas above the microbioreactor membrane. It also provided a large thermal mass for holding the temperature at the desired set point. The interior of the chamber had an area of 11.5 cm by 6.5 cm, and a height of 2.5 cm. This volume was large compared to the volume of the microbioreactor to ensure that gaseous oxygen was in large excess compared to the oxygen consumed by the cells during fermentation. As a result, the chamber could be sealed for the duration of a run once it had been flushed with the desired gas. Temperature was controlled with a water bath that flowed water at the desired setpoint through the chamber base. Temperature was monitored using a thermocouple.

In addition to controlling environmental parameters, the chamber provided optical isolation and optical access for the desired measurements. Optical access was from the top and bottom of the chamber, directly above and below the microbioreactor, respectively, as shown in Figure 2-2.

2.2.4. Biological methodology

2.2.4.1. Organism and medium

E. coli FB21591 (thiC::Tn5 -pKD46, Kan^R) obtained from University of Wisconsin was used as a model organism. *E. coli* cells were cultured in Luria-Bertani (LB) medium with 8 g/L glucose (Mallinckrodt, Hazelwood, MO, USA), 100 μg/L kanamycin (Sigma-Aldrich, Co., St. Louis, MO, USA), and 0.1 mol/L 2-(N-morpholino) ethanesulfonic acid) (MES) (Sigma-Aldrich). Exposure to γ-radiation was proven by experiments to be effective for sterilization for the building materials of our microbioreactor without noticeable changes in properties.

However, to simplify the bench-marking experiments, kanamycin in the culture medium was used to prevent contamination from other bacteria species.

Saccharomyces cerevisiae ATCC 4126 was obtained from the American Type Culture Collection (ATCC, Manassas, VA). Cells were grown at 30°C in YPD or YPGal media. The composition of YPD is: 10g/L yeast extract (Difco, BD Diagnostic Systems, Franklin Lakes, NJ), 5 g/l peptone (Difco), 10 g/L glucose (Sigma-Aldrich, St. Louis, MO), and 50 mg/L streptomycin (Sigma-Aldrich). YPGal is identical to YPD except that 10 g/L galactose (Sigma-Aldrich) was substituted for glucose.

2.2.4.2. Precultures

To ensure reproducible inocula for different fermentation experiments, the inoculum were prepared according to a standardized protocol: single colonies of *E. coli* FB21591 were transferred from LB plates (containing 2 % (wt/vol) agar and 100 µg/L of kanamycin) to 5 mL of sterile LB medium (containing 8 g/L glucose, 100 µg/L kanamycin, and 0.1 mol/L MES) in test tubes. These cultures were then incubated on a roller drum at 60 rpm and 37 °C. When the culture reached an OD_{600nm} of about 1, 1.5 mL of culture medium was transferred from test tubes to 30 mL of the same medium in a 250 mL baffled shake flask. The shake flask was incubated on a horizontal rotary shaker (150–220 rpm, Lab-line 4690, Barnstead International, Dubuque, Iowa, USA) at 37 °C until an OD_{600nm} of about 1 was again reached. The culture medium in the shake flask was then diluted in fresh medium to match an OD_{600nm} of 0.05 and used to inoculate the different bioreactors. Except for the microbioreactor, optical density measurements were performed off-line at 600nm with a Spectronic® 20 Genesys™ spectrophotometer (Spectronic Instruments Inc., Rochster, NY). We used conventional cultivation techniques, including test tubes, baffled shake flasks, and 500-mL stirred-tank (Sixfors®, Infors AG) to benchmark *E. coli*

batch culture in the microbioreactor.

The standard inoculation procedure used in *S. cerevisiae* experiments was similar to the *E. coli* experimental protocol: 5 ml of each medium were inoculated with a single colony from an overnight YPD agar plate (containing streptomycin at 50 μg/liter) and incubated at 30°C on a roller drum at 60 rpm. At an OD_{600nm} of about 1.0, 1.6 ml of culture medium was used to inoculate 30 ml of fresh medium in 500 ml baffled shake flasks and incubated at 30°C on the shaker until the optical density reached about 1.0. At this point the culture was diluted in fresh medium to reach an OD_{600nm} of about 0.05 and used to inoculate microbioreactors. In microbioreactors, optical on-line measurements were made every 20 minutes. Growth data of *S. cerevisiae* cell culture were analyzed and adjusted in term of lag phases.

2.2.4.3. Bench-marking experiments

For bench-marking experiments with test tubes, a total of 13 tubes were filled with 5 mL of the same inoculum derived from a single colony. The tubes were incubated on a roller drum at 60 rpm and 37 °C. Single test tubes were sacrificed at 13 different time points over an 18 hour time period to measure pH and OD_{600nm}. The experiment was replicated four times with independent inoculations. For bench-marking experiments in shake flasks (1 L), pH and OD_{600nm} readings were obtained by taking 1 mL samples at different time points from shake flasks filled with 150 mL of inoculum. Shake flasks were incubated at 37 °C with a shaking speed of 200 rpm. Experiments were repeated four times with independent inocula. For benchmarking experiments with Sixfors® (Infors) reactors, real-time DO and pH readings were obtained in 350 mL working volume using the built-in dissolved oxygen (405 DPAS-SC-K8S/200, Mettler Toledo, Toledo, OH) and pH probes (InPro 6100/220/S/N, Mettler Toledo), respectively. Samples for OD_{600nm} off-line measurement were obtained by syringes through a sampling port at

defined time intervals. The stirring speed was 500 rpm and the air flow rate was set to 1 volume of gas per volume of medium per minute (VVM). In Sixfors stirring was obtained by three rows of six-blade Rushton flat propellers. Three replicate experiments were performed.

For microbioreactor experiments, inoculation was by flowing inoculum liquid through the reactor chamber until all original liquid was flushed out. DO, pH, and OD_{600nm} data were obtained on-line every 10 minutes. Following each fermentation experiment, the volume of the culture (150 μL) was harvested and the final OD_{600nm} and pH values were measured. Calibration curves for OD_{600nm} readings were obtained by filling the microbioreactor with culture fluids with different biomass concentration. The OD_{600nm} reading of the inoculation medium and the final OD_{600nm} reading were then used to calibrate real-time OD_{600nm} measurements. Since the optical absorbance of PDMS changes after being dipped in water (Chang *et al.*, 2003), the microbioreactor was filled with sterile water for more than 6 hours before each experiment to eliminate any potential changes in optical properties. Experiments in the microbioreactor were replicated three times using independent inocula.

2.2.4.4. K_La measurement

The gassing-out method (Stanbury *et al.*, 1995) was used to evaluate K_La values in LB medium (without microbial cells) in the microbioreactor as well as in 500-mL Sixfors® bioreactors. In the Sixfors® system, nitrogen gas was continuously sparged into the medium until the oxygen concentration dropped to zero. Air was then sparged and the DO profile as a function of time was measured by the oxygen electrode. For the microbioreactor, nitrogen was flushed into the headspace over the aeration membrane until the residual DO in the medium was depleted. Then, air was pumped into the headspace and the DO recovery was recorded by the optical sensor. The K_La values were obtain from the following expression:

$$K_L a = -\frac{1}{t}\ln\left[\frac{C^* - C_L}{C^*}\right] = -\frac{\ln(1 - DO)}{t} \quad (2\text{-}1)$$

where t is time, C_L is the dissolved oxygen concentration in the liquid phase, C^* is the saturated dissolved oxygen concentration, and DO (%) is the ratio of $C_L / C^* \times 100$.

The DO sensor response time T_p needs to be excluded from above $K_L a$ calculation. T_p was determined as the time needed to record 63% of a stepwise oxygen concentration change after the sensor was transferred from oxygen-free medium to a well-agitated, oxygen-saturated medium. By assuming a first-order response model, the adjusted $K_L a$ was obtained by fitting DO data as a function of time using the following equation,

$$1 - DO = \frac{T_m \exp\left(-t/T_m\right) - T_p \exp\left(-t/T_p\right)}{T_m - T_p} \quad (2\text{-}2)$$

where T_m is the measured time constant of oxygen mass transfer, (Zanzotto *et al.*, 2004) and $T_m = 1/K_L a$.

2.2.4.5. Comparative global gene expression analysis of *S. Cerevisiae*

Rapid screening for microorganisms exhibiting specific patterns of gene expression and protein production is critical for progress in biological research, biotechnology and the pharmaceutical industry. The analysis of microbial environmental and physiological parameters, linked to global expression technologies (gene, proteins, metabolites), would provide whole-organism information invaluable for characterizing and designing biological systems.

Global genomic expression assays using DNA microarrays permit the exploration of the cells transcriptional state under a wide range of physiological parameters. Microarray analysis has

been widely applied in basic biological research as well as in specialized fields, such as drug screening, environmental testing, and clinical diagnosis (Debouck *et al.*, 1999; Bodrossy *et al.*, 2004). Significant advantages could arise from combining parallel instrumented microbioreactor fermentations with microarray technologies to yield high-throughput gene expression analysis.

In collaboration with Dr. Paolo Boccazzi (a postdoctoral associate in Sinskey's laboratory, Department of Biology, MIT), we use the analysis of global gene expression profiles in *Saccharomyces cerevisiae* grown in glucose and galactose media in batch microbioreactors, to demonstrate the potential biological applications of a high-throughput experimental platform. The galactose utilization pathway is one of the best studied in the budding yeast (Figure 2-3). The wealth of information on this pathway, combined with its relative simplicity, has made it a useful system to evaluate the reproducibility and sensitivity of novel techniques (Ideker *et al.*, 2001; Hood, 2003).

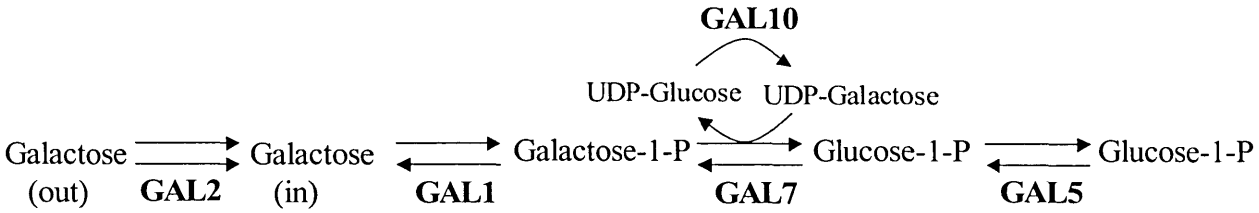

Figure 2-3. Pathway of galactose utilization. *Saccharomyces cerevisiae* metabolizes galactose in a series of steps that start with the transport of galactose into the cell via a permease (GAL2), followed by the transformation of galactose to glucose-6-P via a galactokinase (GAL1), a uridyl transferase (GAL7), an epimerase (GAL10) and a phosphoglucomutase (GAL5).

It is well established that *S. cerevisiae* grown in galactose medium up-regulates the GAL operon (Ideker *et al.*, 2001; Hittinger *et al.*, 2004), which comprises the genes responsible for the catabolism of galactose to glucose-6-P (Figure 2-3). The core genes that allow *S. cerevisiae* to utilize galactose as the carbon source include GAL2, which encodes a permease for galactose

transport into the cell, and GAL1, GAL7, GAL10 and GAL5, the structural genes for galactokinase, uridylyltransferase, epimerase and phosphoglucomutase, respectively. The transcriptional regulation of the GAL operon is not fully understood, but three of the main regulators are encoded by GAL3, GAL80 and GAL4 (Johnston, 1987; Lohr *et al.*, 1995; Ideker *et al.*, 2001). Comparative gene expression analysis studies of *S. cerevisiae* in large scales have been published (Ideker *et al.*, 2001; Hittinger *et al.*, 2004) and are used here as benchmarks.

Total RNA was isolated from two independent fermentations in YPD and in YPGal. Cells were harvested during exponential growth at an OD_{600nm} of about 1.0 and immediately frozen in liquid nitrogen. Total RNA was isolated using an RNeasy kit (Qiagen). For gene expression analysis we applied Affymetrix Yeast Genome S98 Arrays (Affymetrix, Santa Clara, CA) that contain approximately 6,400 Opening Reading Frames (ORFs) of the yeast *Saccharomyces cerevisiae*. Details of the RNA isolation and microarray analysis are given in Boccazzi *et al.* (2006).

2.2.5. CFD simulation of liquid flow in microbioreactors

Flow patterns in the microbioreactor were simulated using CFD-ACE® software (ESI US R&D, Inc., Huntsville, AL, USA). Water was used as the model fluid and the microbioreactor geometry was simplified as a cylindrical chamber of 10 mm diameter and 2 mm depth. The reactor chamber was divided into 0.7×10^6 structured finite elements. The three-dimensional flow in the reactor chamber was simulated by following the angular rotation of the magnetic stir bar until a steady solution was obtained. In each step of the rotation (1° in movement, corresponding to 0.001 second in time step) the solution of the continuity equation and Navier-Stokes equations was obtained within 2000 iterations; steady flow was typically established after 1080 rotations.

2.3. Results and Discussion

2.3.1. Liquid mixing in microbioreactor

The microbioreactor described here is implemented with a magnetic stirring unit for active mixing, in contrast to an existing microbioreactor (Zanzotto *et al.*, 2004) that relied on diffusion. The flow in the microbioreactor is characterized by the Reynolds number:

$$\mathrm{Re}_n = \frac{D^2 N \rho}{\mu} \tag{2-3}$$

where D is the length of the stir bar (from arm to arm), N is the rotation rate for the stir bar. ρ is the density of liquids, and μ is the liquid viscosity coefficient. Using water as the model medium, the Reynolds number for the microbioreactor ranges from 30 (at 180 rpm) to 130 (850 rpm), corresponding to laminar to transitional flow regime in stirred reactors (Biń, 1984; Blanch and Clark, 1996). LB medium was measured to have a 16 % higher viscosity (Ubbelohde viscometer, Technical Glass Products., Inc., Dover, NJ, USA) than pure water and therefore has a lower Reynolds numbers when stirred at same speeds. However, the difference in viscosity did not perturb the stirring speed with the efficient coupling between the stir bar and the magnetic drive. As an indication of the efficiency of mixing, Figure 2-4 illustrates the distribution of phenol red dye in the microbioreactor as a function of mixing time. The indicator color is uniformly distributed throughout the reactor indicating complete mixing within 30 seconds of mixing at stirring speed of 180 rpm.

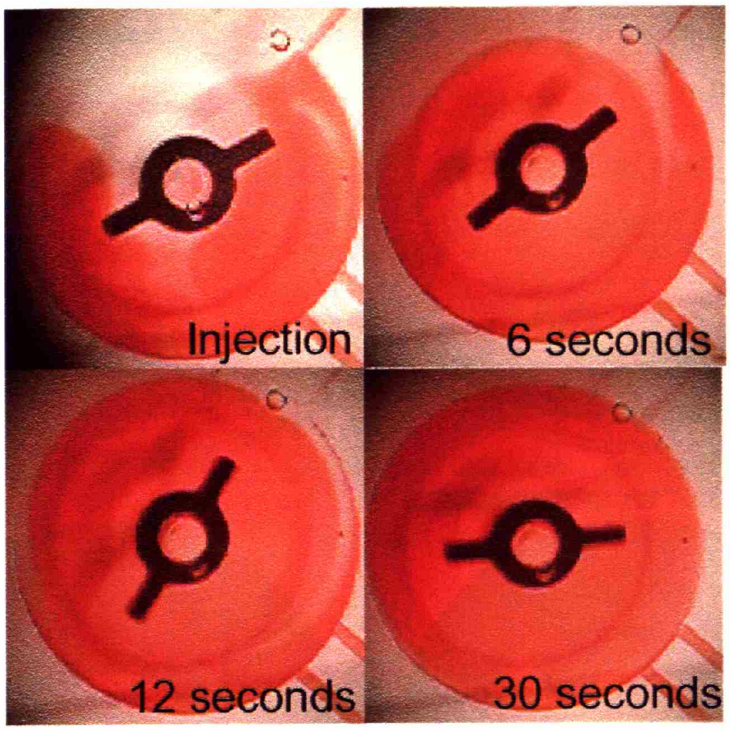

Figure 2-4. Photographs for mixing of phenol red dye in the microbioreactor operating with stirring speed of 180 rpm. Note that the shadow of stir bar is projected and visible at the bottom of the chamber.

Computational fluid dynamic simulations and measurements of the oxygen mass transfer rate provide further characterization of the mixing properties. The steady state liquid flow at 180 rpm, as simulated by CFD-ACE® (Figure 2-5), reveals a secondary vertical flow caused by the horizontal stir bar rotation. This vertical flow contributes to the oxygen mass transportation from the top PDMS membrane to the DO sensor located at the bottom of the reactor. Vuppu *et al.* (2004) also simulated the rotation of a μm-scale rotor, but their rotational flow is in the regime of very low Reynolds number (maximal Re_n of ~ 0.05) and viscous forces dominate over inertial forces with poor mixing as the consequence. Flow in the present microbioreactor has a significantly higher Reynolds number (Re_n of 30~130) and the convective inertial force dominates in this laminar and transitional flow regime. As a readily adjusted parameter, stirring speed has significant effects on mixing in this flow regime, thus allowing for manipulation of

oxygenation in the microbioreactor.

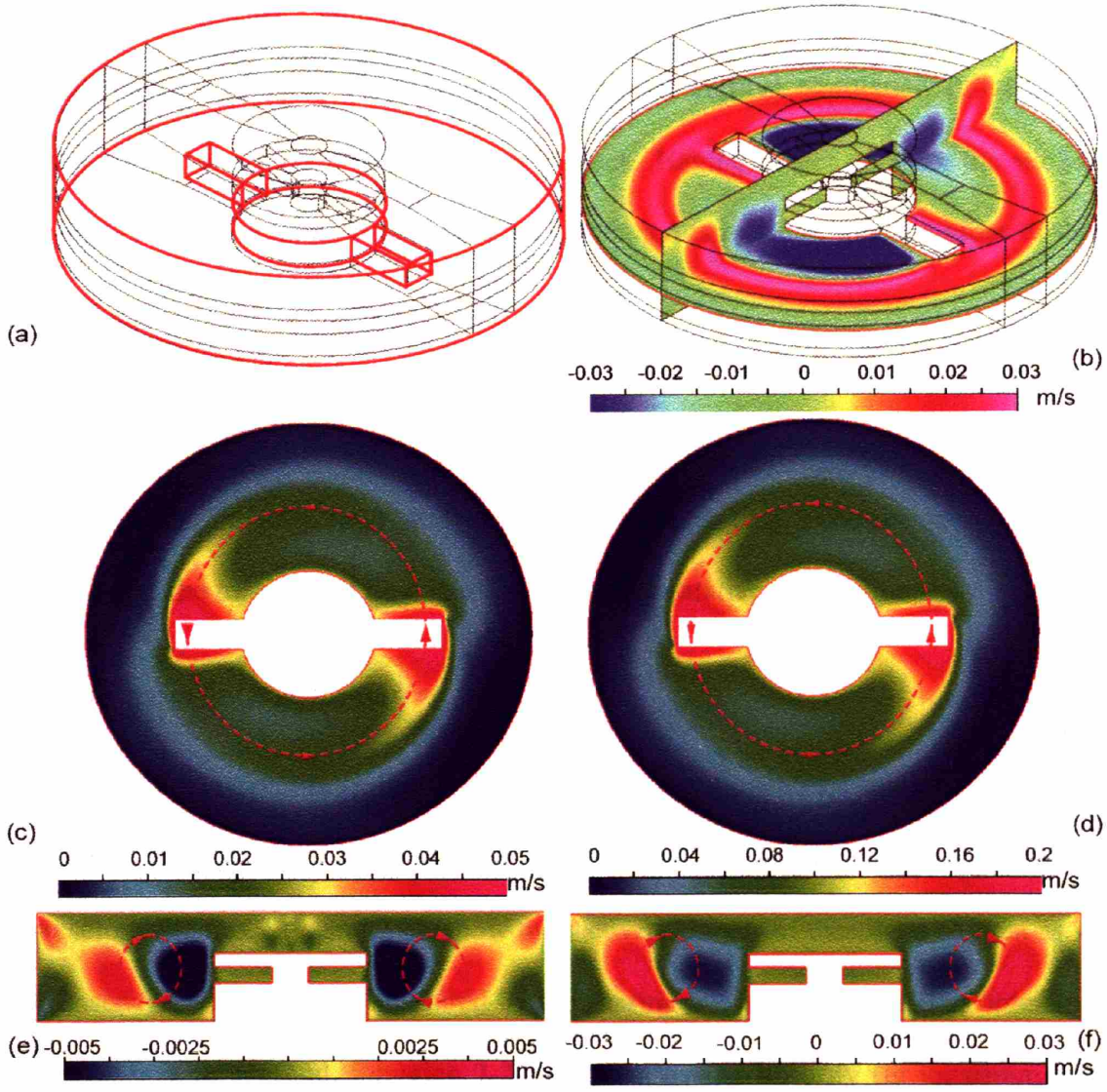

Figure 2-5. CFD-ACE® simulation of medium flow in the microbioreactor operating at stirring speeds of 180 rpm and 700 rpm. (a) Simplified sketch of the reactor chamber and the stir bar. Note the PMMA structures holding the stir bar is not outlined in figure (a). Red solid line in the figure shows the direction of stirrer movement and the dashed line shows the vertical circulation of flow at the given cross-section. (b) Bird's eye of the vertical flow velocity distribution at a horizontal plane in the center and a vertical plane 0.6 mm above the bottom of the microbioreactor that is stirred at 700 rpm.. (c) And (d) Comparison of the magnitude of flow velocity at a vertical plane 0.6 mm above the bottom of the microbioreactor at stirring speed of (c) 180 rpm and (d) 700 rpm. (e) and (f) Comparison of the vertical flow circulation at a horizontal plane in the microbioreactor at stirring speed of (e) 180 rpm and (f) 700 rpm. Note the difference in the scales of legends.

Simulation results were used to optimize the geometry of the reactor chamber. Variables include the vertical position and arm length of the stir bar. Placing the stir bar in the vertical center of the reactor chamber will develop two separate vertical circulation flows above and beneath the stir bar thus reduce the total mixing effect. Having longer arms for the stir bar also confines the vertical circulation flow, given the circulation is in the shoulder regions of the mini stir bar.

It is worth to mention that these conclusions about oxygenation drawn from fluidic simulations are qualitative. Theoretically the CFD simulations can be coupled with mass transfer model to calculate mixing time and correlated with mixing experiments; however, the simplifications in the transitional flow model limit its quantitative applications.

2.3.2. Mass transfer coefficient

Oxygen mass transfer rate in bioreactors is a critical parameter of microbial fermentation. The volumetric mass-transfer coefficient, K_La, is often used as a measure of the aeration capacity of a bioreactor. Figures 2-6a and 2-6b show the recovery curves of dissolved oxygen as well as the DO sensor response curve as measured by the gassing out method. The first order response model for the gassing method, Equation 2-2, is proven by the linearity (in logarithm scale) of curves shown in Figure 2-6. The DO electrode used in the Sixfors® has a response time T_p of 12.7 s at a stirring speed of 500 rpm and a sparging rate of 1 VVM. The K_La in Sixfors® bioreactor is calculated as 48.2 hr^{-1}. The response time of the DO optical sensor in the microbioreactor is 33.6 s (Figure 2-6b). At a 180 rpm stirring speed, the K_La value in the microbioreactor is 22.2 hr^{-1}, which is lower than the K_La value of 48.2 hr^{-1} in the Sixfors® reactor (500 rpm, 1 VVM). Higher oxygen transfer rates can be obtained in the microbioreactor with higher stirring speeds (Figure 2-7); for example, at a stirring speed of 700 rpm, the K_La is

measured as 61.9 hr^{-1}, exceeding the value obtained in bench top reactors.

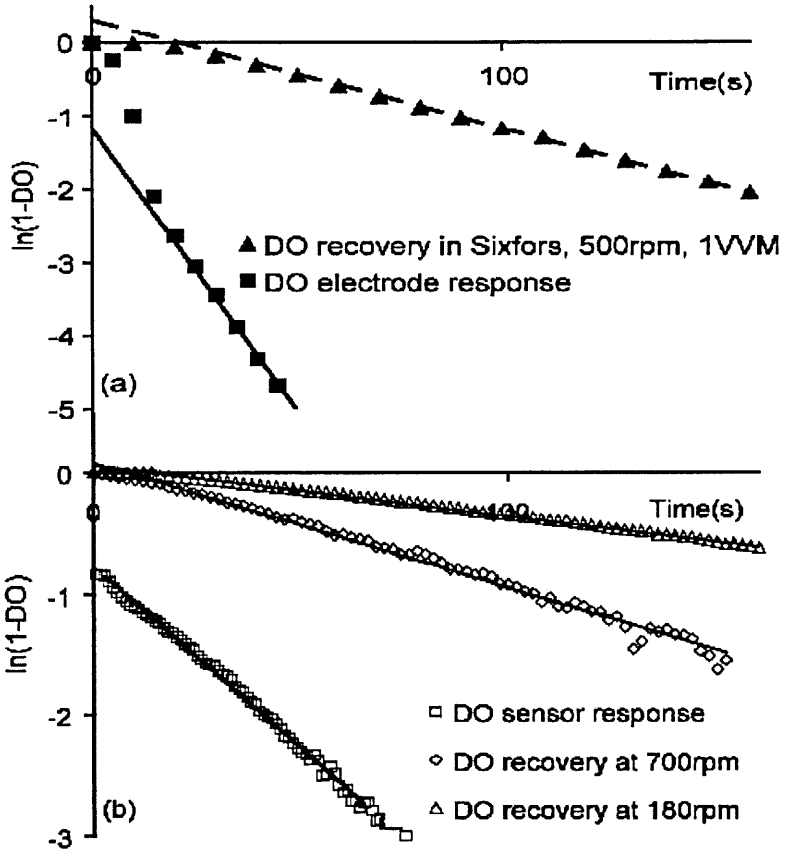

Figure 2-6. Recovery of dissolved oxygen curves as well as the DO sensor response curves (logarithm scale) in (a) Sixfors® reactor (stirring speed of 500 rpm and sparging rate of 1 VVM); and (b) microbioreactor (stirring speed of 180 rpm and 700 rpm).

In the microbioreactor, oxygen is supplied to the medium by oxygen diffusion through the PDMS membrane to the liquid phase. There is no gas sparging through the liquid medium and no moving gas-liquid interface, as a consequence, the specific mass-transfer area a stays constant. Similar to surface-aerated bioreactors (without bubble entrainment), the improvement in $K_L a$ values in the microbioreactor at higher stirring speeds results from better mixing and distribution of dissolved oxygen in the liquid phase.

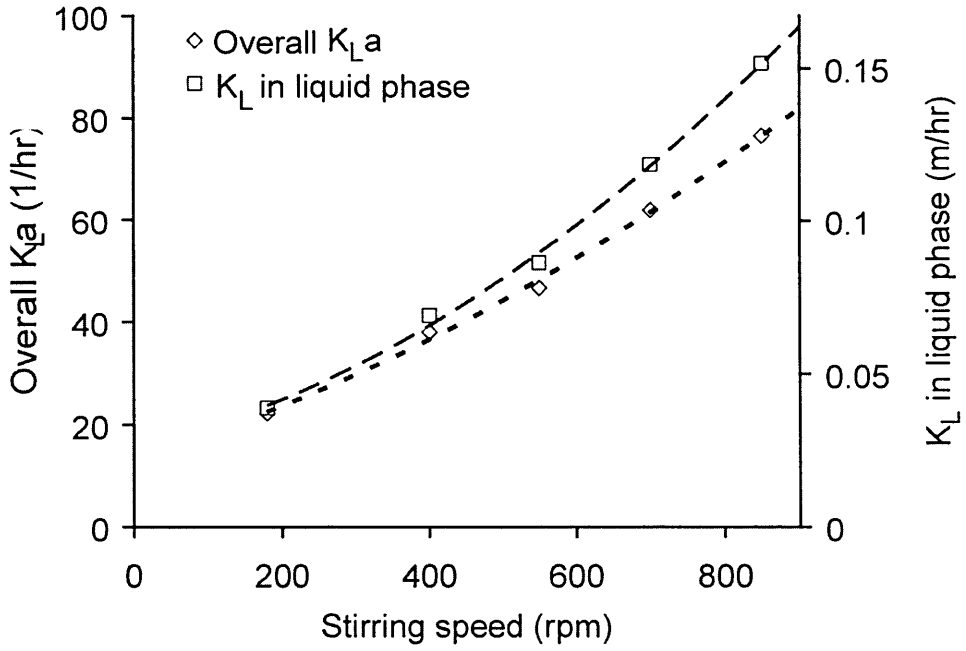

Figure 2-7. Oxygen volumetric mass transfer coefficients as a function of stirring speed in the microbioreactor.

The overall oxygen mass-transfer resistance $1/K_{L,overall}$ in the microbioreactor is the sum of three resistances in series:

$$\frac{1}{K_{L,overall}} = \frac{1}{K_L} + \frac{\delta}{D_{PDMS}H} + \frac{1}{K_G} \tag{2-4}$$

where $1/K_L$ is the mass-transfer resistance in liquid phase, $\delta/(D_{PDMS}H)$ is the diffusion resistance through PDMS, and $1/K_G$ represents the diffusion resistance in air. The mass transfer coefficients and the simple film model are typically used in cases of turbulent flow, such as in traditional large scale fermentors. Nevertheless, with appropriate definition of the mass transfer coefficients (Bird *et al.,* 2002), the concept also applies for the flow conditions in the microbioreactor and it has been applied to similar issues in microtiter plates (Hermann *et al.*,

2002). In particular, it provides a useful means for evaluating the relative importance of the different resistances to oxygen transport into the microbioreactor (Equation 2-4). The diffusivity of oxygen in air is significantly higher than in PDMS and water, thus $1/K_G$ can be neglected compared with the other terms in Equation 2-4. The PDMS membrane has a thickness δ of 100 μm, and the diffusivity of oxygen in PDMS D_{PDMS} is 3.4×10^{-5} cm^2/s (Merkel *et al.*, 2000). The solubilities of oxygen in PDMS and water are 1.69 mmol/L (Merkel *et al.*, 2000) and 0.228 mmol/L (Perry and Green, 1984), respectively. The Henry's constant H, the solubility ratio of oxygen in PDMS and water, equals to 7.4. With a fixed surface aeration area of 90 mm^2, the overall mass transfer coefficient $K_{L,overall}$ ranges from 0.037 m/hr (180 rpm) to 0.13 m/hr (850rpm). The net mass transfer coefficient in water K_L ranges from 0.039 m/hr (180 rpm) to 0.15 m/hr (850 rpm). These values are consistent with or slightly lower than reported literature values for surface-aerated stirred-tank bioreactors (Kawase and Moo-Young, 1990; Kamen *et al.*, 1995). The variation in K_L value with changing stirring speed (Figure 2-7) is similar to the change observed with varying shaking frequency in microtiter plates (Hermann *et al.*, 2002), which have wells of similar volume (200 μL) as the present microbioreactor.

2.3.3. Batch culture results in microbioreactor

We investigated *E. coli* cell growth kinetics in the microbioreactor to demonstrate the feasibility of microbial cultivation in the microbioreactor. Triplicate fermentation experiments were carried out in the microbioreactor at both 180 rpm and 700 rpm stirring speed. The observed OD_{600nm}, pH, and DO values within the microbioreactor (Figure 2-8) demonstrate the reproducibility of cell growth in the microbioreactor under different growth conditions.

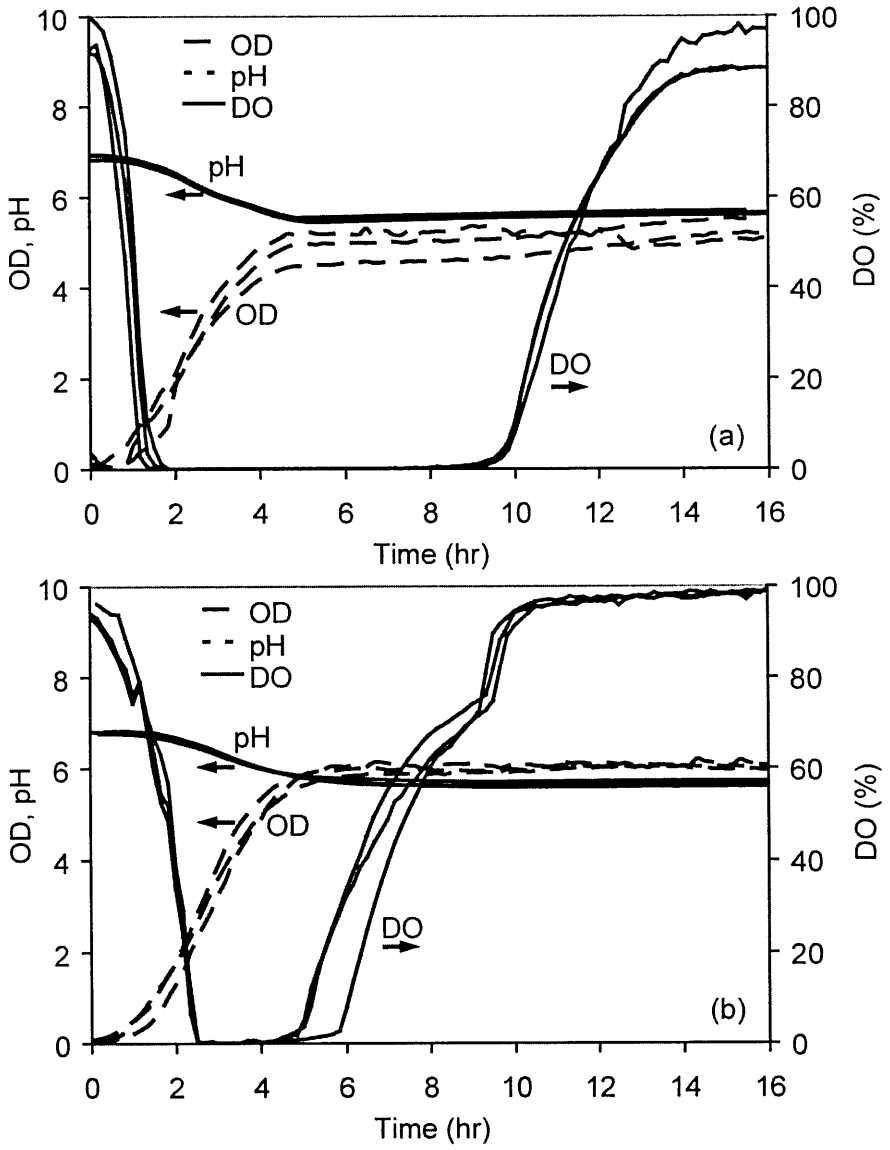

Figure 2-8. Replicate fermentations (n = 3) of *E. coli* FB21591 in LB medium with stirring speed of (a) 180 rpm and (b) 700 rpm.

As a result of the standard inoculation protocol, *E. coli* cells start to grow immediately without any observable lag phase. Consistent with the high growth rate of cells during exponential growth phase, the high demand for oxygen is reflected by the rapid decrease in DO level in the culture medium. Although avoiding oxygen depletion is the best interest for many specific bioprocesses, we intentionally chose oxygen-limited growth conditions for the

cultivation of microbial cells to obtain more information about the microbioreactor itself and to better benchmark the microbioreactor. High-capability oxygenation was not the major pursue for our microbioreactor; the reproducibility and the correlation of the microbioreactor to conventional bench-scale bioreactors are more important for a potentially applicable high-throughput platform with μL volume and on-line measurements.

With a stirring speed of 180 rpm, the DO in the microbioreactor completely depletes at around 1.5 hours of the fermentation and does not start to recover until after 9 hours (Figure 2-8a), when cells enter the late-stationary phase and become limited in nutrients. During this period, as a consequence of anaerobic fermentation the pH level in the medium decreases significantly until cells reach stationary phase at around 6 hours.

Consistent with the K_La measurements, improved oxygenation is observed at higher stirring speeds (Figure 2-8b). With a stirring speed of 700 rpm, the DO level in the microbioreactor depletes after about 2.5 hours of the fermentation and starts to recover at around 5.5 hours, much earlier than the recovery time in fermentations with stirring speed of 180 rpm. With better oxygenation cells grow faster and reach higher biomass concentrations. The final OD_{600nm} with 700 rpm stirring is 6.2 ± 0.17 in contrast to the final OD_{600nm} value of 5.3 ± 0.2 with stirring at 180 rpm.

The reproducibility and flexibility of the microbioreactor is also demonstrated by triplicate *S. cerevisiae* batch culture experiments (Figure 2-9). *S. cerevisiae* ATCC 4126 cells are cultured in YPGal and YPD media. In these experiments the stirring speed is 700 rpm and similar standard inoculation procedure is applied. In YPGal medium, DO depletes at around 10 hours into the fermentation, and starts to recovers around 15 hours, when cells have used the nutrients and enter the stationary phase. In YPGal medium cells reached a maximum OD_{600nm} of 6.87 (± 0.07), and

at this population density the pH and the DO concentration were 6.82 (± 0.09) and 11.2 (± 1.3) %, respectively. In YPD medium, cells reached a maximum OD_{600nm} of 5.2 (± 0.2) with a pH and DO concentration of 6.6 (± 0.1) and 42.1 (± 8.7) %, respectively. In the microbioreactors, the average generation times for *S. cerevisiae* were of 93 (± 3.7) min and 99 (± 10.8) min in YPGal and YPD media, respectively.

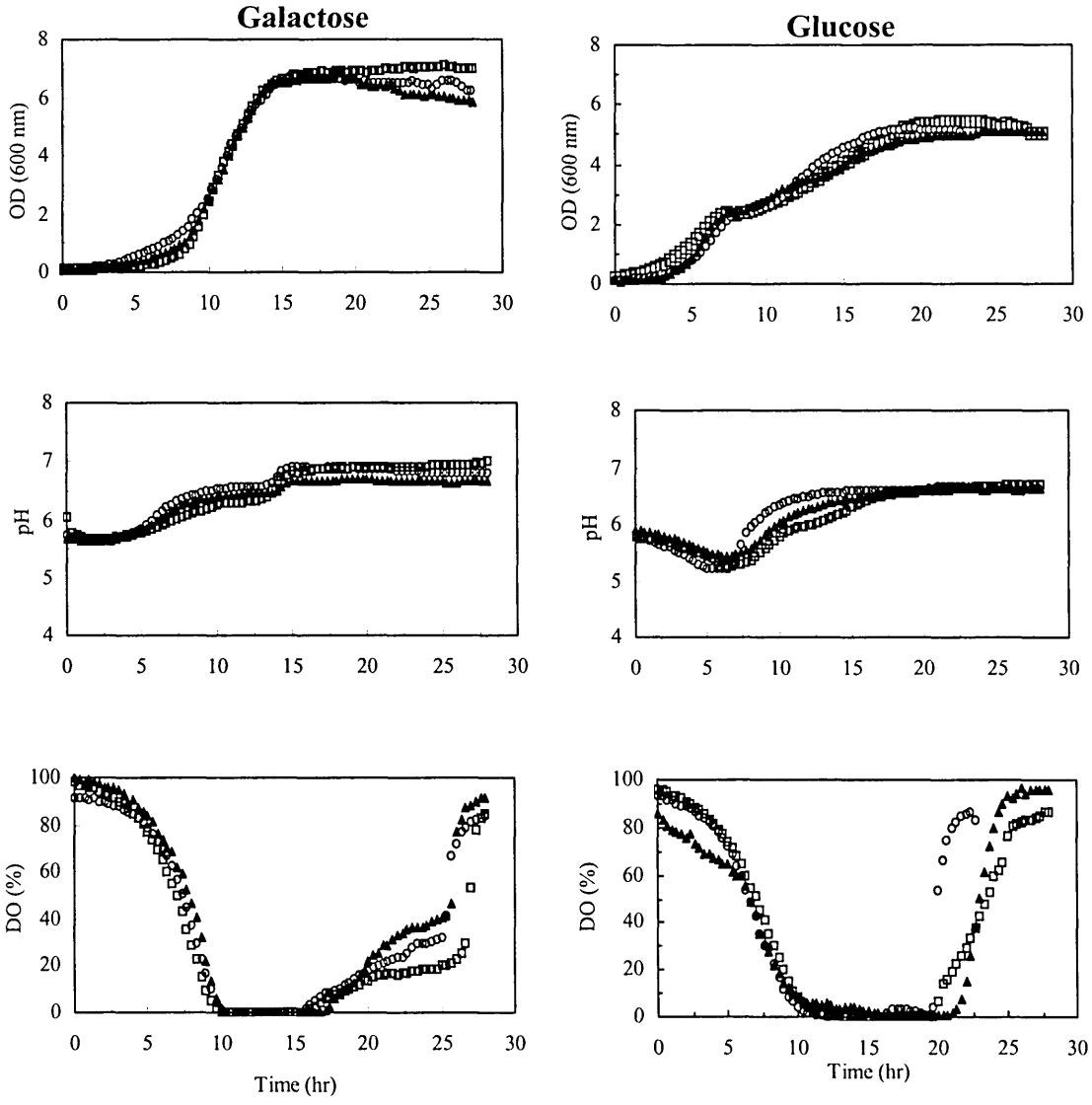

Figure 2-9. Growth data (n = 3) of *S. cerevisiae* in galactose medium (left panels) and glucose medium (right panels).

In YPD we observed a change in the growth rate of the strain after about 7.5 hours of fermentation. This switch was likely due to a diauxic growth (Stahl et al. 2004, Otterstedt et al. 2004; Larsson et al. 1991, Blomberg et al. 1988). During the first part of fermentation the strain grew in a respiro-fermentative mode consuming glucose and producing ethanol and acetate, hence the decrease in pH, and during the second part the strain switched to anaerobic growth with ethanol as carbon source.

2.3.4. Benchmarking fermentations

We compared *E. coli* fermentation growth kinetics obtained in the microbioreactor with growth data from conventional bioreactors, including Sixfors®, test tubes, and shake flasks (Figure 2-10) for benchmarking purpose. Both the time profiles and the standard deviations of the OD curves obtained in the microbioreactor are comparable with other conventional bioreactors (Figure 2-10a). The highest biomass was obtained with the microbioreactors stirred at 700 rpm, followed by the Sixfors® bioreactors (500 rpm, 1 VVM) and the shake flasks (200 rpm in shaking speed), and then by the microbioreactor stirring at 180 rpm. These results are consistent with the oxygenation characteristics in the reactors, including both the K_La data and the DO profiles during batch fermentation (Figure 2-10c). As a dynamic process, the recovery of DO in bioreactors happens when glucose becomes limiting, and this recovery is significantly slower in less oxygenated reactors (microbioreactor operating at 180 rpm), and cells grow anaerobically for longer period of time.

The pH curves for the microbioreactor and those from all other bioreactors (Figure 2-10b), as well as the DO profiles (Figure 2-10c) from the microbioreactor and the Sixfors® are all similar. In our experiments, test tubes and shake flasks were not equipped with DO sensors; but the

oxygenation can be estimated by the growth rate and final OD level (Figure 2-11). Cell growth in

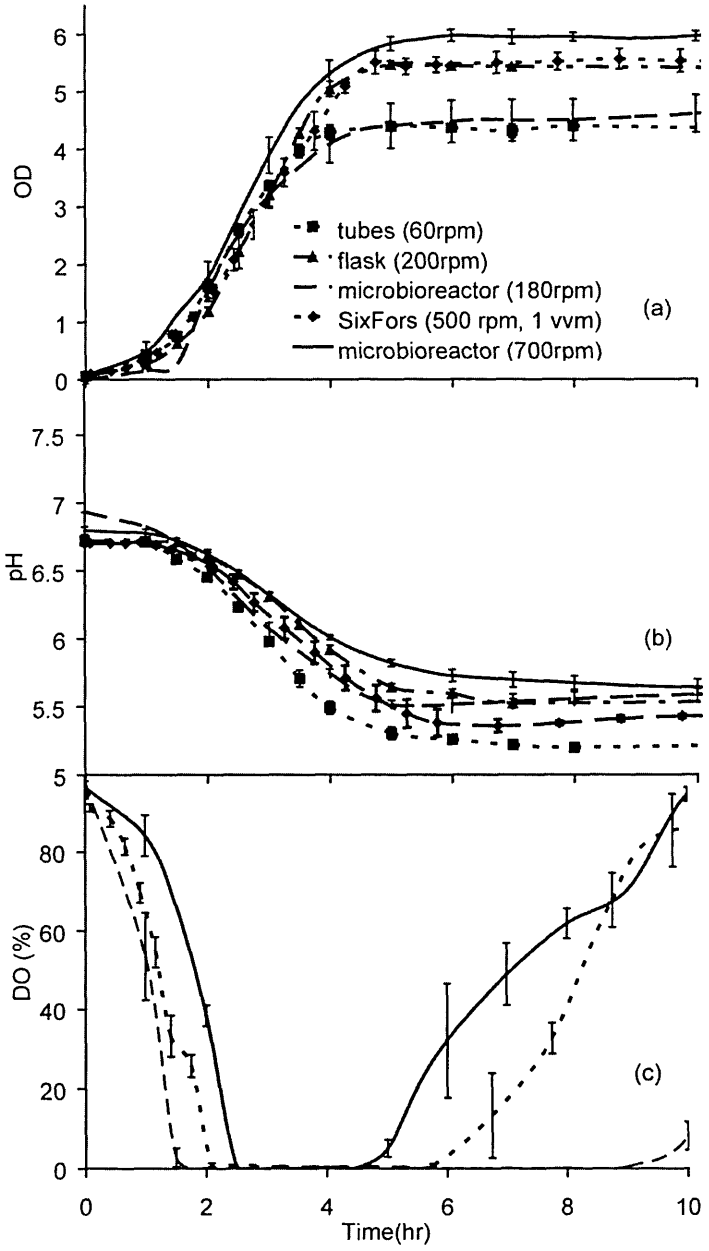

Figure 2-10. Comparison of *E. coli* FB21591 growth kinetics in LB medium in the microbioreactor (n = 3, stirring speed at 180 rpm and 700rpm, respectively) with conventional bioreactors including test tubes (n = 4), shake flasks (n = 4), and Sixfors (n = 3). Each growth curve represents the average value with standard deviation from replicate experiments carried out in separate bioreactors. (a) OD_{600nm}. (b) pH. (c) DO.

test tubes has the lowest final OD_{600nm} (4.23 ± 0.01), which can be attributed to the low oxygenation level. Gupta and Rao (2003) reported a K_La value in baffled shake flasks with 100 mL filling volume and shaking speed of 250 rpm as ~ 59.2 hr^{-1}. Because a lower shaking speed and a larger filling volume are used here, the K_La value in our shake flasks would be expected to be less than the reported value. This assumption is consistent with our experimental data: the cell growth rate, the final biomass concentration, and the final pH level in shake flasks (1.39 ± 0.06 hr^{-1}, 5.35 ± 0.18 and 5.59 ± 0.02, respectively) are close to the values obtained in Sixfors® (1.55 ± 0.03 hr^{-1}, 5.37 ± 0.06, and 5.61 ± 0.47, respectively). The ability to change mixing in the microbioreactor by different stirring speed enables the control of oxygenation and also allows varying growth kinetics ranging from shake flasks conditions to those characterized conventional bench-scale stirred-tank bioreactors, such as Sixfors®. Variations in data, especially for OD_{600nm} data obtained in our microbioreactor (5.29 ± 0.2 at 180rpm and 6.20 ± 0.17 at 700rpm), are comparable with those from flasks and Sixfors bioreactors.

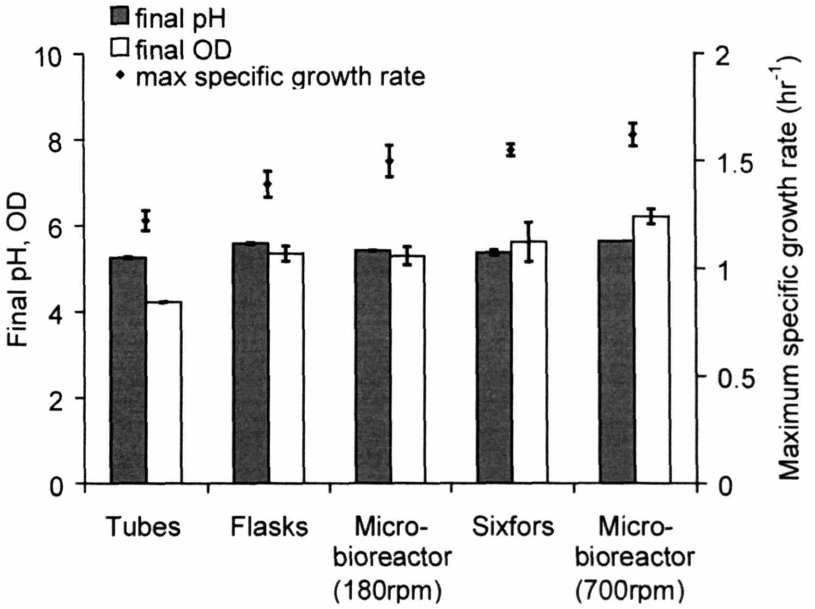

Figure 2-11. Comparison of final OD_{600nm}, pH, and maximal growth rate in *E. coli* FB21591 batch cultures in different bioreactors.

2.3.5. Application: global gene expression analysis of yeast cells

Reproducible growth kinetics of *S. cerevisiae* grown in the microbioreactors are demonstrated in Figure 2-9; the reproducibility is especially good considering that individual fermentations were run on different days from independent colonies. Real-time measurements of growth kinetics in the microbioreactors allowed harvesting the cells at an OD_{600nm} of about 1 for RNA isolation for the investigation of global gene expression analysis. Figure 2-12 shows the physiological status of the cells at harvesting time. At an OD_{600nm} of 1.0, the average pH of both media was 5.9 - 6.2, and the DO concentrations were on average 11.2 % in YPGal medium and 76.7 % in YPD medium.

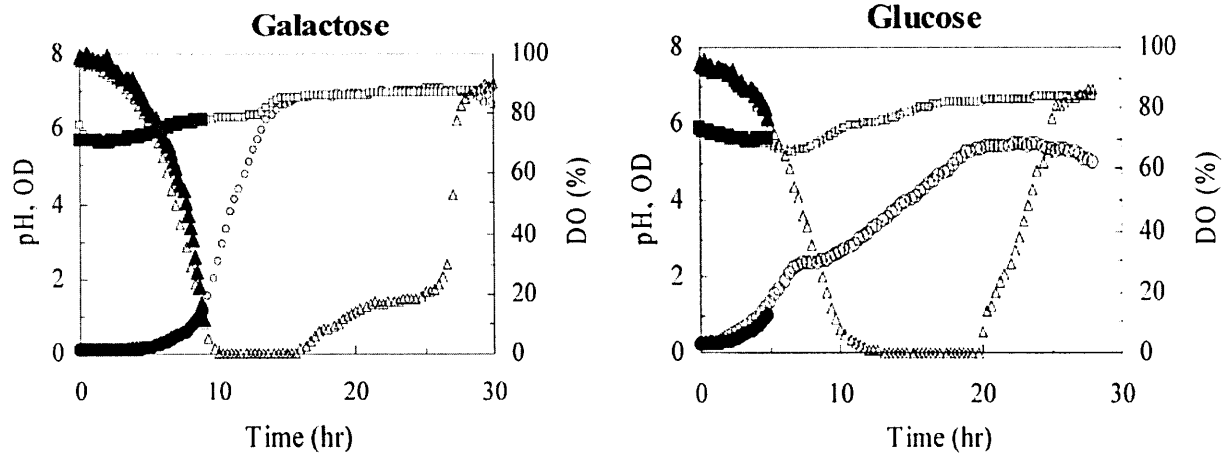

Figure 2-12. Reproducibility of complete fermentations (open symbols) growth kinetics of *S. cerevisiae* grown in galactose and glucose media when fermentations were sacrificed at OD_{600nm}=1 (closed symbols). Real-time measurements of OD_{600nm} (circles), pH (squares), and DO (triangles) were taken every ten minutes.

To assess differential gene expression profiles under the two growth conditions, up-regulated genes were identified based on significance and fold change. The array-to-array reproducibility was excellent and the R square of normalized intensities of duplicate samples of cells grown in the same medium and plotted against each other was above 0.97. More details of

up-regulated genes in *S. cerevisiae* grown in YPGal and YPD media are given in Boccazzi *et al.* (2006).

In *S. cerevisiae* grown in YPGal, four genes of the galactose pathway GAL1, GAL2, GAL7 and GAL10 were up-regulated more than 125-fold (Figure 2-13). GAL5 was expressed but not found to be up-regulated. The two transcriptional regulators GAL3 and GAL80 (Figure 2-3) were up-regulated 8- and 7.5-fold, respectively. GAL4, a third regulator, was not found to be up-regulated. These results are in close agreement with previous reports (Johnston 1987; Lohr *et al.* 1995).

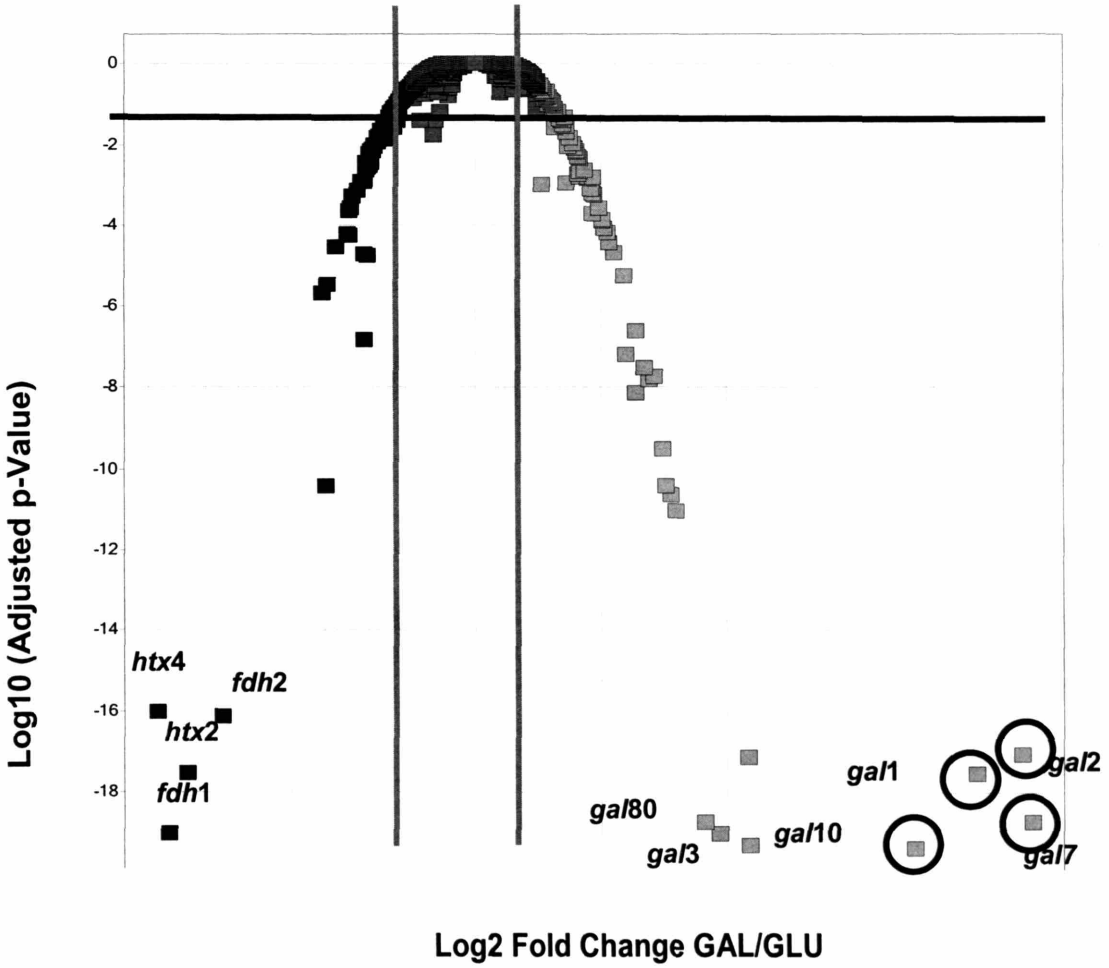

Figure 2-13. Volcano plot of differential gene expression in *S. cerevisiae* grown in galactose and glucose media.

Among the most up-regulated genes in *S. cerevisiae* grown YPD medium were two genes coding for high affinity glucose transporters, HXT4 and HXT2, whose expression increased 34.3- and 21.6-fold, respectively, and two NAD-dependent formate dehydrogenase genes, FDH2 and FDH1, whose expression increased 29.8- and 16-fold, respectively (Figure 2-13).

2.4. Conclusion

A 150 μL membrane-aerated and actively mixed microbioreactor in PMMA and PDMS was designed and fabricated. PMMA and PDMS were chosen as materials for the bioreactor, for their good optical transparency to visible light, biocompatibility and mechanical rigidity, low cost, as well as their potential for large-scale manufacturing; the latter characters should allow the microbioreactor to be disposable. Optical sensors for OD_{600nm}, pH, and DO real time measurements were integrated into the microbioreactor.

Active mixing facilitates oxygenation in membrane-aerated bioreactors and enables larger culture volume for bio-analysis, while still maintaining reasonable levels of oxygenation for cell growth. The volumetric mass-transfer coefficient, K_La, was characterized to range in $20 \sim 75 hr^{-1}$, which is comparable to those from conventional bench-scale bioreactors. Growth kinetics, in terms of time profiles and final values of OD_{600nm}, pH, and DO measurements, were reproducible for the batch microbioreactors and corresponded closely to those observed with conventional experimental culture methods, including test tubes, shake flasks, and bench-scale stirred tank bioreactors (Sixfors®). With this ability to mirror observations obtained in conventional systems coupled with reproducible growth, the small reactor volumes, and the on-line measurements of DO, pH, and OD in microbioreactors show promise as for high throughput bioprocessing.

Global gene expression analysis of *S. cerevisiae*, an extensively studied eukaryotic model

system and the galactose pathway, was used as an example to evaluate the potential applications for the novel technology. *S. cerevisiae* fermentation experiments were on-line monitored up to the point where samples were taken. Sufficient mRNA was separated out of cells grow in either medium to perform microarray hybridizations. Spot intensities between duplicate arrays of each growth condition correlated favorably. During microbioreactor cultivation in galactose medium, the core genes of the galactose pathway, GAL2, GAL1, GAL7 and GAL10 were up-regulated more than 100-fold. Furthermore, two major positive regulators of this pathway, GAL3 and GAL80, were up-regulated at least 7.5-fold. Among the most up-regulated genes in cultures grown in glucose medium were HTX4 and HTX2 which encode high affinity glucose transporters. Yeast cells grown in the microbioreactors described here exhibit physiological and molecular characteristics which parallel those of large-scale cultures, demonstrating that microbioreactors are a step toward high-throughput analysis of yeast and bacterial strains.

Chapter 3. Microchemostat- continuous culture in microbioreactor

3.1. Introduction

In a chemostat, microbial cells reach a steady state condition at which cell biomass production, substrates and the product concentrations remain constant. These features make the bioreactor operated with a continuous culture mode a unique and powerful tool for biological and physiological research. Continuous culture offers the possibility of screening and selecting microorganisms in a constant environment on the basis of different growth rates at different substrate concentrations by setting volumetric flow rate of feed and effluent streams at a steady state (Harder and Kuenen, 1977). An example is the selection of ethanol-tolerant strain by using a two-stage continuous culture (Kim, 1978). In addition for screening of microorganisms, the continuous process is useful for finding the optimal culture conditions for a chosen strain.

However, continuous culture is often expensive and time-consuming. Normally the culture begins as a batch process and is transferred to a continuous process by starting feeding the reactor with nutrients and draining medium solution from the reaction system. Long starting and transient time is needed before the system reaches a steady state and valuable data are obtained (Kubitschek, 1970). The tradeoff for a set of higher quality data by continuous culture is a lower quantity. Typical applications of continuous culture are in physiological and ecological research for microorganisms. Screening typically employs batch vessels, such as shake-flasks or test tubes (Parekh, 2000). Miniaturization of existing continuous bioreactors can potentially reduce the effort of continuous experiments thus to make continuous culture a widely applicable routine for bioprocess development.

We present a polymer-based microbioreactor system integrated with OD, pH, and DO real-time measurements for continuous cultivation of microbial cells. *E. coli* cells are continuously cultured in a 150 μL, membrane-aerated, well-mixed microbioreactor fed by pressure-driven flow of fresh medium through a microchannel. Chemotaxis, i.e. back growth of bacterial cells into the medium feed channel, is prevented by local heating the microchannel. By using poly(ethylene glycol) (PEG)-grafted poly(acrylic acid) (PAA) copolymer films, the inner surfaces of PMMA and PDMS of the microbioreactor are modified to generate bio-inert surfaces resistant to non-specific protein adsorption and cell adhesion. The modified surfaces of microbioreactor effectively reduce wall growth of *E. coli* for a prolonged period of cultivation. Steady state conditions at different dilution rates are demonstrated and characterized by steady OD, pH, and DO levels.

3.2. Materials and Methods

3.2.1. Microbioreactor design

The microbioreactor was fabricated from four PMMA layers and two PDMS layers (see Figure 3-1). The microbioreactor chamber (diameter 10 mm, depth 2 mm, total volume of 150 μL) and three connecting channels (depth 250 μm, width 250 μm) were fabricated in three bottom PMMA layers (1 mm, 1.5 mm, and 0.5 mm in thickness, Goodfellow Corp., Devon, PA, USA) by using a computer-numerical-controlled (CNC) milling machine. The three layers were thermally bonded using a mechanical press (140 kPa, 145°C for 90 mins). A thin layer (100 μm) of spin-coated PDMS covered the reactor chamber and served as the aeration membrane. PDMS was spin-coated at a speed of 1200 rpm for 25 seconds and then baked at 70°C for 2 hours for curing. To facilitate device assembly and hermetical sealing, this PDMS layer was bonded with

a 5 mm-thick PDMS gasket layer. The PDMS layer was covered with an additional layer of stainless steel grid (B-PMX-062, Small Parts Inc., Miami, FL, USA) fixed by a homemade PDMS O-ring to provide a perforated membrane structure with 40% opening area. The stainless steel grid significantly reduces bulging of PDMS membrane and makes the reactor volume constant despite of potential fluctuations in fluidic pressure. However, the grid also reduces oxygenation in the microbioreactor. Optimal aeration is not the primary objective for our chemostat application and it can be partially compensated by faster stirring speed in the reactor chamber. A top PMMA layer was used to provide a rigid support in the mechanical assembly.

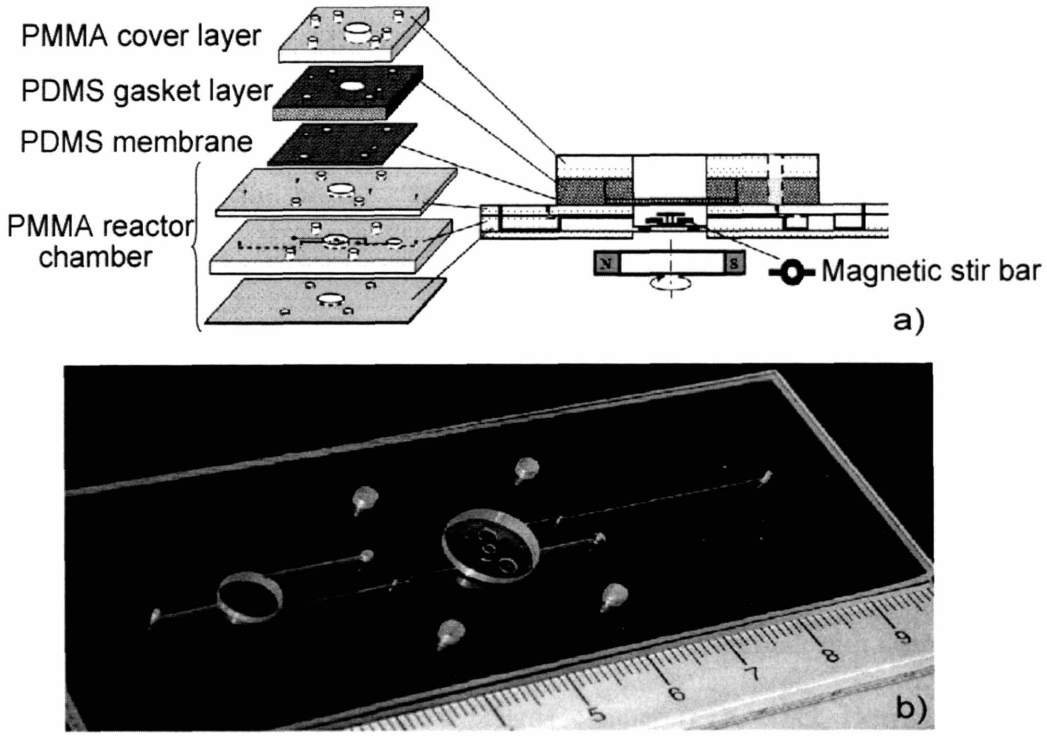

Figure 3-1. (a) Schematic view of the longitudinal section of the microbioreactor utilized for continuous culture studies; (b) Photograph of the empty PMMA chamber of the reactor (middle layer for reactor chamber) with the magnetic stir bar in the center.

3.2.2. Cell-resistant surface modification

A coating technology was developed by a collaborator, Dr. Hyun-Goo Choi (a postdoctoral associate in Jensen's laboratory), using poly(ethylene-*r*-propylene) copolymer- grafted poly(acrylic acid) (PAA) copolymer films (PAA-*g*-(PEG-*r*-PPG)) to generate bio-inert surfaces capable of effectively reducing non-specific cell adhesion on both PDMS (Choi *et al.* 2003) and PMMA surfaces (Zhang *et al*, 2004) in the microbioreactor. PAA-*g*-(PEG-*r*-PPG) copolymer was synthesized using an amidation reaction to graft H_2N-(PEG-*r*-PPG)-OCH_3 (Jeffamine XTJ-234, Huntsman Co., Houston, TX, USA) chains to the carboxylic acid groups on the PAA (Sigma-Aldrich, Co., St. Louis, MO, USA) backbone (Moeser *et al.*, 2002) with a grafting ratio of 50%. In a typical synthesis, a total of 23 g of the two polymers in the desired stoichiometric ratio was added to a reaction vessel. The mixture was heated to 180 °C for 2 hours under a bubbling flow of N_2 that provided mixing, prevented oxidation, and expelled water produced by the condensation reaction. The product was cooled to room temperature and dissolved in deionized water to produce a 33 wt% stock solution. Completion of the reaction was verified by the disappearance of free amine in a Ninhydrin test (Moeser *et al.*, 2002; Curotto and Aros, 1993).

The surface modification protocols, as shown in Figure 3-2, started with O_2 plasma treatment for 30 seconds at 0.15 Torr in a Harrick plasma cleaner (PDC-32G, Harrick Scientific) for PDMS and reduction with 0.4 mol/L of $LiAlH_4$ in ether solution for 30 min for PMMA to generate hydroxyl groups on the surfaces. PDMS and PMMA layers were then immersed in a solution of 1 wt% ethanol solution of *N*-(6-aminohexyl) aminopropyl trimethoxysilane (AHPTS, Gelest, Inc. Morrisville, PA, USA) for 18 hours. After being removed from solution, rinsed with ethanol, and dried under the stream of N_2, AHPTS-coated PDMS and PMMA layers were

assembled into a microbioreactor. In the final step, the PAA-*g*-(PEG-*r*-PPG) copolymer films were assembled on the AHPTS-coated PDMS and PMMA surfaces by flowing an aqueous solution of the polymer (6 wt%, pH 7.4) through the microbioreactor, followed by rinsing with distilled water and drying under N_2.

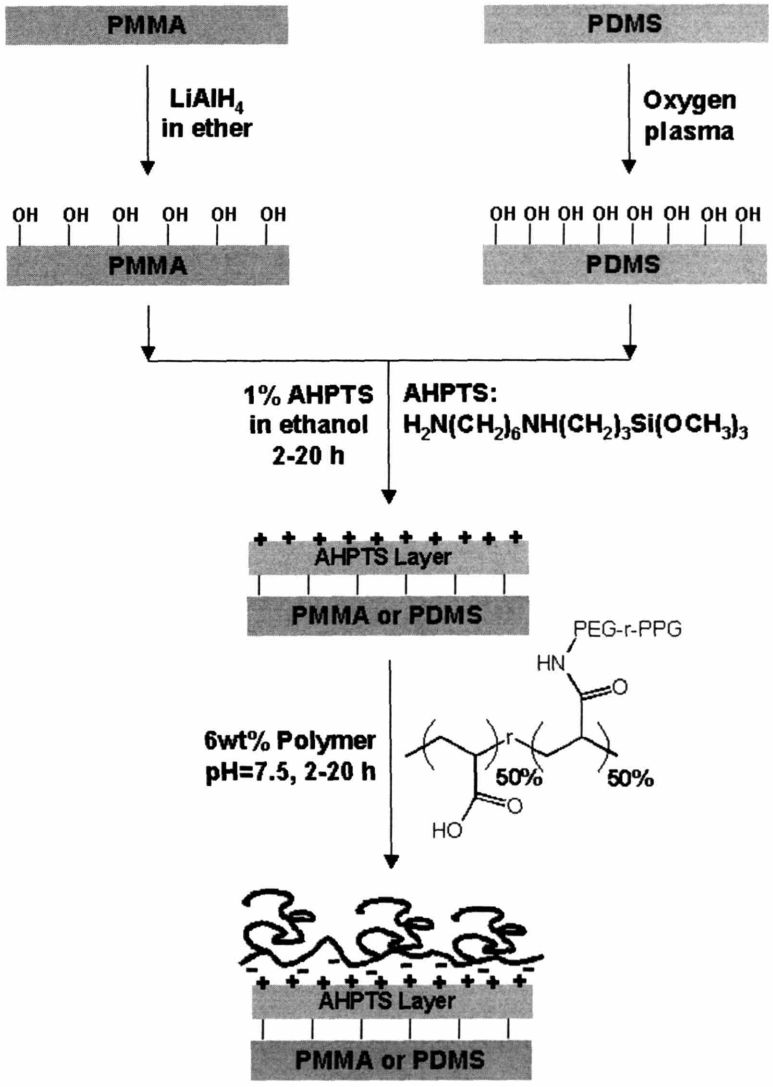

Figure 3-2. Schematic illustration of surface modification of PMMA and PDMS using PAA-*g*-(PEG-*r*-PPG) copolymer films.

3.2.3. Local temperature control in microbioreactor

Small connecting ports (660 μm in diameter) were drilled into the PMMA chip at two inlets

(for inoculation and medium feeding, respectively) and two outlets (for exit to waste and sampling, respectively) of the microbioreactor. Stainless steel tubes (23 gauge, Small Parts, Inc., Miami Lakes, FL, USA) were fixed into these ports by epoxy and connected to polyethylene tubings (1/32" outer diameter, Becton Dickinson, Franklin Lakes, NJ, USA). Fresh medium in a 10 mL glass syringe (Gastight, Becton Dickinson and Company) was pumped and fed to the microbioreactor by a syringe pump (PHD2000, Harvard Apparatus Inc., Holliston, MA, USA). The other side of the reactor was connected to a pressurized water reservoir (at 300 mm H_2O) that served as the effluent collector and also kept the reactor at a constant, positive pressure.

In the microchemostat, medium continuously flows through the microbioreactor, implying that motile bacteria, e. g. *E. coli*, can potentially migrate upstream into the nutrient reservoir. Two steps were taken to eliminate this chemotaxis behavior. First, the cross-section of the inlet microchannels were made small (250 μm × 250μm). For typical flow rates (0.5 μL/min to 2 μL/min) the average linear flow rates (130 ~ 500 μm/s) were significantly higher than the average migration speed of *E. coli* cells (20~80 μm/s; Maeda *et al.*, 1976). Second, we used a local heater (HP-127-1.0-0.8P, TE Technology, Inc., Traverse City, MI, USA) to raise the temperature of the feed line to ~70 °C, which reversed the driving force for chemotaxis, since the cells moved away from the region of high temperature (Maeda *et al.*, 1976; Adler, 1976). The high temperature zone provides an additional advantage of pasteurizing effect on cells. At the exit side of the chemostat, a peltier thermoelectrical cooler (HP-127-1.0-0.8P, TE Technology) reduced the local temperature of a 40 μL effluent reservoir (1.5 mm deep and 6 mm in diameter) to 4 °C to keep cells at low temperature and significantly reduce metabolic activity to facilitate off-line sampling for further analysis. Thin pieces of copper (1 mm in thickness) were placed underneath each section (heater, bioreactor, and cooler) within each region (Figure 3-3) to ensure

constant temperature. The chamber temperature was measured by a thermal couple (TP-2444, TE Technology) and maintained at 37°C by a temperature controller (TC-24-10, TE Technology).

In order to evaluate the thermal design, the temperature distribution in the microbioreactor (Figure 3-3) was simulated by the finite element method using Femlab® software (version 3.1, Comsol, Inc., Burlington, MA, USA). Free convection boundary condition was applied to simulate the heat loss into air; and the thermal energy transferred by the liquid flow in the microchannels was decided to be insignificant thus excluded in the simulation.

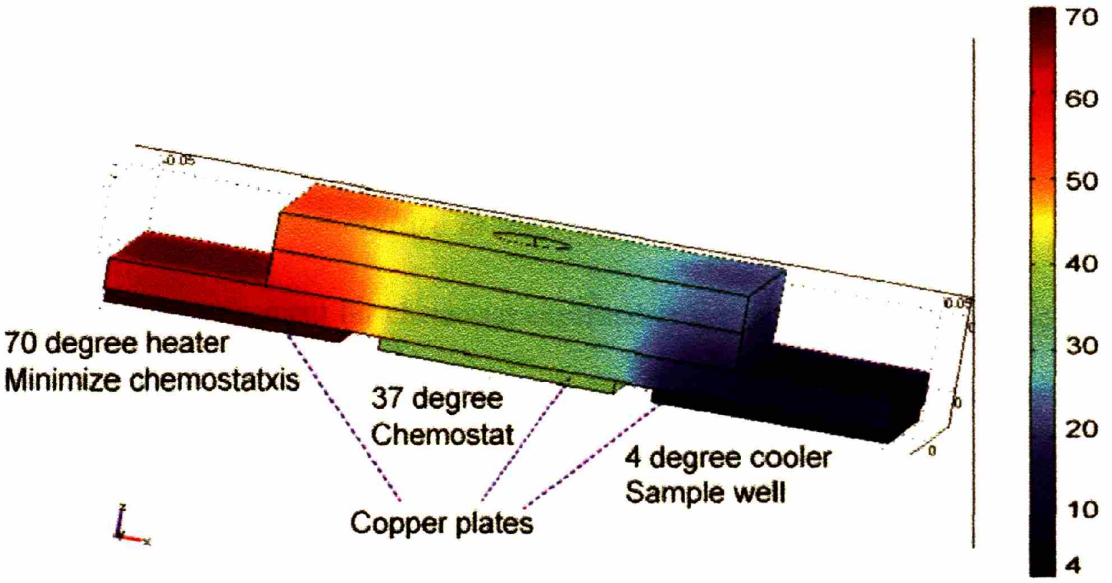

Figure 3-3. Femlab simulation of temperature control and distribution in the microbioreactor. Microbioreactor chamber and microchannels are located at the bottom side of the device, thus temperature disturbances by native convection of air are not significant.

3.2.4. Biological methodology

Two culture media were used for different experiments: LB rich medium containing 8 g/L

glucose, 100 mg/L kanamycin (Sigma-Aldrich), and 0.1 mol/L MES (Sigma-Aldrich), and MOPS minimal medium (Teknova, Inc., Hollister, CA, USA) containing 1 g/L glucose, 100 μmol/L thiamine (Sigma-Aldrich), and 100 mg/L kanamycin.

In order to test for any potential contamination of the medium, the medium in the feeding tubing was collected after each experiment and added to test tubes containing 5 mL of sterile LB medium. Turbidity measurements of the test tubes after incubation at 37 °C were used to detect growth in feed medium. After completion of the culture, *E. coli* cells adhering on the PMMA and PDMS surfaces in the microbioreactor chamber were captured by optical microscope (Nikon TE300). Safranin (Sigma-Aldrich) was used to stain *E. coli* cells on the PMMA surface.

3.3. Results and Discussion

3.3.1. Steady state cell culture in microchemostat

A critical requirement for chemostat experiments is the ability to achieve and sustain steady state conditions. Figure 3-4 shows an example of continuous culture experiments with *E. coli*, starting with an inoculum of concentrated and metabolically active cells in MOPS medium. After inoculation, cells utilized the carbon source, glucose, in the medium and consumed all available oxygen, thus DO level rapidly dropped to zero within a few hours. Correspondingly, the pH level of the culture broth decreased as a result of acetic acid byproduct formation due to fermentation (Han, *et al.*, 1993). OD_{600nm} in the microbioreactor increased at the beginning indicating rapid cell growth, and decreased slowly due to limited glucose in the feeding stream and slow feeding rate of 0.5 μL/min. The recovery of pH was significantly faster because little acid was produced after oxygen starts to recover. After about 80 hours, DO, pH, and OD_{600nm} reached stable levels and steady state conditions in the microchemostat were established.

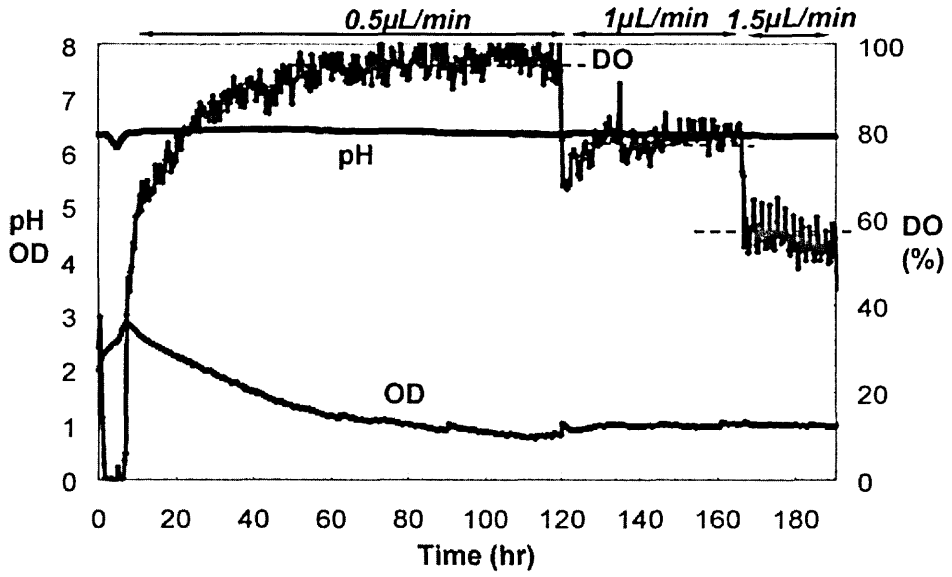

Figure 3-4. Steady states in *E. coli* microchemostats at medium feeding rates of 0.5 μL/min, 1 μL/min, and 1.5 μL/min, respectively.

The net increase rate of bacterial biomass in suspension X is given by the simple mass balance (Herbert *et al.*, 1956):

$$\frac{dX}{dt} = \mu X - DX \tag{3-1}$$

where μ is the specific growth rate and D is the dilution rate. At steady states the growth rate equals the dilution rate:

$$\mu = D = \frac{F}{V} \tag{3-2}$$

With a medium feeding rate F of 1 μL/min and a reactor volume V of 150 μL, the specific cell growth rate μ, which equals the dilution rate D, was 0.4 hr^{-1}. This relatively low growth rate was characterized by a DO level as high as ~ 81%, and the steady state was maintained for ~ 8 turnover times. Correspondingly, the OD_{600nm} level was ~ 1.05 and the pH level was 6.5.

In order to demonstrate that different steady states can be established by varying the dilution

rate, the medium feed rate was increased sequentially from 0.5 μL/min to 1 μL/min and to 1.5 μL/min. Steady state conditions were maintained for at least 8 turnovers at each dilution rate. The observed steady DO levels were 94%, 77%, and 56%, respectively (Figures 3-4 and 3-5). Lower DO levels at higher dilution rates are direct indications of faster growth and metabolism rates. Aerobic metabolism in the microchemostat resulted in relatively stable pH level in the culture medium at different dilution rates due to sufficient oxidative catabolism and the pH buffering from phosphates in the MOPS medium. The measurement for biomass concentration, OD_{600nm} level also remained at a stable level of ~ 1 (biomass concentration of ~ 0.46 g cell dry weight/L), despite the changes of different dilution rates; this is consistent to bioprocess stoichiometry observed in conventional bioreactors when glucose was used as the sole carbon and energy source for *E. coli* aerobic cultivation (Harvey, 1970; Shuler and Kargi, 2001).

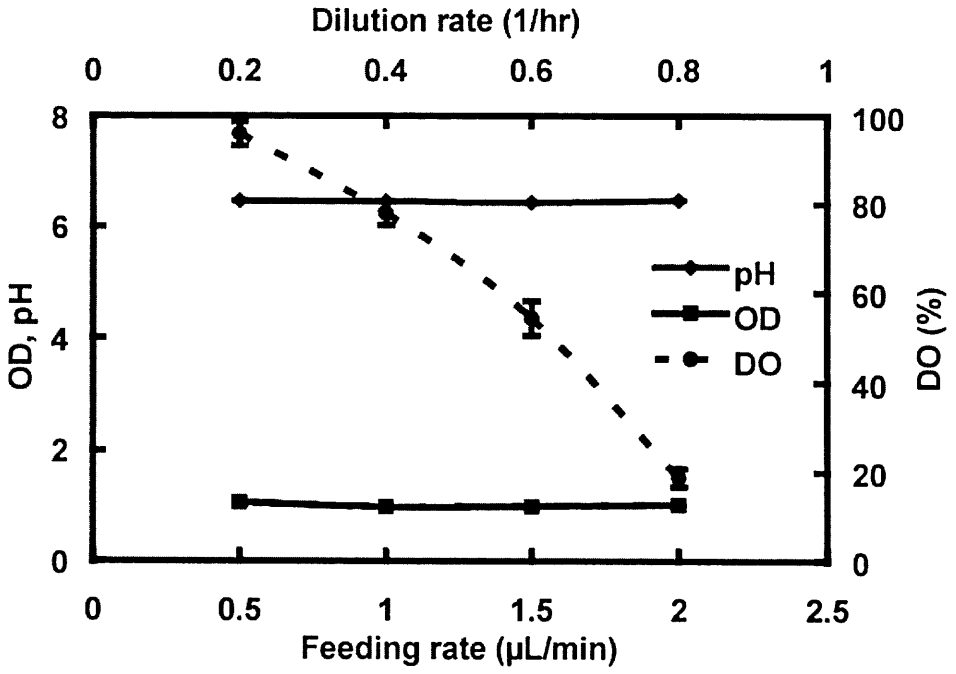

Figure 3-5. Steady state conditions of *E. coli* culture in MOPS medium with the microchemostat operating at different dilution rates.

In a different experiment LB rich medium containing 8g/L glucose was fed into microbioreactor at a flow rate of 2 μL/min. This rich supply of carbon sources was dominant over oxygen mass transfer in the microbioreactor. At the beginning of the reaction cells utilized all available oxygen to build up biomass, as a result, DO level dropped to zero in 2 hours. The pH level of the culture broth decreased at the beginning as a result of the biomass production, and then increased when fed with fresh medium. The steady conditions balance medium feed rate and cell growth rate. OD_{600nm} level increased significantly at the beginning of the experiment and slowly stabilized. At about 20 hours DO, pH, and OD_{600nm} reach stable levels and chemostat conditions are established (Figure 3-6a). In a carbon-rich continuous culture, OD_{600nm} is more sensitive to flow fluctuation due to direct dilution, as indicated by slight fluctuations in OD_{600nm} during the steady state.

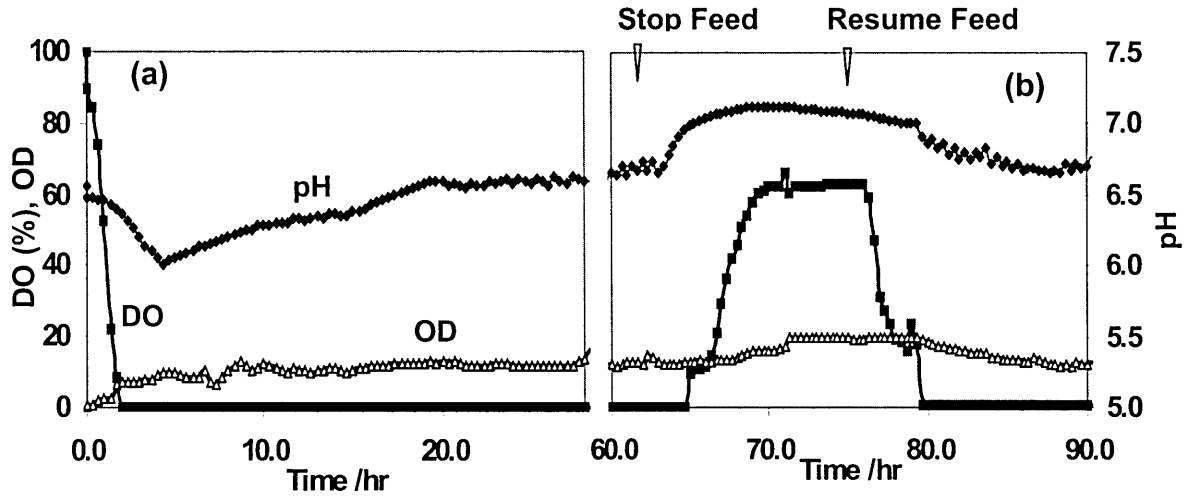

Figure 3-6. Steady state condition of *E. coli* culture obtained in LB medium with the 8 g/L of glucose, 0.1 mol/L MES, and 100 mg/L kanamycin. Medium feeding was set as 1.5 μL/min.

Disturbances in flow rate, temperature, or medium concentration will impact this dynamic balance. Figure 3-6b exemplifies the case when at around 65 hours the medium feeding was

intentionally stopped. At beginning the operation was batch, in which OD_{600nm} increased and then stabilized. In the mean time DO level recovered to ~60%. These trends were reversed when medium feeding was resumed.

Generally only continuous culture with limited nutrient supply is defined as chemostat, thus carbon rich culture is not the major focus for the study here.

3.3.2. Inhibition of back-growth and wall-growth of E. coli

With the implementation of local heating of the medium feeding channel, chemotaxis and back growth of *E. coli* cells were effectively eliminated. Liquid medium upstream to the heated zone was incubated in fresh LB medium, and no cell growth was observed. In contrast, cells were present upstream of the unheated feeding channel.

The extent of cell wall growth in the microbioreactor was also investigated. Figure 3-7 shows the comparison of un-modified and PAA-*g*-(PEG-*r*-PPG)-modified PDMS and PMMA surfaces of the microbioreactor after *E. coli* chemostat cultures. After a prolonged period (7 days) of cell culture, typical surface densities of *E. coli* on the unmodified PMMA and PDMS surfaces were estimated as 4.6×10^6 cells/cm^2 and 2.8×10^6 cells/cm^2, respectively. On the other hand, the PAA-*g*-(PEG-*r*-PPG)-modified PMMA and PDMS surfaces exhibited large reduction in *E. coli* adhesion by 92% (3.9×10^5 cells/cm^2) and 93% (2×10^5 cells/cm^2), respectively, relative to the unmodified PMMA and PDMS surfaces. By implementing the PAA-*g*-(PEG-*r*-PPG)-modified PDMS and PMMA surfaces into the microbioreactor, adhesion and wall growth of *E. coli* in the microbioreactor were effectively reduced. As an estimate, the number ratio of wall attached cells over suspension cells is ~11% for unmodified microbioreactor and ~0.8% for PAA-*g*-(PEG-*r*-PPG) copolymer films-coated microbioreactor.

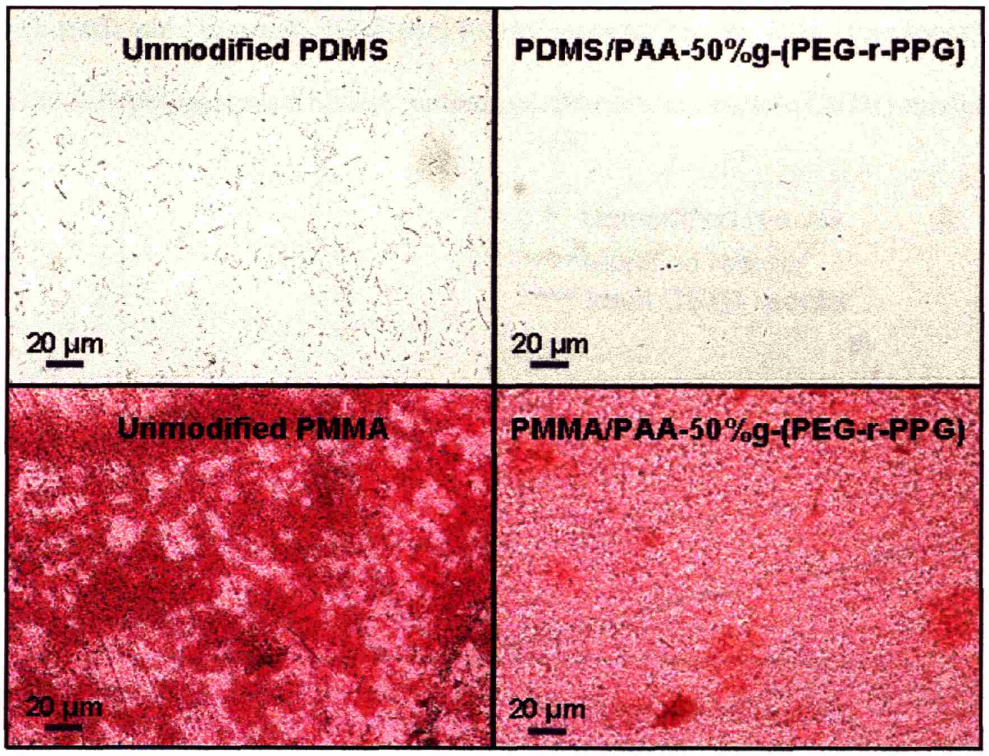

Figure 3-7. Comparison of *E. coli* adhesion and wall growth of *E. coli* cells on PDMS and PMMA surfaces after continuous culture for 7 days in the microbioreactor. Cell adhesion on PAA-*g*-(PEG-*r*-PPG)-modified PDMS and PMMA surfaces were significantly reduced by 93 % and 92 %, respectively, relative to the unmodified surfaces.

The effects of cell wall growth on bioprocess kinetics in the microbioreactor were further investigated by wash-out experiments, as summarized in Figure 3-8. In glucose-limited microchemostat experiments, as a result of a sudden increment in medium feeding rate, most suspension cells were washed out of the microbioreactor and OD_{600nm} in the microbioreactor decreased dramatically in a short period of time (less than 20 minutes, Figure 3-8). However, few attached bacterial cells were washed out by the high medium flow rate; instead these cells were surrounded by large amount of fresh medium and started to reproduce at the maximum growth rate. The resulting rapid recovery in growth was characterized by the steady increases in absorption and decreases in DO (Figure 3-8). This behavior is consistent with reported

phenomena (Larsen and Dimmick, 1964) and kinetic models (Moser, 1988) that incorporate wall growth into the conventional well-mixed continuous stirred tank reactor (CSTR) model.

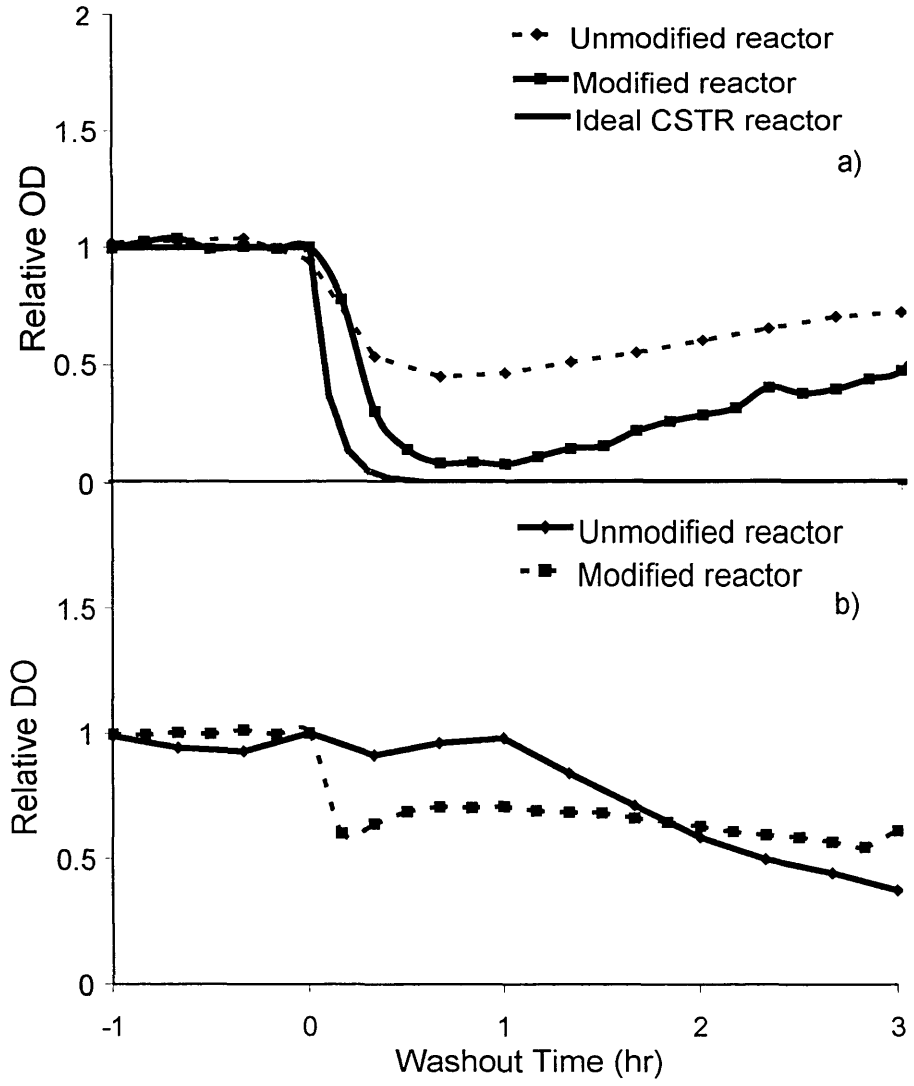

Figure 3-8. Cell wash-out experiments in microchemostat. Wash-out experiments started with an increment of the medium feeding rate to 25 μL/min (turnover time of 12 mins), which was significantly faster than the maximum reproduction rate of *E. coli* cells (doubling time of 23 ~ 27 mins). (a) Comparison of OD_{600nm} after wash-out. Steady OD_{600nm} levels before wash-out in unmodified and modified reactors are 1.00 and 1.01, respectively. (b) Comparison of DO after wash-out. Steady DO levels before wash-out in unmodified and modified reactors are 18% and 82%, respectively.

The minimum OD_{600nm} value observed in the wash-out experiment can be used to characterize the extent of cell wall growth. A comparison of Figure 3-8a and 3-8b revealed that

the significantly less wall growth of *E. coli* is observed in the microbioreactor modified with PAA-*g*-(PEG-*r*-PPG) copolymer films than in the unmodified microbioreactor, well consistent with the cell count data (Figure 3-7). In the microchemostat with modified reactor surfaces, the deviation from the expected behavior was much less significant, indicating that the employed method for surface modification is sufficiently effective to avoid effects of wall growth.

3.4. Conclusions

A 150 μL membrane-aerated and actively mixed microbioreactor was designed and fabricated for continuous culture of microbial cells. With the combination of single-phase, pressure-driven medium feed at slow flow rates, local temperature control in the microbioreactor device, as well as the formation of a PEG-grafted PAA copolymer films on both PMMA and PDMS surfaces, steady state of *E. coli* culture was obtained and sustained in the microchemostat with glucose as the only limiting substrate for growth. Bacterial chemotaxis and back growth were effectively inhibited by local heating in the medium feeding channel. Wall growth of bacterial cells in the microbioreactor was significantly reduced by the cell-resistant surfaces coated with PEG-grafted PAA copolymer films, even after a prolong period of time cell cultivation. As a result, cell growth in microchemostat was dominated by the suspended cells in the microbioreactor chamber.

Time profiles of OD_{600nm}, pH, and DO measurements demonstrated the dynamic balance between cell growth rates and medium feed rates at steady state conditions. Kinetics and cell growth stoichiometry in the microchemostat were consistent with phenomena reported in conventional stirred-tank bioreactors, but with 10^3 times smaller volumes than that of typical bench systems. The ability to control the growth rate of *E. coli* by varying the medium feed rate

implies that the microchemostat could be an effective tool in investigations of cell physiology and metabolic rates. Integration of the microbioreactors into a multiplexed format will enable parallel operations, as for micro batch reactors (Section 5-3; Szita *et al.*, 2005), which should offer a platform towards high throughput systems to be used in analysis of biochemical processes.

Chapter 4. Evaporation Driven Fed-Batch and pH-Controlled Microbioreactor

4.1. Introduction

In the previously chapters microbioreactors were demonstrated for reproducible batch and continuous cultures of microbial cells. This chapter deals with the control of the environmental variables, specifically the control of pH and fed-batch operation.

In batch and fed-batch reactions, the excretion of organic acids byproducts by *E. coli* is a result of fermentative metabolism that occurs in response to insufficient oxygen (Phillips and Johnson, 1961) or the presence of excess carbon substrate due to the Crabtree effect (Doelle *et al.*, 1982; Johnston *et al*, 2002). By-products of *E. coli* anaerobic fermentation, e.g. acetate, succinate, formate, lactate and ethanol (Aristidou *et al.*, 1999) influence culture environments and lead to an undesired decrease of pH, which negatively affects both biomass concentration and cell morphology. Accurate pH control at specific set points does not directly address the issue of fermentative metabolism, but is necessary for exploring optimum culture conditions with higher yield for biomass or products. In glucose-feeding fed-batch processes the formation of growth-inhibiting acidic by-products can be significantly reduced by preventing incomplete substrate oxidation and excess carbon sources in the culture medium (Korz *et al.*, 1995). Feedback control strategies for glucose feeding to maintain the DO value in the bioreactor in a certain range have been applied for high density cell cultures, as reported by Åkesson et al. (2001) and Whiffin *et al.* (2004).

While conventional stirred tank bioreactors add base, acid, and glucose solutions drop-wise, the microbioreactor system feeds solutions by continuous flows. This brings unique challenges

for the design of microbioreactors, such as the chemotaxis of motile cells, as discussed in Chapter Three. Diffusion of chemical solutions in the continuous flow system is also an important issue that must be addressed. Most important of all, feeding of base and/or glucose can greatly increase the liquid volume in a microliter bioreactor.

As a novel solution for these non-conventional challenges, a fed-batch microbioreactor system is developed by using water evaporation as an outlet for liquid feed to maintain a constant volume in the microbioreactor. Designs and experimental results for passive or active feedings controls are compared. A closed-loop pH active control system is built up by applying pressure-driven microflow and commercial microvalves for base and acid feeds. Together with passive replenishment of pure water, the control system successfully maintains the pH value within a physiological range preserving cell metabolism and obtains a higher yield for biomass. In addition, closed-loop glucose feeding system based on DO measurement is also designed and demonstrated for fed-batch applications. This demonstrates the feasibility and potential of DO control and fed-batch processes with high biomass/products yields in the microbioreactor.

4.2. Evaporation Driven Passive Feeding System

As a first step, the batch reactor described in Chapter Two was tested to prove the feasibility of passive feeding driven by water evaporation. The same experimental setup and biological methods were used, except that a concentrated NaOH or glucose solution was connected to the microbioreactor and served to replenish water evaporation. A balance between the contracting pressure of the bulging of PDMS membrane and the static pressure by the elevated liquid reservoir kept the reactor volume constant, as the inflow liquid passively replenished water loss by evaporation through the PDMS membrane. Pellets of desiccant (anhydrous calcium sulfate, W.A. Hammond Drierite, Xenia, Ohio) was placed in the heated aluminum chamber (Figure 2-2)

to remove moisture from the head space above PDMS membrane and increase water evaporation. The evaporation rate for natural convection was determined to be 4 μL/hr by weighting pellets.

4.2.1. Feeding of glucose

Figure 4-1 compares DO curves in the microbioreactor for typical *E. coli* fermentations with 8 g/L glucose and 0.1 mol/L MES medium in LB rich media. For both batch fermentation and experiments with glucose passive feeding, the DO level dropped rapidly to zero during exponential growth phase, when the actively growing cells had a strong demand for oxygen. As the cells entered the stationary phase, the oxygen demand dropped and the diffusion across the PDMS membrane returned the DO level to saturation. Addition of nutrient (glucose) appeared to increase the duration of the growth phase, and delay the recovery of DO to its saturation level. However no significant difference in the final OD values was observed due to the absence of pH control.

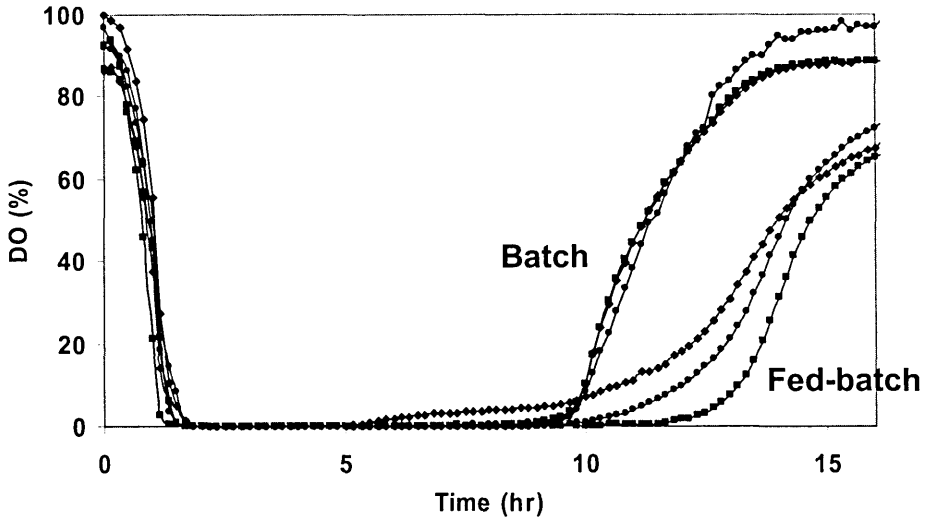

Figure 4-1. DO curves from batch experiments and experiments with passively feeding of glucose (2g/L glucose concentration, 4 μL/hr feeding rate).

4.2.2. Feeding of NaOH solution

The pH curves in Figure 4-2 show a decrease to pH 5.6 in batch fermentation. This pH drop was reduced by feeding a diluted base solution (0.01 mol/L NaOH). When a strong base solution (0.1 mol/L NaOH) was used, pH decreased even less during cell growth phase and strongly increased thereafter. In the particular example, the strong base solution was administered 80 minutes after the fermentation run had started with cell growth in early phase.

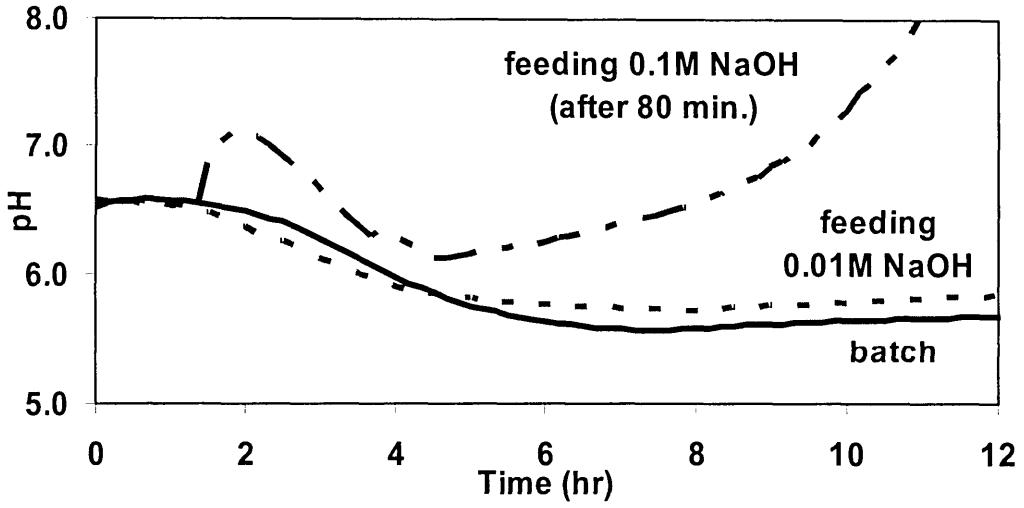

Figure 4-2. Time courses of pH curves from batch experiments and experiments with passively feeding of NaOH solutions (concentration of 0.01 mol/L and 0.1 mol/L, respectively). Feeding of 0.1 mol/L NaOH solution started at 80 min in the experiment.

4.2.3. Limitations of passive feeding

The above results demonstrate that the environmental conditions in microbioreactors can be monitored and manipulated as a fed-batch process. However, passive feeding driven by water evaporation is not a practical solution. Evaporation can control glucose or base feeding but not both. In the case of pH control, the demand for base feeding in bioreactors is complicated by the

feeding load exponentially increasing during fermentation (in pace with biomass accumulation) until nutrients are depleted or hazardous byproducts accumulate to a certain level. Although the water evaporation rate from the microbioreactor can be manipulated by changing air moisture and mixing in the headspace, the dynamic range is not sufficient to meet the demand. Furthermore, the slow-response time of water evaporation makes control difficult. Finally, different experiments could have different feeding rates, and changing the rate for water evaporation is not a solution compatible with parallel operation of multiple bioreactors.

4.3. Active Feeding System

Active delivery of compounds (acid, base, and glucose) and closed-loop control were rendered feasible by applying both passive feeding of water and active feeding of compounds using commercial microvalves. To utilize the water evaporation from the microbioreactor as the water outlet for feed streams, the rate was kept at a constant level, and preferably at the maximum rate. On the inflow side, the sum of the actively fed volumes plus the passively fed volumes equaled to the water evaporation rate. Acid (HCl) and base (NaOH or NH_4OH) can be actively added to the system for pH control, and glucose or other carbon sources can be actively addedd to control dissolve oxygen and cell density in fed-batch cell cultures.

4.3.1. Microbioreactor design

The microbioreactor was fabricated by thermal bonding of two PMMA chips (thickness of 1.6 mm for the top piece and 1 mm for the bottom piece, respectively), as illustrated in Figure 4-3. Thin layer of PDMS membrane and thick PDMS gasket were mechanically assembled by a rigid PMMA cover. The depth of the reactor chamber was 2 mm and the diameter was 10 mm. Together with the bulging of PDMS membrane at 2500 Pa static pressure (pressurized by a water

reservoir elevated at a height of 25 cm), the microbioreactor had a total volume of 230 μL. Five fluidic ports for inoculation, exit for inoculation, water replenishment, and base and acid/glucose feeds connected the reactor with the external setup. Connecting microchannels with cross-section of 250 μm by 250 μm were designed to minimize diffusion of chemicals.

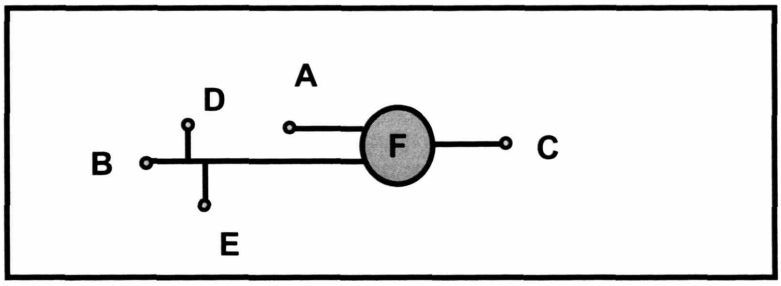

Figure 4-3. Illustration of microbioreactor used for pH control and fed-batch experiments. Port A – inoculation; B - water replenish; C – exit during inoculation and closed after that; D – base feeding; E – acid/glucose feeding. F indicates the reactor chamber. Details in the reactor chamber

The microbioreactor was placed in an aluminum chamber equipped with a 4 mm-diameter fan (12V DC, Radioshack) and maintained at 35°C by water circulation. A cylinder containing compressed dry air (Airgas Inc., MA) connected to the reactor chamber via a flow meter provided a steady air flow at 5 ccm.

4.3.2. Calibration of evaporation rate

The evaporation rate was measured by the change in pH of a buffer solution during passive feeding of base. The Henderson-Hasselbach equation (Skoog, *et al.*, 1992) was rearranged used to back calculate the amount of base added to the system:

$$base_{added}(mol) = C \cdot V \cdot \left(\frac{10^{pH-pK_a}}{10^{pH-pK_a}+1} - \frac{10^{pH_0-pK_a}}{10^{pH_0-pK_a}+1} \right) \qquad (4\text{-}1)$$

This equation is valid for buffer solutions with single pKa. C is the buffer concentration; V is

the total volume of microbioreactor; pH_0 is the initial pH value in the buffer.

In the calibration experiments the microbioreactor was loaded with a buffer solution of known concentration C and pressurized by an elevated base solution reservoir (with known concentration) at 0.25 m height. Evaporation rates at different conditions were calculated by measuring the changes in pH value during experiments. Equation 4-1 was also applied to calculate the base feed rates in the active feeding scheme (described in the next section) when the microvalves were opened at different time durations.

4.3.3. Active feeding

A nitrogen gas cylinder was used to pressurize two liquid reservoirs (made in polycarbonate) to 10 psi and to drive the liquid feeds (Figure 4-4). Liquid was injected into the reservoirs by syringes through 0.45 μm syringe filters (Acrodisc®, Pall Corporation) before experiments. Liquids flowing out of the reservoirs were controlled by micro dispensing valves (INKX0514300A, The Lee Company, Westbrook, CT). PEEK tubing (poly(oxy-1,4-phenyleneoxy-1,4-phenylene-carbonyl-1,4-phenylene), 50 μm inner diameter, 1/16" outer diameter, and 58 cm in total length (Upchurch Scientific, Oak Harbor, WA) were connected to the reservoirs with valves via tubing connectors (TUTC3216930L, The Lee; P702, Upchurch Scientific). These small-diameter tubes were used to increase the flow resistance and limit liquid injection volume to the order of μL per valve opening. Before experiments, plugs of strong acid and base solutions (0.2 mol/L and 1 mol/L, respectively) were injected in tubes on the downstream side of microvalves via four-way manual valves (V-100L, Upchurch Scientific). During experiments working liquids from the liquid reservoirs flowed through the PEEK tubes and microvalves to push acid or base solutions into the microbioreactor. This effectively prevented direct contact of microvalves with corrosive solutions. The same procedure was

applied to glucose feed for the ease of sterilization.

The microvalve was controlled by a spike-and-hold driver circuit (IECX0501350A, The Lee Company) connected with 24 V and 3 V DC power supplies. The valve was opened upon receiving of a 5 V control signal from the computer via the driver circuit. The driver circuit reduced the signal amplitude to 3 V to maintain the microvalve at the open status for certain duration of time, until termination of the control signal triggered closure of the microvalve.

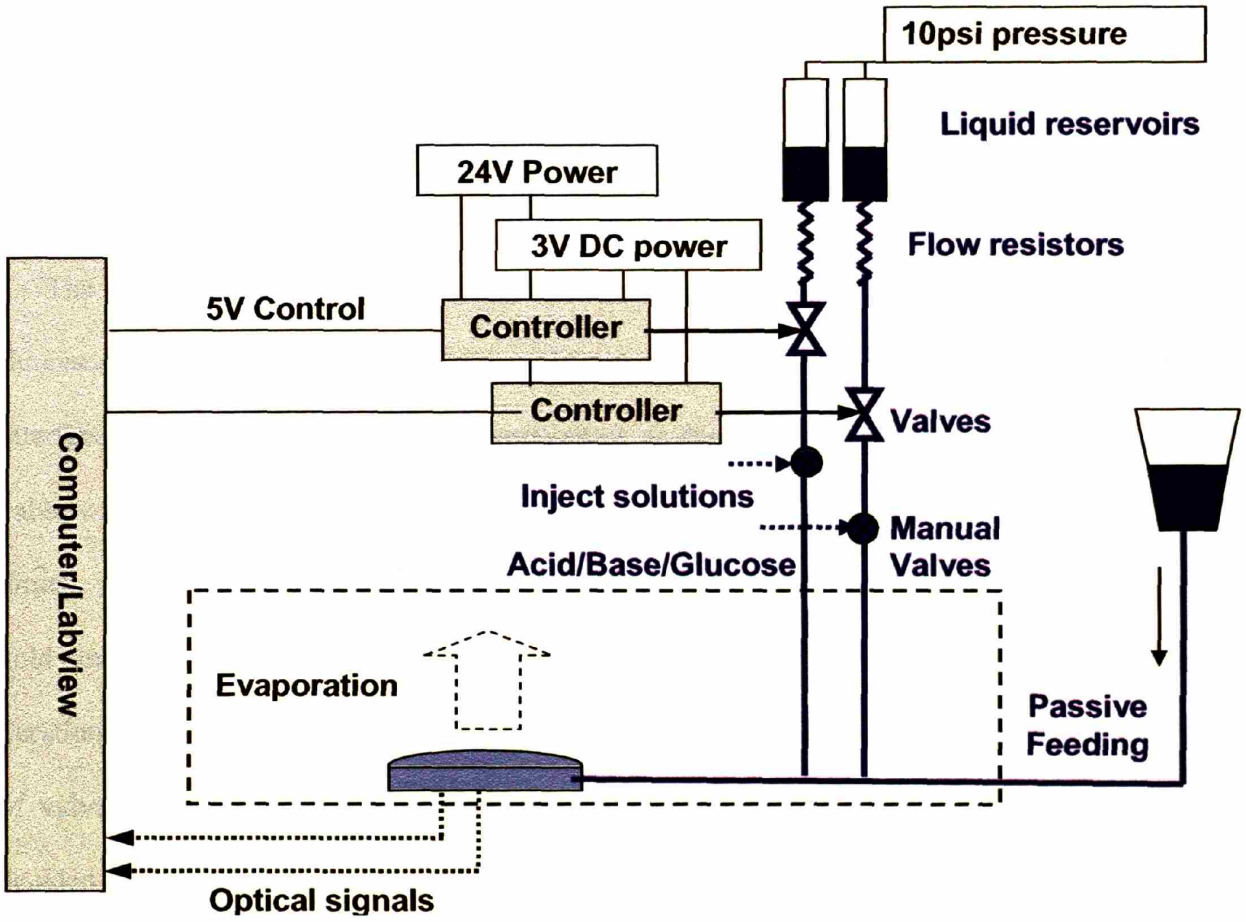

Figure 4-4. A schematic illustration of microbioreactor system and control loops by combining water evaporation with active feed of water from an elevated reservoir and active feed of chemical compounds using microvalves. Dash line indicates the aluminum chamber containing microbioreactor. Thick solid lines indicate fluidic tubes and microchannels, while thin solid lines indicate electronic cables for power and signal transfer. The GPIB interface card and optical measurement setup are not shown in the figure.

A water reservoir was elevated to a height of 0.25 m to passive replenish water into the microbioreactor. This passive feed provided a constant water flow unless the active feed microvalves were opened, in which case the active feeds dominated due to the higher driving pressure. The active feed lines were connected as side branches (Port D and E in Figure 4-3) to the water feed channel (Port B in Figure 4-3), and the time averaged active feeding rates were always less than the evaporation rate of water. In the experiments, the evaporation rate was maximized by applying a fan to improve air mixing inside the aluminum chamber and by flowing dry air at 5 ccm through the chamber.

4.3.4. Closed-loop pH control

The pH measurements in the microbioreactor, represented as a phase shift signal from the fluorescent sensor, were obtained every 5 minutes by a Labview program through a GPIB interface card (PCI-GPIB, National Instruments), as described in Chapter Two. The phase shift value was compared by the Labview program with two setpoints, defining the upper and lower limits. A 5-volt valve opening signal was sent from the GPIB interface card to the spike and hold circuits that operated the microvalves. The base or acid microvalve was opened for specific duration of time if the phase shift reading was out of range as defined by setpoints. The duration of valve opening, which controlled the volume of liquid fed into the microbioreactor, was decided based on the error in phase shift (proportional controller) and the difference from the last phase shift reading (derivative controller). The PD control scheme was used to accurately control pH value between setpoints and to shorten the response time in fluidic microchannels. If the phase shift reading was more than 0.1 pH unit (1^{o} in phase shift) away from the setpoints, the base/acid valves would be opened at a maximal time (15 seconds), which was decided by the total volume of water evaporation (~3.6 μL) from the microbioreactor in 5 minutes. The valve

opening signals and actuation time data used by the spike and hold circuits were saved in a log file together with other information including the pH and DO phase shifts and OD amplitude data during cell cultivation experiments. Integral controller was not applied in these experiments due to the slow response time in the continuous flow control system.

4.3.5. Glucose feeding and closed-loop DO control

For fed-batch experiments, in addition to the closed-loop pH control, glucose solution (with certain concentration) was fed into the microbioreactor as a response to certain DO level in the microbioreactor measured as a phase shift signal from the fluorescent sensor to realize a closed-loop control. The DO phase shift reading from the microbioreactor was compared by the Labview® program with a certain setpoint defining the lower limit for DO value. Once the measured DO value was higher than the setpoint value, a 5-volt valve opening signal was sent to the spike and hold circuit to open the microvalve for glucose feeding.

4.4. Results and Discussion

4.4.1. Evaporation in microbioreactors

Figure 4.5 shows the total evaporated volumes as functions of time. In these experiments evaporation rates were measured by passive feeding and titration of 0.5 mol/L K_2HPO_4 solution by 0.01 mol/L NaOH.

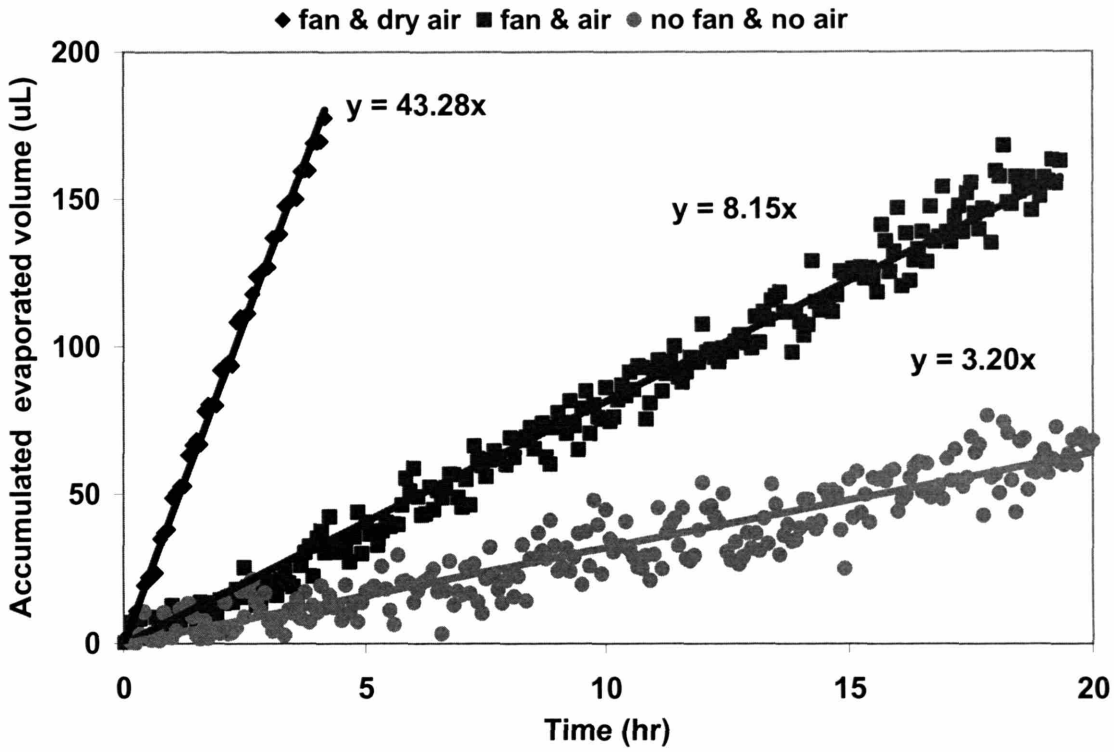

Figure 4-5. Water evaporation rate in the headspace above the microbioreactor for three controlled conditions - mixing with a fan and dry air, mixing with a fan and humid air, or no mixing and no air flow. The fan was located in the reactor chamber. Dry air from a compressed air cylinder was flowing at a rate of 5 ± 1 ccm; humid air (~20% humidity) came from an air pump at a rate of 5 ± 1 ccm. The linear fits are shown corresponding to the points obtained at different air-mixing conditions with R^2 values of 1.00 (fan and dry air flow), 0.98 (fan and air flow), and 0.89 (no fan and no air flow), respectively.

Clear linear correlations with R-square values close to 1 demonstrate stable water evaporation rates at these conditions. As a lower bound when there was no mixing or air flow in the headspace, the evaporation rate was measured as 3.2 μL/hr, which is very close to the value measured by the weight increase of desiccant pellets, as discussed in Chapter Two. The maximum rate of 43 μL/hr was obtained when a fan was used to mix the headspace through which 5 ccm dry air was flowing.

4.4.2. pH control in fermentation experiments

Figure 4-6 shows the experimental results of closed-loop pH control for *E. coli* cell cultivation in rich LB medium containing 8 g/L glucose, 0.1 mol/L MES, and 100 μg/L KAN. In the first 6 hours of the experiment, fermentative metabolism of glucose dominated since glucose is the preferred carbon source for *E. coli*. As a result of acetate production during fermentation, the pH value in the microbioreactor dropped below the first pH setpoint of 6.65, and base feed was actuated. For a few minutes the pH value was 0.1 pH unit (1° in phase shift signal) lower than the setpoint, and the base feed was actuated with the maximal opening time of 15 s.

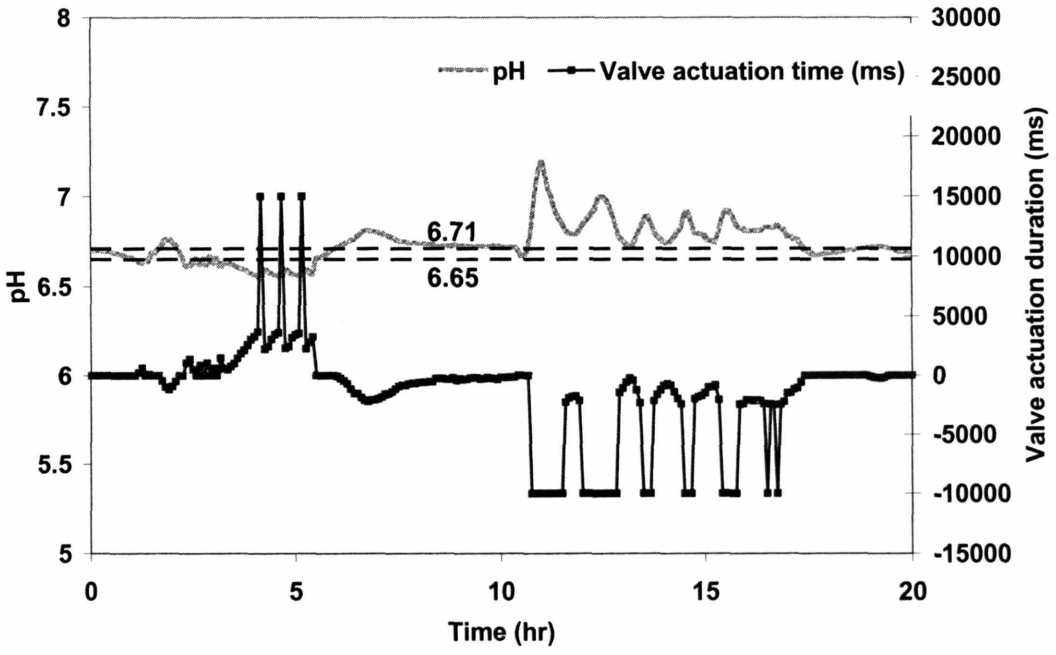

Figure 4-6. pH control in cell cultivation of *E. coli* FB21591 in rich LB medium containing 8g/L glucose, 0.1 mol/L MES, and 100 μg/L KAN. 1 mol/L NaOH and 0.2 mol/L HCl were used, with maximal actuation time durations for base and acid valves set as 15 s and 10 s, respectively. Actual valve actuation durations are shown in the figure, with positive numbers indicating base valve opening times and negative numbers indicating acid valve opening times. Time constants for proportional and derivative controllers were 0.25 and 0.5, respectively.

Once glucose in media had been consumed after 6 hours in fermentation, cells grew by utilizing other carbon sources in LB rich media. In this process cells started to accumulate basic byproducts, as proved by results from control experiments, in which LB was used as the only carbon source for cell culture and final pH of the culture was as high as 8.3. In the pH control experiment, after 6 hours in the culture the acid feed was actuated when pH value was higher than the second setpoint of 6.71. Maximum actuation duration of 10 s for the acid valve was in effect when pH value was higher than 6.83. Overshoots in the base were observed (Figure 4-6) suggesting that the concentration of acid solution used (0.2 mol/L) was insufficient to fully compensate the production of basic byproducts during fermentation. Concentrated acid solution needs be used in further investigation and optimization of pH control. The first and highest overshoot at 11 hours in the experiment was caused by the transition of carbon source from glucose to LB. Further optimization of the control system would reduce these issues.

Despite the difficulties mentioned above, the active feeding and closed-loop control system successfully maintained the pH value in the microbioreactor within a physiological range of 6.68 ± 0.15 for most of the cultivation time. As a result of a healthier culture, higher biomass yield was obtained (OD_{600nm} ~ 8.3) (Figure 4-7).

In the batch microbioreactor without control, the pH decreased significantly owing to fermentation after 2 hours in the experiment. The DO level only recovered after ~ 8 hours in the experiments. As a result the final OD_{600nm} level in the batch culture was as low as ~ 4.1. This value is significantly lower than the results reported in Chapter Two as a larger culture volume was used here with the same PDMS aeration area. With pH control, bacterial cells were metabolically active for a longer period of cultivation time and the DO level recovered after 16 hours of experiment. A higher biomass yield was obtained with a final OD_{600nm} of ~ 8.3.

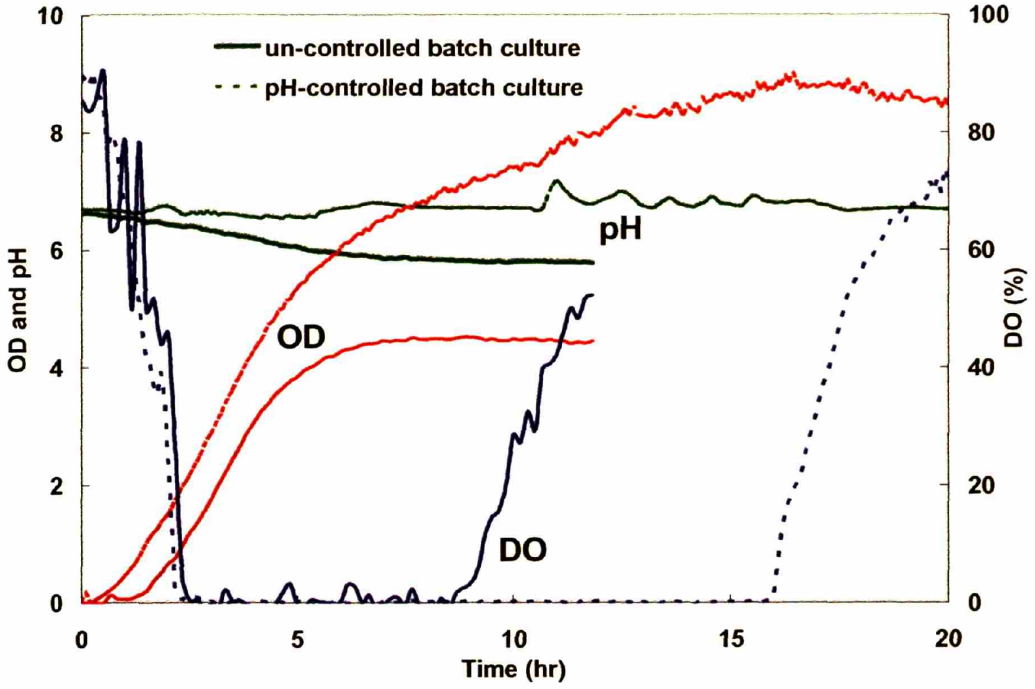

Figure 4-7. Comparison of pH, DO, and OD_{600nm} curves for *E. coli* FB21591 cell cultures with (dash lines) and without (real lines) pH-control. The rich LB medium contained 8 g/L glucose, 0.1 mol/L MES, and KAN.

Similar phenomena were observed in batch cultures with 20 g/L glucose (Figure 4-8). Without pH control, the growth kinetics in culture media with 20 g/L glucose were very similar to those with 8 g/L glucose, except the DO level started to recover after 12 hours in the experiment. In this set of experiments *E. coli*, a fast growing bacteria, was cultivated in the rich medium with very rich supply of glucose but limited supply of oxygen. These fermentative cell cultivation conditions were intentionally selected to make the needs for active feeding very demanding. As shown in the figure, pH control by using 1 mol/L NaOH did not fully compensate acetate production during the fermentation stage and a higher concentration of base and an optimized control algorithm would be required. Still, the pH value during the time course of fermentation was controlled within the physiological range to maintain active cell metabolism. As a result the DO level did not recover during 30 hours of cultivation time and the final OD_{600nm}

in the microbioreactor reached 8.64, which was significantly higher than that of un-controlled experiments (~ 4.1).

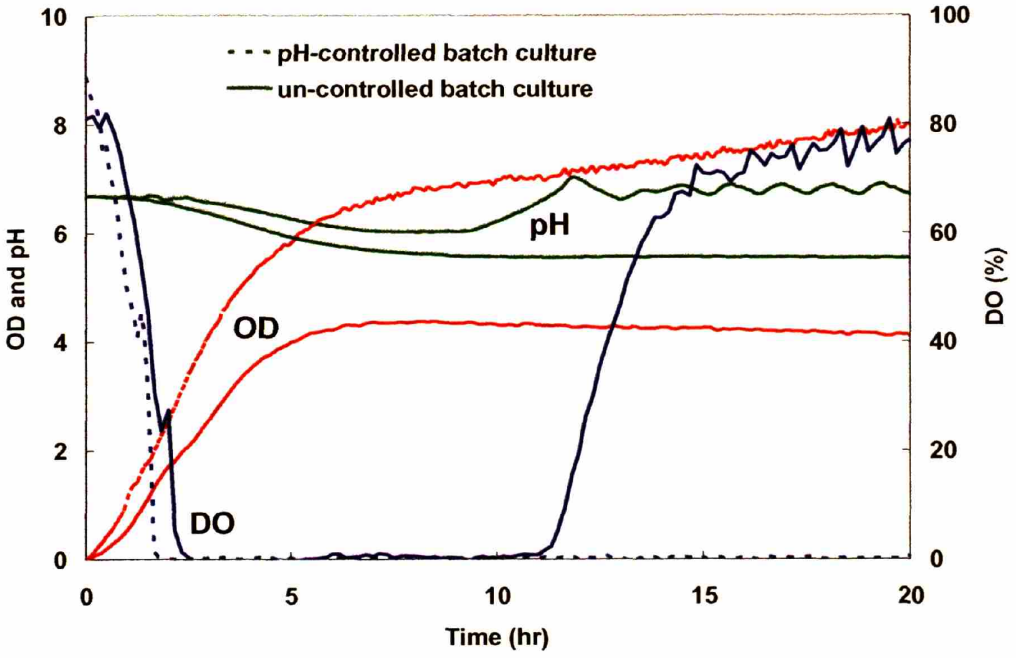

Figure 4-8. Comparison of pH, DO, and OD_{600nm} curves for *E. coli* FB21591 cell cultures with (dash lines) and without (real lines) pH-control. The rich LB medium contained 20 g/L glucose, 0.1 mol/L MES, and KAN.

4.4.3. Feedback glucose feeding

A fed-batch experiment, started with standard inoculum of *E. coli* FB21591 in LB medium containing 2 g/L glucose and 0.1 mol/L MES, is shown in Figure 4-9. Delivery of 40 g/L glucose and 1 mol/L NaOH solutions were feed-back controlled based on DO and pH readings, respectively. The same PI control strategy discussed earlier was applied for pH control. For glucose addition, when the DO value in the microbioreactor, represented by a phase shift reading, became higher than the 40% saturation setpoint, a constant volume of 1.34 µL glucose

solution was fed into the microbioreactor.

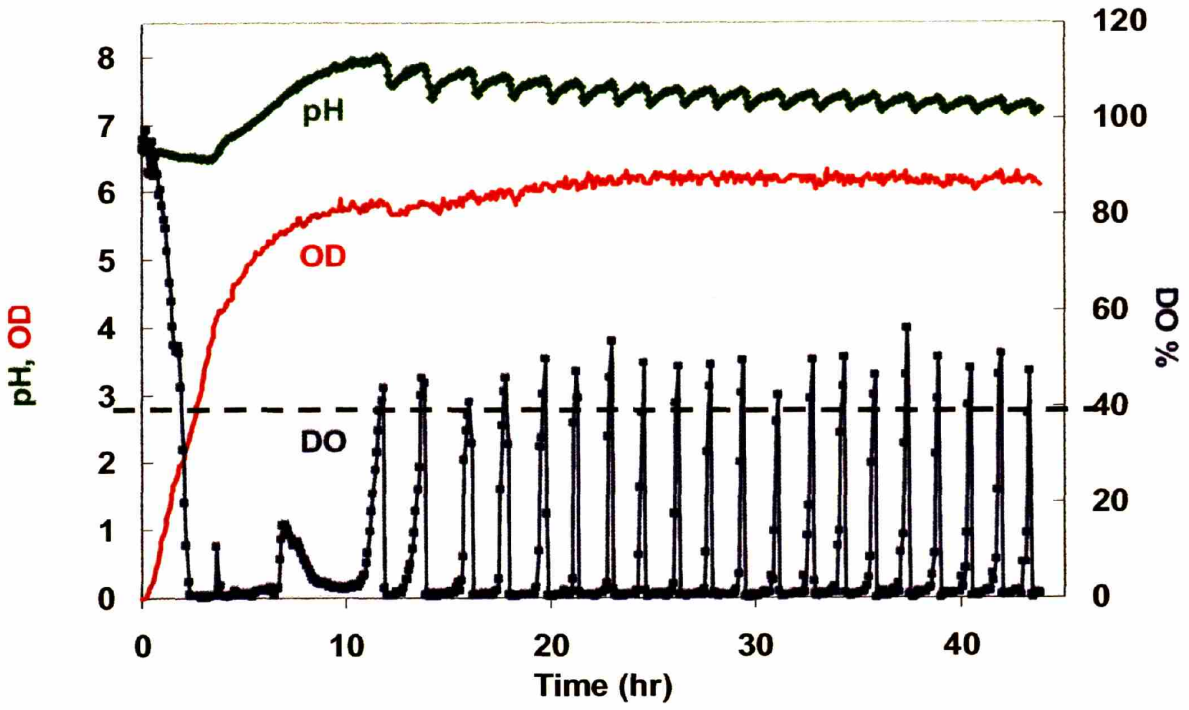

Figure 4-9. Comparison of pH, DO, and OD_{600nm} curves for *E. coli* FB21591 cell cultures with (dash lines) and without (real lines) pH-control. The rich LB medium contained 20 g/L glucose, 0.1 mol/L MES, and KAN.

In the first two hours of experiment, DO decreased and reached zero level due to a strong oxygen demand by fast cell reproduction, as indicated by the rapid increase in OD. This fermentation process lasted about 10 hours before DO recovered. In the mean time pH value decreased at fist due to the fermentation using glucose as the carbon source, and then increased to the basic direction as a result of cell growth utilizing LB medium, as discussed in Section 4-4-2. The DO reading recovered when carbon sources in the culture medium was depleted after 10 hours, and quickly dropped to zero after the glucose-feeding valve was actuated.

This periodically recurring phenomenon indicated that too much glucose was fed into the microbioreactor in every cycle (~ 2 hours) in order to avoid fermentative metabolism; acid feeding will be necessary to maintain pH within physiological limits. Nonetheless, this

experiment demonstrated the potential to control DO level within certain range to obtain a healthy and well-controlled cell physiology, high bioproduct yields, and high density cell culture.

4.5. Conclusion

Design and fabrication of a fed-batch system was proposed for pH control and glucose feeding in the μL-volume microbioreactor. Water evaporation through the PDMS cover membrane was designed to serve as the water outlet for the microbioreactor and maintained the culture volume constant. Titration of pH buffer solution in the microbioreactor by base solution was used to characterize the rate and stability of water evaporation. Fresh solutions such as base and carbon sources were allowed to enter the microbioreactor while microbial cells and solutes were kept in the culture to realize an effective fed-batch process.

Applications of passive and active feeding were discussed, and a combination scheme was designed in the microbioreactor system. Active addition of base, acid, and glucose solutions was driven by pressure and controlled by commercially-available microvalves. A Labview program in the computer measured the pH values during fermentation and manipulated the opening time for microvalves as a proportional-derivative controller. DO value was used for the feedback control of glucose feeding using a microvalve.

Closed-loop pH control was demonstrated for *E. coli* cell cultivation in rich media. This was a challenging system due to the large demand for base feed during anaerobic fermentation, and the demand for acid feed due to the secondary metabolism when LB was used as an alternative carbon source for growth. The control system successfully maintained the pH value in the microbioreactor within a certain physiological region, in spite of these challenges. Significant extensions of cell growth, as indicated by longer recovery time in dissolved oxygen levels and significant improvements in biomass yield (reflected by higher final OD_{600nm} values), were

observed in pH-controlled batch culture experiments with the same initial glucose concentrations of 8 g/L and 20 g/L. Furthermore, feed-back control of glucose feeding based on DO level in cell culture demonstrated the feasibility and potential of using fed-batch process to realize high density cell culture.

These results demonstrate the concept of using water evaporation and active feeding for control of fed-batch microbioreactors. Cell cultivation conditions during the time course of experiments are not only monitored as in batch operations but also effectively manipulated as in continuous culture and fed-batch operations. These features could make the microbioreactor technology a promising approach for high-throughput bioprocess developments.

Chapter 5. Integrated Microbioreactor Cassette and Multiplexed System

5.1. Introduction

In the previous chapters, single disposable microbioreactors with integrated sensors were demonstrated for batch, fed-batch, continuous culture operations, and they greatly simplified the effort per fermentation experiments. Based on these investigations, parallel operation of multiple microbioreactors need be developed to make the technology viable for high-throughput data acquisition. This requires a platform on which disposable microbioreactors can be set-up rapidly and with which real time information in fermentation processes can be obtained. In addition, the microbial cultivation data in multiple reactors must be reproducible.

As a collaboration effort with Gerardo Perozziello,[1] the work presented in Section 5-2 focuses on the integration of bioreactors into a reactor cassette with fluidic and optical coupling interfaces to external instruments. The cassette design, made possible by a specifically designed multilayer plastic thermal-bonding procedure, enables scaling out to a multiplexed, high-throughput batch/fed-batch/continuous cell culture platform. This unit automatically aligns with external fluidic and optical components and addresses the need for rapid set-up and ease of operation of bioreactors for high-throughput bioprocessing.

For the external optical measurement setup, a prototype multiplex system is developed and presented in Section 5-3 in collaboration with Dr. Nicolas Szita, a postdoctoral associate. In this

---

[1] Gerardo Perozziello was a visiting PhD student from Department of Micro and Nanotechnology, Technical University of Denmark, DTU Building 345 East, DK-2800 Kgs.Lyngby, Denmark. His thesis supervisor was Prof. Oliver Geschke*

prototype we used a single macroscopic interface for measurements in multiple parallel microbioreactors. Reproducibility was demonstrated by experimental results from the operation of four batch microbioreactors. Section 5-4 presents design of a prototype of multiplexed system with higher degree of integration.

5.2. Integrated Microbioreactor Cassette

5.2.1. Design and fabrication of microbioreactor cassette

Microbioreactors for batch, fed-batch, and continuous culture operations were discussed in previous chapters. Efforts were focused on features and functionalities specific for different applications, especially those of microfluidics controls. The task was to unify the systems to allow operation flexibility. Furthermore, the microbioreactor cassettes should be disposable and separated from external housing instruments (fluidics, optics, electronics, and computer) thus greatly reducing the mechanical complexity in setting up and running multiple microbioreactors. Devices described in previous chapters were assembled manually by mechanical compression using bolts and nuts. Besides being a slow step in the setup procedures, alignments of optical sensors also affected reproducibility in measurements. The setup procedure for fluidic connections was also slow. All these issues needed to be addressed in the new design.

Here we describe our efforts in the packaging of a microbioreactor system by integration of microfluidic connectors and optical plugs. The microbioreactor consisted of five thermally-bonded PMMA layers (Figure 5-1). Precise thermal bonding of PMMA with different glass transition (TG) temperatures was performed in two steps: three bottom layers (layers C, D, and E, material purchased from Goodfellow Corp.) were bonded at a temperature of 140°C and then bonded with top two layers (purchased from MSC Industrial Supply, Co.) at a lower temperature

of 120°C. Thermal bonding was performed using a home-made mechanical press, described in detail in Appendix A.

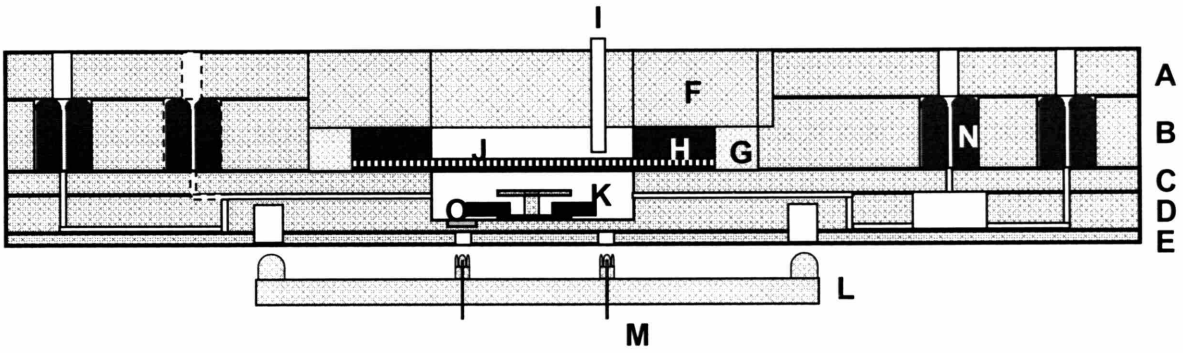

Figure 5-1. Cross-section of an integrated microbioreactor cassette. A-E, thermally bonded PMMA layers; F- PMMA cork; G- PDMS gasket and aeration membrane; H- Silastic O-ring; I- optical fiber fixed by F; J- grid for holding the PDMS membrane; K- magnetic mixer; L- PDMS optical plugs; M- optical fibers and micro-lens; N- fluidic interconnections; O- pH and DO fluorescent sensors.

Pictures of individual parts and the assembled device are shown in Figure 5-2 and 5-3, respectively. In the center of the device, a round reactor chamber was fabricated with a built-in magnetic spin bar mixer (K) for mixing of fermentation medium. The geometry of the reactor chamber was the same as described in Chapter Three. A thin layer of spin-coated PDMS (G) covered the reactor chamber and served as the aeration membrane. This thin PDMS layer was held by a thicker PDMS layer (shape of an O-ring with an inner diameter of 20 mm, an outer diameter of 25 mm, and a thickness of 3 mm; the O-ring was fabricated by a negative mold in polycarbonate) to facilitate the assembly of the device, and covered by a stainless steel grid structure (J) to prevent bulging. A PMMA cork (F) with an outer diameter slightly larger (13 μm larger in diameter) than the inner diameter of PMMA housing frame (machined in A and B) was pressed down on the PDMS (G) and an Silastic O-ring (part H, inner diameter of 10mm, outer diameter of 20 mm, and height of 3 mm) for sealing. The O-ring was molded out of Sylastic®

RTV silicone elastomer (Dow Corning) by a polycarbonate negative mold. A small hole in the cork also aligns an optical fiber (I) for the OD transmission measurement. Two recesses (O) at the bottom of the bioreactor chamber accommodated pH and DO fluorescence lifetime sensors. Recesses beneath these sensors in the bottom PMMA layer accommodate and passively align optical connectors (M) connecting the microbioreactor system to external instruments.

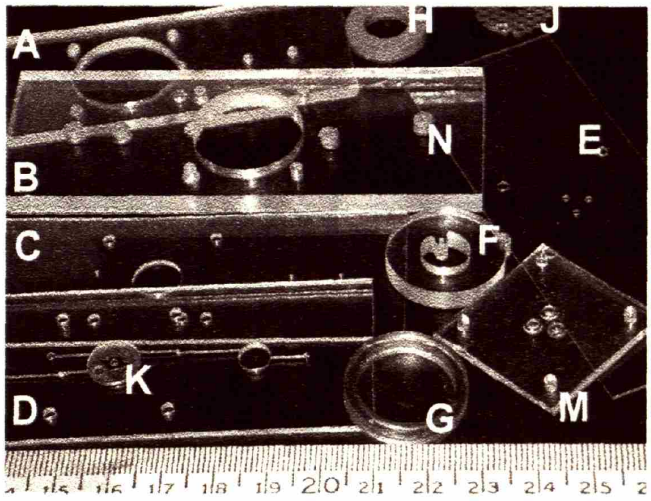

Figure 5-2. Overview of individual parts - letters refer to Figure 5-1.

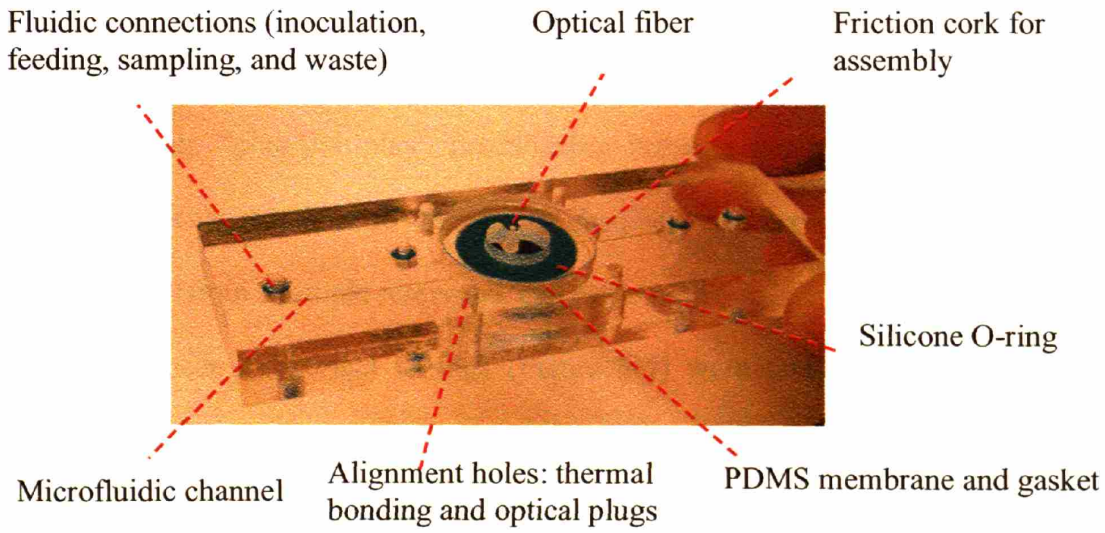

Figure 5-3. Top view photograph of assembled and bonded microbioreactor "cassette".

The above design allowed the reactor cassette to be cleaned and reused by replacing PDMS membranes after experiments. An alternative prototype was proposed to make the whole cassette disposable and would be applied when cassettes become large-scale manufactured. As shown in Figure 5-4, the PDMS membrane was permanently fixed in PMMA layers after thermal bonding and the grid structure was molded in PMMA layer B.

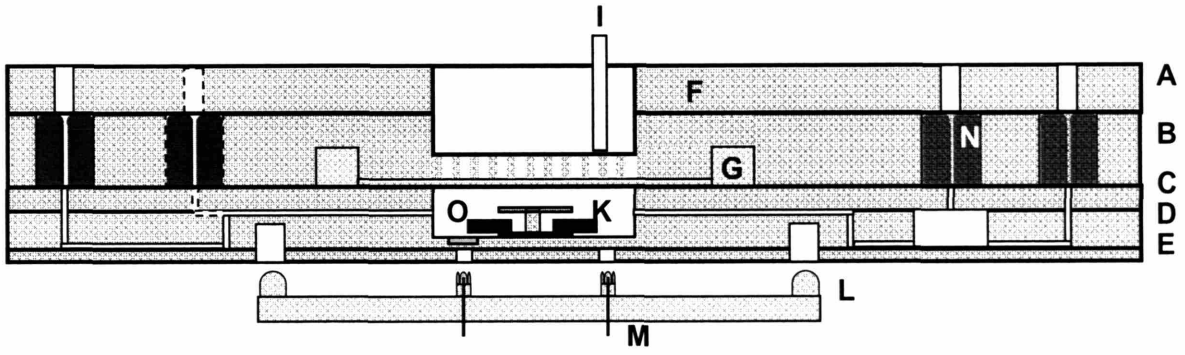

Figure 5-4. Cross-section of disposable cassette - letters refer to Figure 5-1.

5.2.2. "Plug-in-n-play" fluidic interface

The fluidic interface between a microbioreactor and external fluidic units was composed of custom-made elastomer O-rings integrated in the PMMA device (Figure 5-1). They allowed aseptic self-sealing, "plug-in-n-play" functionality between the external tubes with internal microfluidic channels that lead to the reactor chamber, and served for inoculation, reagent-feeding, sampling (from a sample reservoir), and waste outlet.

The custom-made cylindrical O-rings (Figure 5-5) were fabricated from Sylastic® RTV silicone elastomer (Dow Corning). The elastomer rings were cast from stainless steel molds reproducing the negative shape of the rings, having an outer diameter of 4.2 mm and an inner diameter of 0.2 mm and a depth of 4.6 mm. The stainless steel molds were CNC-machined at high rotation speed of 8000 rpm by a 2 mm-diameter ball-head endmill (MSC Industrial Supply)

at high rotation speed and electropolished to obtain a smooth surface.

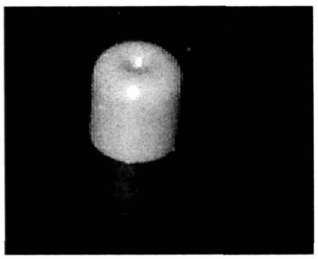

Figure 5-5. Sylastic® O-ring serving as fluidic connector.

Elastomer O-rings were cured at room temperature for more than 12 hours to obtain a Young modulus (E) of 4.5 MPa (Perozziello *et al.*, 2006). They were then embedded into housings machined in a thick PMMA layer and were fixed by a cover PMMA layer when the two layers were thermally bonded (cf. Figure 5-1; Appendix A). The housings for the O-rings have slightly smaller diameter of 4.1 mm and smaller depth of 4.45 mm, so that after O-rings were embedded in the housings they were compressed by pressure, and the center holes in the O-rings were sealed. 1.5 mm-diameter through-holes were drilled in the covering PMMA layer corresponding to the positions of center holes in O-rings to allow access. When stainless tubes (1.2 cm long, 23 gauges, Small Parts, Inc.) connecting with external fluidic tubing were plugged into the center hole of the O-rings, the elastomer expanded and accommodated the tubes to make a fluidic connection. This process is reversible and the sealing can withhold pressure up to 90 psi without leakage (Perozziello, *et al.,* 2004).

5.2.3. Microlens as optical interface

A similar "plug-in-n-play" strategy was also applied to the optical interface between external measurement setup and disposable florescence sensors inside of the microbioreactor cassette. Integrated microlens and optical connectors (Figure 5-6) were molded out of PDMS (Sylgard 184, Dow Corning) in an aluminum mold fabricated by conventional milling using a 2 mm-

diameter ball-head endmill (MSC Industrial Supply, Co.) and mechanically polished using a shaft grider kit (Dremel, MSC) and polishing paste (Novus Plastic Polish, MSC).

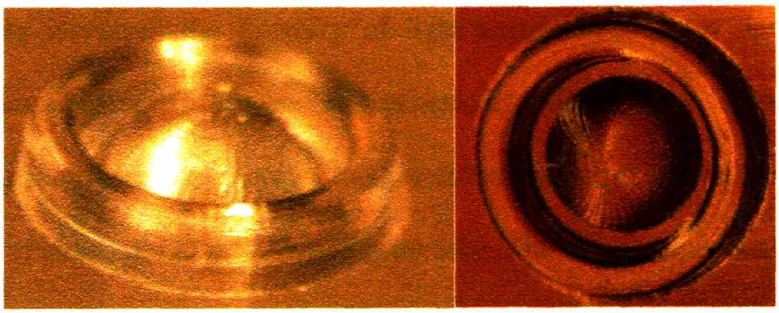

Figure 5-6. Side view and top view of microlens and alignment ring around the microlens.

The aluminum mold ensured the replication of the negative shape of the microlens and four pillars to fix the optical plug for packaging. The negative of the lenses had a diameter of 2 mm and the plug had an overall height of 10 mm. The upper part was composed of 5 mm long aluminum columns that were aligned concentrically to the lenses as guide channels for optical fibers. Figure 5-7 shows an optical plug integrated with three PDMS microlens for on-line measurements of OD (center fiber), pH and DO (double fibers fibers at the two side locations).

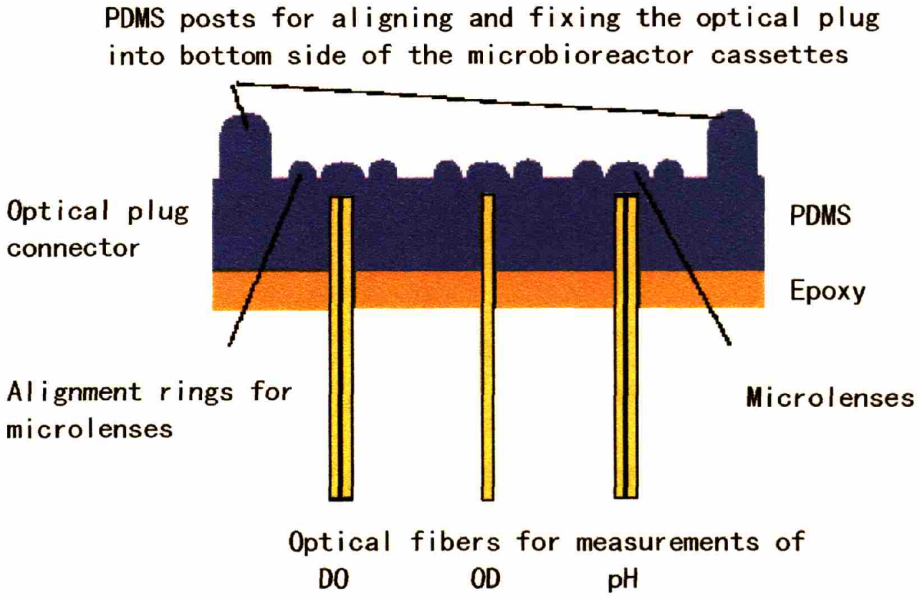

Figure 5-7. Cross-section view three microlenses assembled with optical fibers.

With optical fibers fixed in the middle of the optical plugs and a smooth, hemispherical outer surface shape on the other end facing towards the optical sensors in the bioreactor, the optical plugs effectively increased the intensity of light transmission from optical fibers to optical sensors thus increasing signal-to-noise ratio of optical measurements. A two dimensional model was developed using ray optics theory. Images of the light distribution showed good agreement with the model (Perozziello *et al.*, 2006; Figure 5-8). The measurements show a maximum light intensity from the plugs, which was 50% higher than from the cleaved optical fibers and significantly more focused with respect to lateral distribution of light. Even in presence of slight misalignments away from the center, the focusing effect by the microlenses made coupling of light more efficient comparing to butt-end coupling techniques,. Further details on the fabrication and characterization of the microlenses can be found in Perozziello *et al.* (2006).

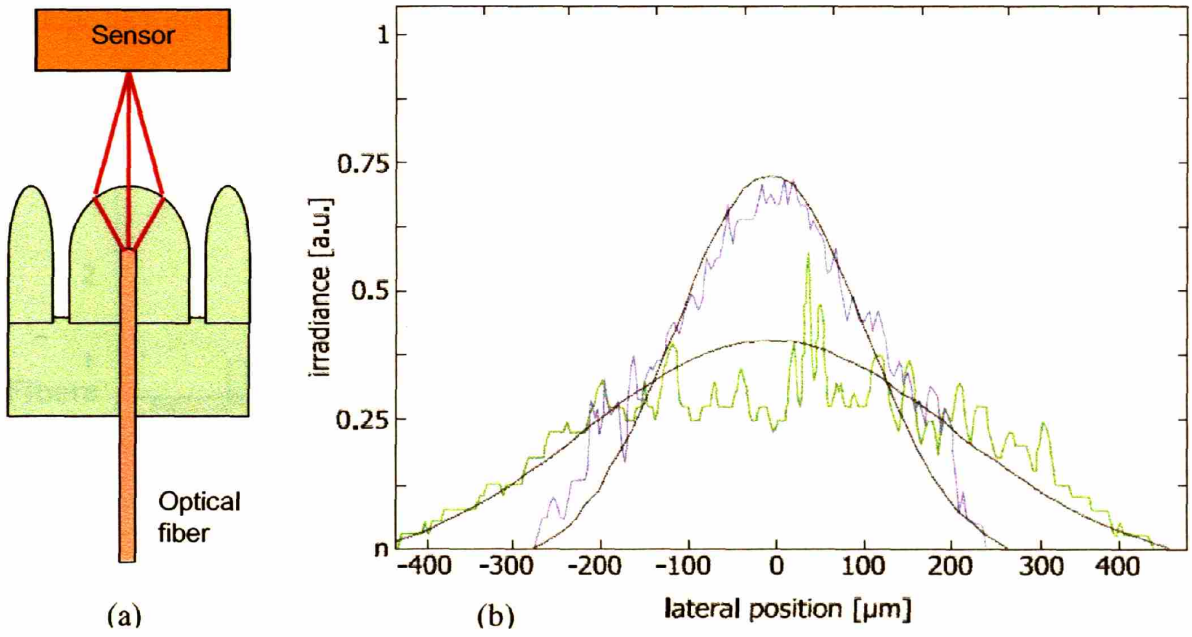

Figure 5-8. (a) Illustration of focusing effect by PDMS microlens (b) Intensity of the light versus lateral distribution of a cleaved fiber (green line) and optical microlens (blue line). Calculation values are obtained by the two-dimensional model, with details described by Perozziello *et al.* (2006).

In practice the focusing effect depended on the axial and radial positions of optical fibers

fixed in the back side of microlenses. As shown in Figure 5-7, for pH or DO measurements two optical fibers (plastics fibers were 1 mm and 0.6 mm in diameter, BFL 37-1000 from Thorlabs, Inc., and FVA500550590 from Polymicro Technology LLC, Phoenix, AZ, respectively.) were aligned parallel in each microlens as analogs to the bifurcated optical fibers presented in Chapter Two. One fiber (1 mm in diameter, Thorlabs) was fixed in the center of plug for the OD reading. Calibration and optimization of positions for pH and DO reading aimed to maximize the intensity of light from the fluorescent sensor to improve the signal-to-noise ratio of measurements. For the OD measurement the objective was to obtain parallel transmission light and improved reception on the other side of the device. Different focal points were designed in the optical plug (Figure 5-9) for the different measurements. The refractive indexes for PDMS, air, PMMA, and water were 1.43 (Horvath *et al.*, 2003), 1.49 (Defaude *et al.*, 2005), and 1.33 (Wikipedia Coordination), respectively. A layer of epoxy was used to permanently fix the fibers in perpendicular position and align with external mechanical housing.

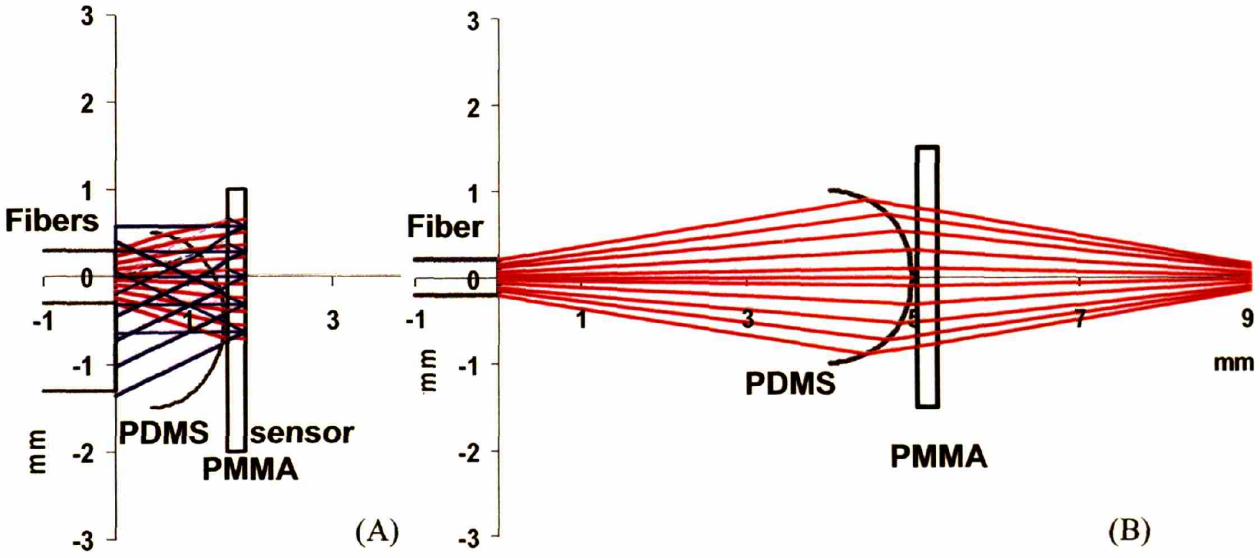

Figure 5-9. Calculated focusing effects by PDMS microlens on pH/DO measurements (a) and OD reading (b).

In addition, the alignment ring around the microlens (cf. Figure 5-6) was fabricated with a size comparable to the size of the cavity beneath the microbioreactor (1.6 mm from the center, 1 mm high and 0.4 mm wide). The mold was fabricated using a 0.4 mm-diameter ball-head endmill, TR-2-0130-BN, Performance Micro Tool, Janesville, WI.). The alignment ring helped positioning of optical fibers to optical sensors and made setup procedures significantly easier and faster (Figures 5-8 and 5-10).

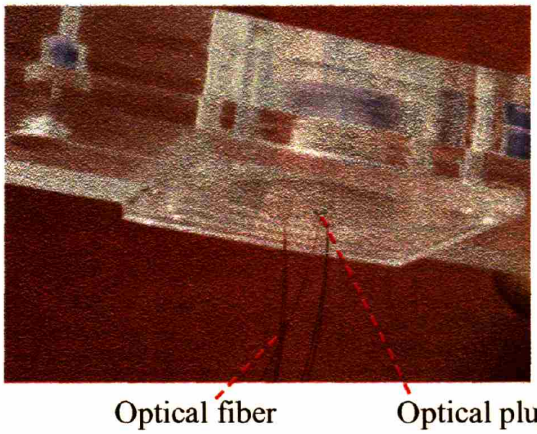

Figure 5-10. Bottom view photograph of optical microlenses assembled with optical fiber housing. Fibers for demonstration here were 0.25 mm in diameter. Epoxy and external mechanical support are not shown.

5.3. Step Motor-Controlled Multiplexed System

A prototype multiplexed microbioreactor system for parallel operation of four microbial fermentations is described in this section to demonstrate the concept and potential of high-throughput bioprocessing. The microbioreactor devices described in Chapter Two were held on an aluminum platform, which rested on support rails mounted to the sidewalls of an aluminum enclosure (Figure 5-11). Pins in the support rail maintained proper alignment for optical measurements. An optical fiber extension (part I shown in Figure 5-1) served as waveguide for OD measurements for the microbioreactor.

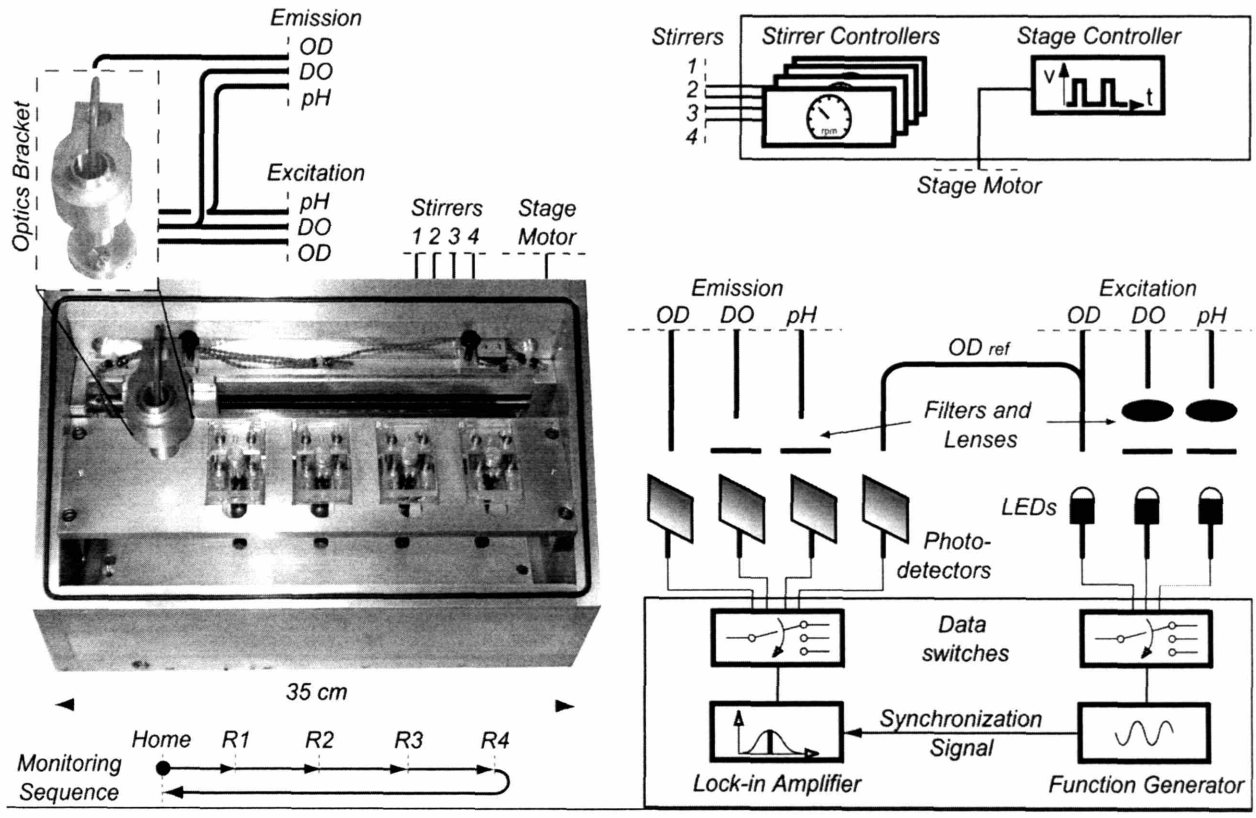

Figure 5-11. Photograph of the multiplexed microbioreactor system embedded in a schematic of the instrumentation. The multiplexed system is loaded with four stirred batch bioreactor. The optics bracket (detailed photographic view) contains the optical fibers for monitoring of OD_{600}, DO, and pH, as described in Chapter Two. The enclosure of the multiplexed system was sealed with a top lid (not shown).

The aluminum stage was attached to the rear wall of the enclosure and the slider motion was controlled with a stepper motor (Type 23T1, Velmex) which permitted an axial step resolution of 5 μm for the optical bracket. Outboard limit switches (P/N 3-8515, Velmex) prevented over-travel of the bracket. The optics bracket scanned over the microbioreactors in stop-and-go sequences executed by computer control algorithms. The process parameters were measured and recorded for each reactor using lifetime fluorescence and absorbance methods. In a typical monitoring sequence, the optical bracket would sequentially read all four microbioreactors and then return to its initial home position, waiting for the start of the next cycle.

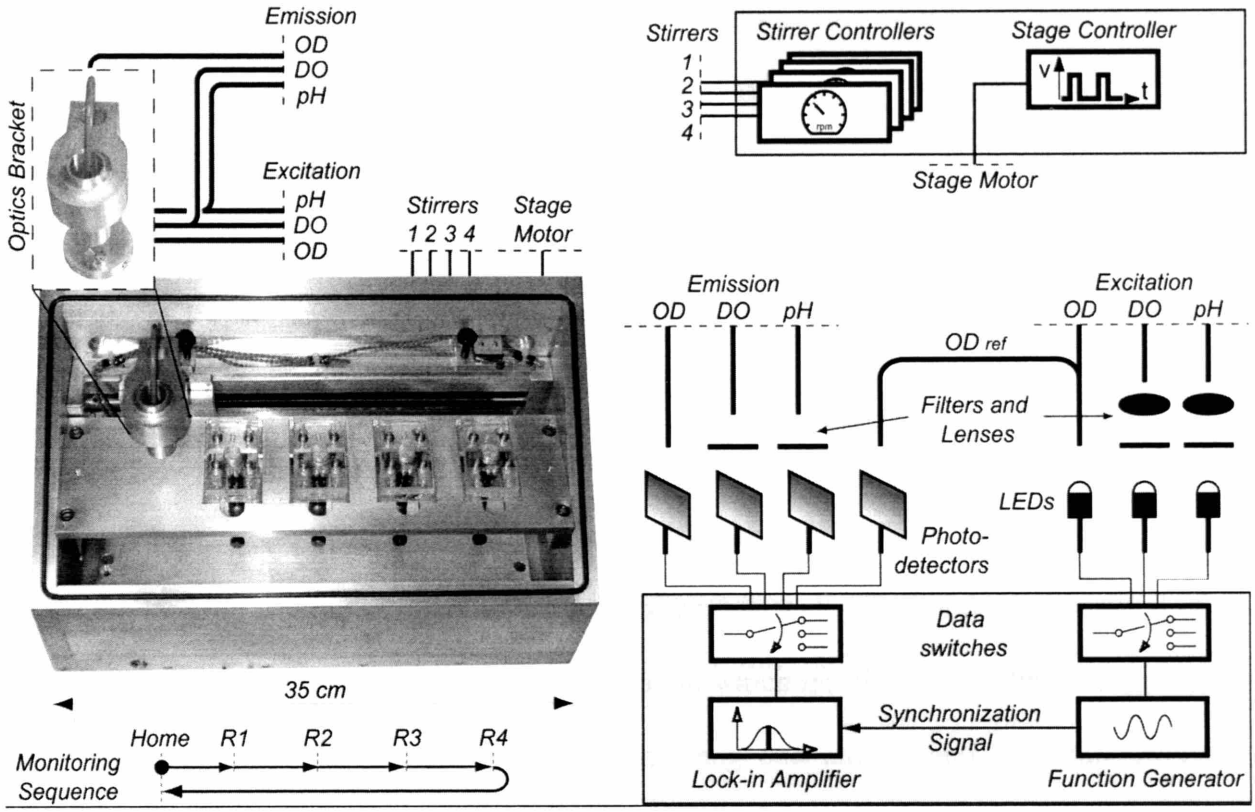

Figure 5-11. Photograph of the multiplexed microbioreactor system embedded in a schematic of the instrumentation. The multiplexed system is loaded with four stirred batch bioreactor. The optics bracket (detailed photographic view) contains the optical fibers for monitoring of OD_{600}, DO, and pH, as described in Chapter Two. The enclosure of the multiplexed system was sealed with a top lid (not shown).

The aluminum stage was attached to the rear wall of the enclosure and the slider motion was controlled with a stepper motor (Type 23T1, Velmex) which permitted an axial step resolution of 5 μm for the optical bracket. Outboard limit switches (P/N 3-8515, Velmex) prevented over-travel of the bracket. The optics bracket scanned over the microbioreactors in stop-and-go sequences executed by computer control algorithms. The process parameters were measured and recorded for each reactor using lifetime fluorescence and absorbance methods. In a typical monitoring sequence, the optical bracket would sequentially read all four microbioreactors and then return to its initial home position, waiting for the start of the next cycle.

The platform included openings at the bottom for optical access. An optics bracket mounted to a slider on a single-axis stage (Unislide, P/N MA2512K2-S2.5, Velmex, NY, USA) held optical fibers (custom-made, RoMack Fiberoptics) above and below the microbioreactors. The bracket was attached to a slider on a stage and sequentially read the microbioreactors from reactor R1 to R4, starting from the home position. Stage controllers operated the motors for stage motions. The optical and electrical leadthroughs were placed in the rear wall of the enclosure below the motorized stage. Swagelok tube fittings (SS-6-UT-1-4BT, Swagelok, OH, USA) were mounted to the rear wall, and used to clamp the optical fibers at the fiber break-out (i.e. at the location where the fibers bifurcated) to the rear wall. The break-out consisted of an aluminum cylinder with an outer diameter of 9.5 mm, which matched the inner diameter of the tube fitting bore. For the electrical wires of the magnetic motors and the limit switches, provisions in the rear wall were made for circular plastic connectors (Tyco Electronics P/N 1445759-1, Newark InOne, MA, USA). System-wide temperature control was achieved by flowing water from an external heated bath (Thermostat C10-B3, Haake, MA, USA) through the base of the housing.

A total of three bifurcated optical fibers were attached to the bottom of the bracket to monitor DO and pH sensors at the bottom of the microbioreactors, and to introduce light for the OD_{600} measurements. An optical fiber collected the transmitted light above the reactors. To maximize signal intensity, the z-position of the fibers both above and below the microbioreactors was adjustable. This was performed with cylinders that held the fibers, and were able to slide inside vertical bores machined within the bracket. The positions of the fibers with respect to the cylinders, and the position of the cylinders with respect to the bracket, were fixed with set screws.

Four magnetic stirrers were attached underneath the reactor platform. The stirrers were comprised of a DC torque mini motor (Faulhaber1212 E 006, Instech Laboratories, Plymouth Meeting, PA) with a gear (Spur gear head 12/3, transmission ratio 9.17:1, Instech) and a permanent magnet (long neodymium iron boron, diameter 6.3 mm, length 6.3 mm, Instech) attached to the rotating shaft. The gear was chosen to permit stirring speeds between 200 and 1500 rpm. Individual motor controllers (MC50, Instech) allowed independent stirring of each reactor. The total height of motor, gear and shaft was approximately 47 mm with a diameter of 10 mm. The motors were held on a separate plate, which could be exchanged to quickly reconfigure the number of stirrers and their distance from each other. The magnetic flux obtained with these permanent magnets was strong enough to perform reliable magnetic stirring from a distance of approximately one inch.

Parallel microbial fermentations with *E. coli* were carried out in four stirred microbioreactors. Details for microbial strain, culture medium, inoculation preparation are described in Chapter Two. After inoculation, the LabVIEW® routine for the multiplexed system was initiated. The control algorithm executed the stop-and-go sequences for the optics bracket. Starting from the home position (Figure 5-11), the bracket stopped at each reactor, such that the optical fibers from the optics bracket would align with the OD_{600} waveguide from the reactor top layer and the DO and pH sensors in the reactor bottom, and the respective fermentation parameters were measured. The travel speeds in between the measurements and the travel speeds from and to the home position were 1 mm/s. One scanning sequence took approximately 7 min to complete. A sampling rate of 10 min was chosen, which is sufficient to determine growth kinetics of even fast growing bacterial species, such as *E. coli*. Stirring speed was set at 700 rpm.

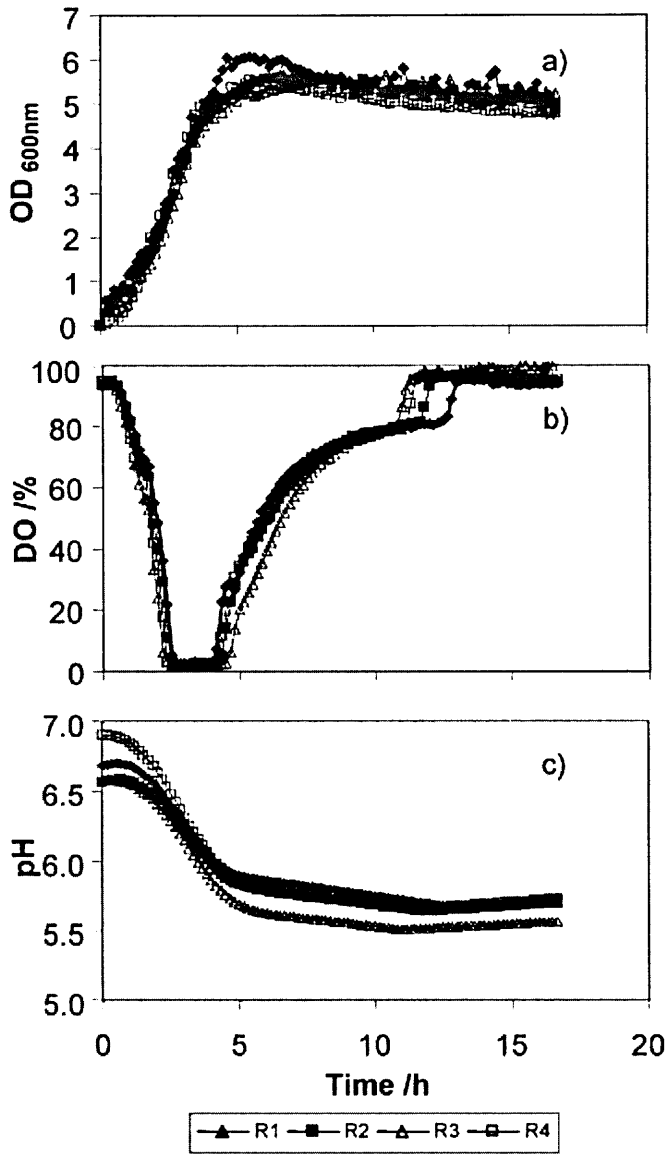

Figure 5-12. Parallel fermentations of *E. coli* performed in four microbioreactors and real-time measurements of: (a) OD600, (b) DO, and (c) pH. R1 to R4 indicate individual reactors.

In the fermentation experiments, *E. coli* cells reached the stationary phase after 6 hours and achieved an average maximum OD of 5.6 with a CV better than 6% (Figure 5-12a). The oxygen concentrations after reaching 0% remained low for a short period of time and recovered to 100% after 12 hours (Figure 5-12b). The starting pH values were between pH 6.6 and 6.9, and changed little in the first hour of the microbial fermentations, most likely as a result of the buffering

capacity of the MES added to the medium, then dropped significantly for approximately 4 hours to below pH 6 due to strong acid production, and finally reached a minimum of 5.6 after approximately 12 hours (Figure 5-12c). The four microbioreactors showed reproducible performance in terms of the measured process parameters. During exponential growth phase, the calculated standard deviations were less than or equal to 0.38 for OD_{600}, 14% for DO, and 0.16 for pH. Fermentation data indicate expected and healthy cell growth behavior with good reproducibility in growth profiles.

5.4. Design of Multiplexed System without Moving Parts

In the previous section a prototype multiplexed system was demonstrated to have good reproducibility. In this multiplexed system, a set of motor-controlled optics were used monitor multiple reactors without scaling the cost for optics. The setup for optical measurements, especially the function generators, data switches, and lock-in amplifier were too expensive to replicate for each reactor.

One major problem of the motor-controlled system was that the scanning/reading speed for individual reactor limited the number of parallel reactions. It took about 2 minutes to obtain readings of OD, pH, and DO from each microbioreactor. Given the measurement intervals of 10 (or 20) minutes, this limits the scale of parallelization to 5 (or 9) microbioreactors. The application of customer-built or commercial optical parts also makes the prototype expensive for large scale multiplexing.

A new design of multiplex system without moving parts is illustrated in Figure 5-13. Each reactor cassette in the multiplexed system, as described in Section 5-2-3, is equipped with a set of optics for OD, pH, and DO measurements.

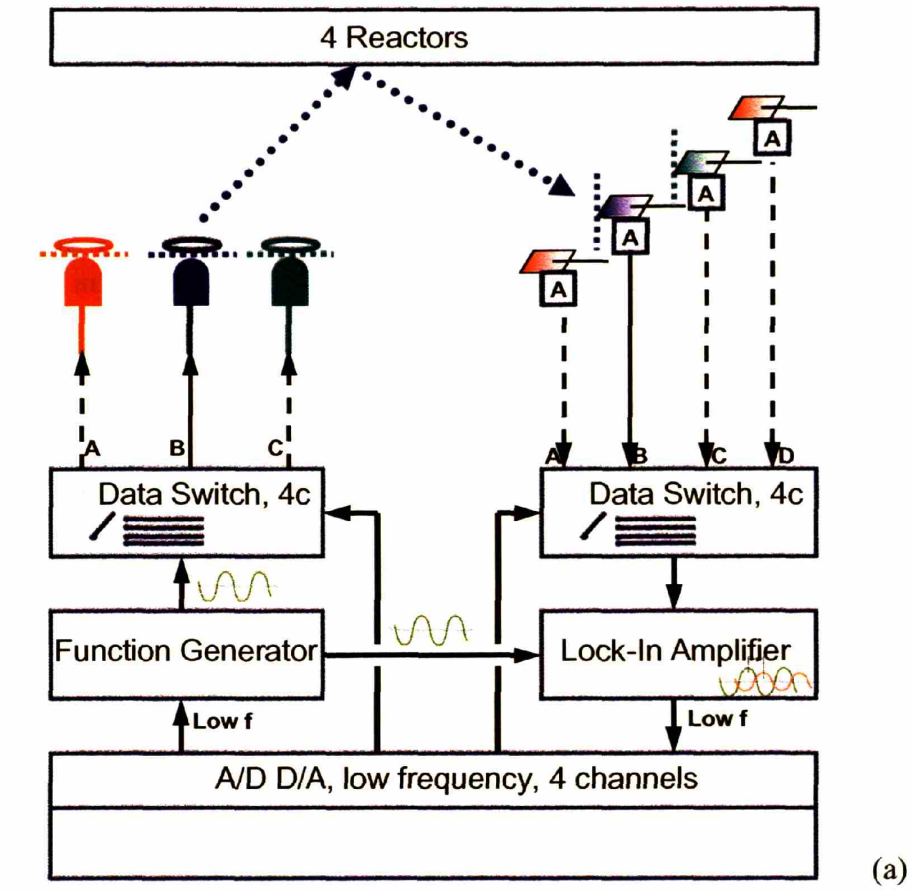

(a)

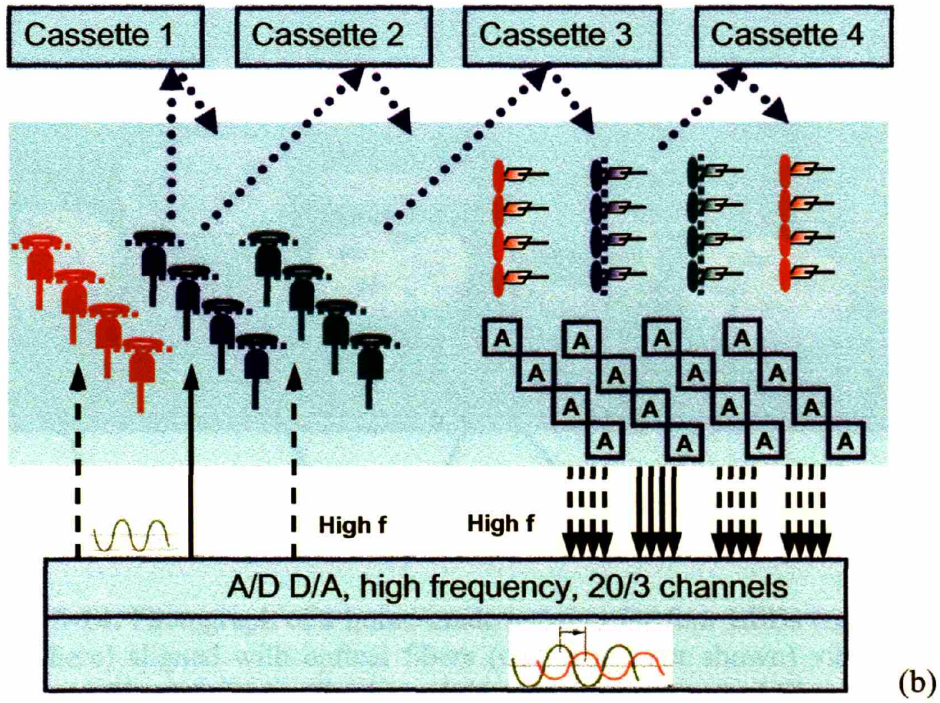

(b)

Figure 5-13. (A) Illustration of single reactor setup, as well the multiplexed

system discussed in Section 5-3. Channels A and D are OD measurements, B for pH measurement, and C for DO measurement. Commercial bundles of photodetectors are used in all measurements. Channel B is shown as the current reading channel. (B) Illustration of the new design for a multiplexed system without moving parts. Different from the previous design, a high-frequency A/D D/A card (2 MHz, National Instruments) is required for sending discrete sinoidal signals to LED's and receiving signals from photodetector. Phase-shift and intensity information are analyzed by Labview® software rather than by a lock-in amplifier.

Inexpensive parts including the optical lenses (5 cm in diameter, Thorlabs), optical fibers (Thorlabs and Polymicro), the photodectors (Thorlabs) are applied in the system, and home-built electronical amplifiers are used to reduce the cost of individual measurement setup. Expensive parts, including optical filters and the high frequency A/D D/A card for data acquisition and control purposes, are shared by all parallel setups. Figure 5-14 shows a prototype of four LEDs integrated by sharing one optical filter.

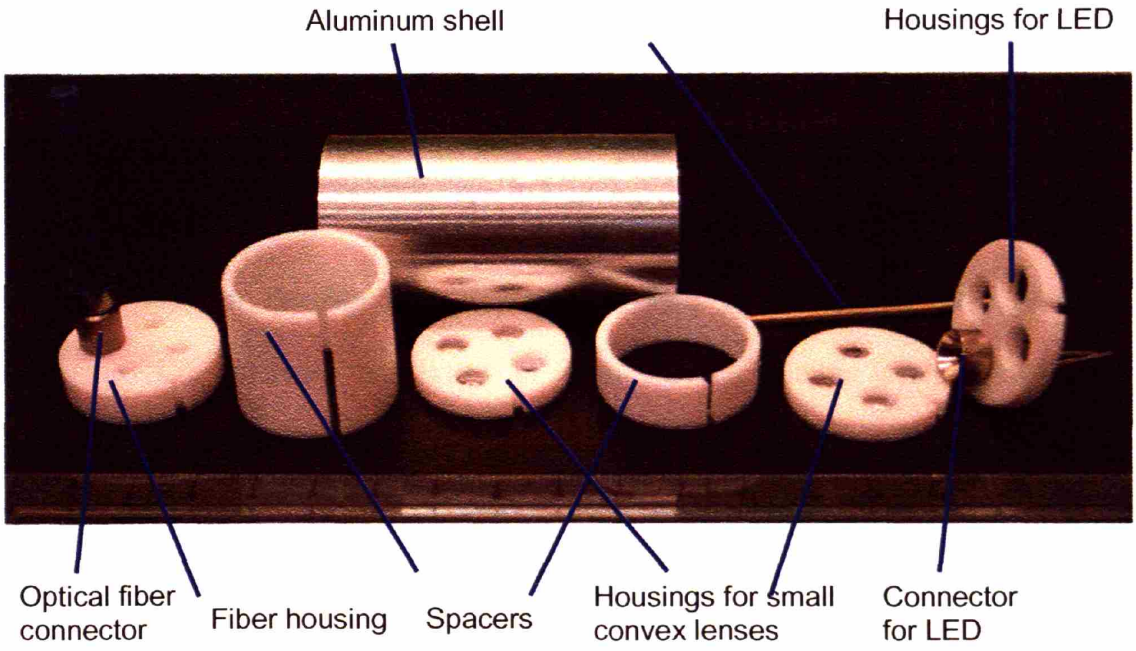

Figure 5-14. Photograph of a home-made housing for four LEDs (only one LED shown here) aligned with optical fibers (only one fiber shown) via mechanical connectors (Thorlas; Radio Shack) and through a shared optical filter (not shown). The distances from LEDs to the filter and from the filter to lenses were optimized and fixed by spacers to allow maximal light intensity received by optical fibers.

5.5. Highlights and Future Opportunities

Different from previous chapters that focused on functionalities and controls of individual microbioreactors and exploration of different applications in bioprocess developments, this chapter aims to address issues of packaging and parallelization for high throughput data acquisition, bringing the microbioreactor technology a step further to being widely applied in bioprocess discovery and development.

The proposed approach is to separate the system into two parts: the bioreactor cassette, and the external measurement and control system. The reactor cassette is a reactor system integrated with all the technologies discussed in previous chapters, which make it applicable to batch, fed-batch, and continuous culture operations. The building materials for the cassette are inexpensive, and the fabrication process is compatible with large-scale manufacture. Most importantly, the cassette interfaces with the external system seamlessly for both physical connection and data acquisition. This advance was made possible by the invention and integration of optical and fluidic connectors, as described in Section 5-2. Finally a pre-packed, clean cassette would significantly reduce the mechanical complexity before and during biological experiments.

The key issue in developing multiplexed systems as prototypes for high-throughput bioprocessing is to increase the extent of parallelization without scaling the number of measurement instruments. In the first prototype a step motor was applied to use one set of optics for four parallel batch microbioreactors. Fermentation data indicated healthy and expected cell growth behavior with good reproducibility of the OD_{600}, DO, and pH profiles. A second prototype of multiplexed system was designed and fabricated to eliminate moving parts to allow higher extent of integration and scaling. Parallel measurements and data analysis would be directly controlled by the computer interfaced with a high-frequency data acquisition card.

Figure 5-15 envisions a future parallel-operated microbioreactor system. The system is composed of four parts. In the center of the system is the device chamber, which contains the housing platform for microbioreactor cassettes. Fluidic connectors, or fluidic motherboards (Perozziello et al., 2006) connected with external reservoirs via microvalves and tubings, allow fast setup of microbioreactors in the platform. For illustration purpose a platform with only four reactors is shown in the figure. Optical fibers and connectors are fixed in the housing platform allowing accesses to the reactor cassettes from bottom and top sides. These fibers are physically connected with optical light sources (LEDs and filters, in the left hand side of the box, shown in Figure 5-15) and detection units (optical filters, photodetectors, and amplifier circuits, in the right hand side of the box, shown in Figure 5-15). Data are collected and sent to the computer. The last part is the control box sitting at the bottom of the system. This box is integrated with control functions, such as power supply, temperature, stir speeds, air pressure, air flow rate and moisture, microfluidic feeding (via microvalves), and amplifying circuits. All these functions are monitored and controlled by the front panel on the external face of the system.

In this bioreactor system, only the housing platform in the middle of the chamber is accessed by end users. Analogous to photo spectrometers used in biological laboratories, the ideal microbioreactor system should be fully-integrated and user-friendly.

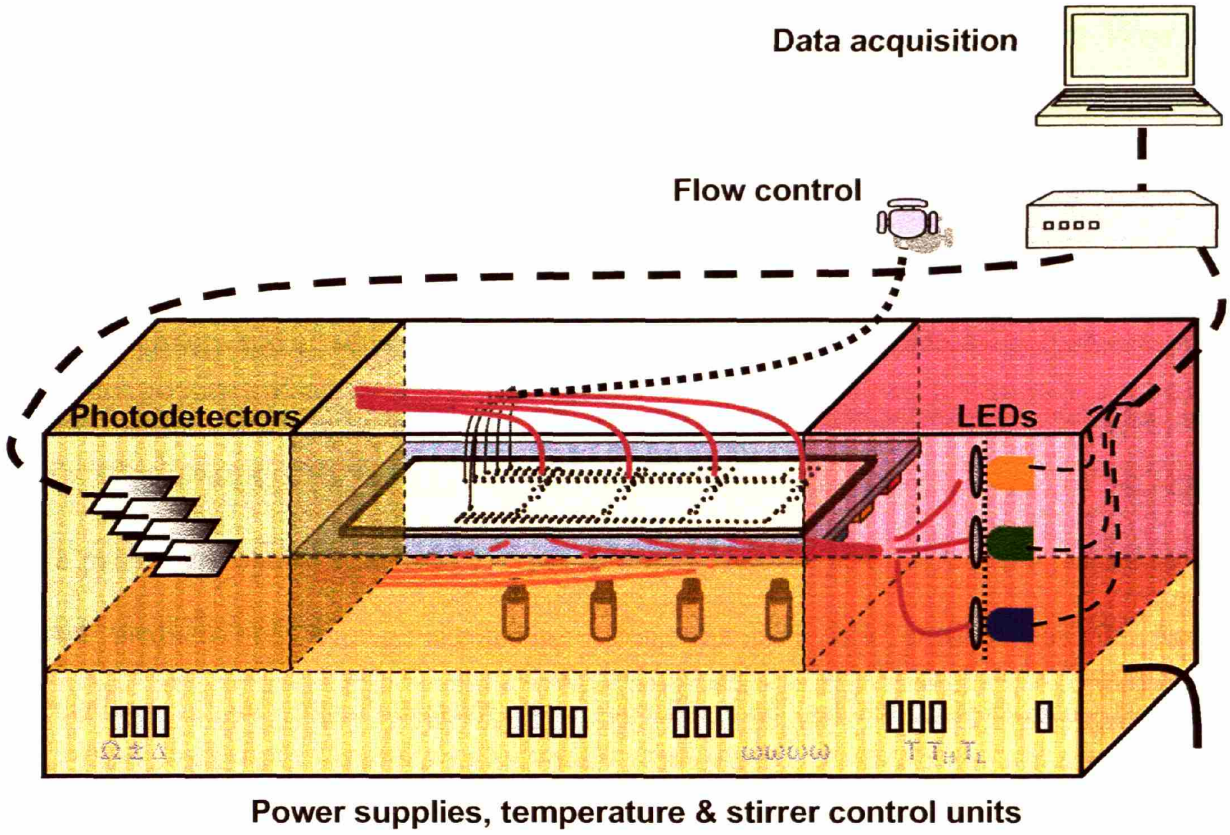

Figure 5-15. Envision of a multiplexed bioreactor system for high-throughput bioprocess developments. Microbioreactor cassettes are shown to be placed in the housing platform in the middle of system chamber. Thin dashed lines separate different regions in the system. Dotted lines are used to illustrate fluidic connections. Thick dashed lines indicate electronical cable connecting the computer, data requisition card, photodetectors, and LED units. The thick solid line at the right-hand side corner illustrates power supply for the system, and shadow solid lines in the chamber indicate the optical fibers used for measurements.

Chapter 6. Conclusions and Recommendations for Future Work

6.1. Conclusions

This thesis has demonstrated the feasibility of cultivation of microbial cells in microliter-volume bioreactors and of allowing flexible operations and effective controls for bioprocessing. In Chapter Two, membrane-aerated and actively-mixed microbioreactors were designed and fabricated out of PMMA and PDMS. Optical sensors were integrated to monitor the important growth parameters optical density (OD), pH, and dissolved oxygen (DO) under conditions of different medium and mixing/oxygenation. Reproduciblity was ensured and the batch fermentations in the microbioreactor were benchmarked against conventional lab-scale bioreactors to demonstrate the similarity in growth kinetics of bacteria at the two scales. Upon the establishment of the reproducibility the microbioreactor was used for biological applications such as global gene expression analysis of *S. cerevisiae* in culture media with different carbon sources. Yeast cells grown in the microbioreactors exhibited physiological and molecular characteristics which parallel those of large-scale cultures. With this ability to mirror observations obtained in conventional systems coupled with reproducible growth, the small reactor volumes, and the on-line measurements of DO, pH, and OD in microbioreactors fulfill the fundamental requirements as a practical bioreactor.

Active mixing facilitates oxygenation in membrane-aerated bioreactors and more importantly, together with external fluidics units it allows the microbioreactor to be operated in continuous and fed-bath modes, which are very important operations for bioprocessing. In Chapter Three, microchemostat, the continuous culture of microbial cells was made possible by the integration of new approaches, including single-phase, pressure-driven medium feed at slow

flow rates, local temperature control in the microbioreactor device, as well as the formation of a PEG-grafted PAA copolymer films on both PMMA and PDMS surfaces. Steady state of *E. coli* culture was obtained and sustained in the microchemostat with glucose as the only limiting substrate for growth. Wall growth of bacterial cells in the microbioreactor, a common challenge for microscale device, was significantly reduced by application of cell-resistant surface coatings, even after a prolong period of time cell cultivation. Another important issue for continuous flowing biodevices, bacterial chemotaxis and back growth were effectively inhibited by local heating in the medium feeding channel. These advances enabled cell growth kinetics and stoichiometry to be obtained in microchemostat consistent with phenomena reported for conventional stirred-tank bioreactors, as indicated by the time profiles of OD, pH, and DO measurements during steady states.

Chapter Four presented a microbioreactor system for the fed-batch cell culture. The microbioreactor utilized water evaporation as a water exit for the microbioreactor and a combination of active feeding of base and acid, and passive feeding of water. Feeds were pressure-driven and closed-loop controlled by microvalves. The proportional-derivative controller successfully maintained the pH value in the microbioreactor within a physiological scale during the time course of *E. coli* cell cultivation in rich media. Extensions of cell growth and significant improvements in biomass yield were observed in pH-controlled batch culture experiments. Feedback control of glucose feeding using DO reading in the microbioreactor was also demonstrated. These results demonstrated the concept of a fed-batch microbioreactor with well-controlled environmental condition for cell cultivation.

As a practical, user-friendly platform that would meet the needs for high-throughput bioprocess developments, the system was designed as two separate parts: disposable

microbioreactors preferably in the form of plastic cassettes, and a fixed housing including expensive optical components and instruments. In Chapter Five microfluidic connectors and PDMS microlens were presented and integrated in a microbioreactor cassette serving as "plug-in-and-play" interfaces with external fluidic and optical instruments. These connectors not only greatly simplified the setup procedure for the cassette but also helped to increase the accuracy and reproducibility in measurements. Multiple layers of PMMA chips were thermally bonded and a PDMS aeration membrane was embedded to make the cassette a disposable monolithic device. For the second part of the platform, a step-motor controlled multiplexed system was designed and demonstrated for parallel operations of four batch microbioreactor. Reproducible growth kinetics comparable to bench top systems was obtained in this setup. Finally an integrated bench scale microbioreactor platform for bioprocess development was proposed.

6.2. Outlook and Recommendations for Future Work

In the initial stages of this work, one of the major tasks was to decide how the microbioreactor would meet the engineering standards for bioprocess developments. For operations of batch, fed-batch, and continuous cell cultivations, the control over environmental conditions is critical for allow flexibility. We believed that the flexibility in operations and ability to monitor process variables would give the microbioreactor technology advantages over simple assay bioreactors, such as 96-well microplate, and provide comparable performance to conventional stir-tank bioreactors in bioprocessing.

With the completion of this thesis, we can begin to answer these questions. The results we have presented demonstrate that in its current incarnation, the microbioreactor is a promising tool for many applications bioprocess developments, such as on-line measurements of growth kinetics, genome-wide expression analysis, pH control, and even continuous culture of bacterial

cells. We were assured by the reproducibility and comparable phenomena observed in the microbioreactor behavior, as reflected by the measured growth parameters (OD, pH, and OD) and benchmarked by conventional bioreactors.

On the other hand, the applicability of the microbioreactor in bioprocessing still need to be further explored. To some extends this thesis focuses on proofs of concepts and the solutions we proposed may not be the optimal answer to the question. Engineering optimizations are needed to make the microbioreactor applicable for a wide range of operation conditions and different types of microbial strains. For example, the geometry of the magnetic stir bar in the microbioreactor can be optimized and machined in shaft-shape to improve mixing and oxygenation.

The micro scale bioreactors were made to mimic the results from bench-scale reactors. The design and fabrication of the microbioreactor benefited from the polymer microfabrication and precision machining technologies. However, we were also limited by the availability of fabrication technologies and utilities. Improvements can be made by applying the recent advances of polymer technologies. Laser-ablation will make the microscale features as small as 5 μm in polymers; high speed air turbine milling machine with rotating speed of up to 50,000 rpm will yield better surface finishes in devices; hot-embossing technology will replicate microdevices will better accuracy and reproducibility while give very smooth surfaces on polymers. These technologies will allow more functionality to be added in the microbioreactor.

Another area we believe as the most important area in which future work can focus is the further integration of multiplexed system for parallel operation of multiple microbioreactors. We have developed and presented a prototype system with limited extends of integration using four parallel microbioreactors to prove the concepts. Further integration of the system will allow

autonomous operation of multiple (> 4) microbioreactors with seamless interfaces. This is necessary to obtain economies of scale for the obtaining cost advantages of microbioreactors and will greatly increase the throughput for biological applications. We designed a first version of such a future bench-scale microbioreactor platform. Concerted multidisciplinary efforts will be needed to make instrumented, multiplexed microreactors common tools in bioprocess engineering.

References

Akgün, A., Maier, B., Preis, D., Roth, B., Klingelhöfer, R., Büchs, J. A novel parallel shaken bioreactor system for continuous operation. *Biotech. Prog.* **2004**, *20*, 1718-1724.

Adler, J. The sensing of chemicals by bacteria. *Scientific American* **1976**, *234*, 40-47.

Åkesson, M., Hagander, P., Axelsson, J.P. Avoiding acetate accumulation in *Escherichia coli* cultures using feedback control of glucose feeding. *Biotech. Bioeng.* **2001**, *73*, 223-230.

Aristidou, A.A., Bennett, G. N., San, K.-Y. Metabolic flux analysis of *Escherichia coli* expressing the *Bacillus subtilis* acetolactate synthase in batch and continuous Cultures. *Biotech. Bioeng.* **1999**, *63*, 737-749.

Balaban, N.Q. Szilard's dream. *Nature Methods* **2005**, *2*, 648-649.

Balagaddé, F.K., You, L., Hansen, C.L., Arnold, F.H., Quake, S.R. Long-term monitoring of bacteria undergoing programmed population control in a microchemostat. *Science* **2005**, *309*, 137-140.

Bin, A.K. Mass transfer to the free interface in stirred vessels. *Chem. Eng. Commun.* **1984**, *31*, 155-183.

Bird, R.B., Steward, W.E., Lightfoot, E.N. *Transport phenomena*. **2002,** Wiley & Sons, Inc.

Blanch, H.W., Clark, D.S. *Biochemical engineering*. **1996**, Marcel Dekker, Inc.

Blomberg, A., Larsson, C., Gustafsson, L. Microcalorimetric monitoring of growth of *Saccharomyces cerevisiae*: osmotolerance in relation to physiological state. *J. Bacteriol.* **1988**, *170*, 4562-4568.

Boccazzi, P., Zanzotto, A., Szita, N., Bhattacharya, S., Jensen, K.F., Sinskey, A.J. Gene expression analysis of *Escherichia coli* grown in miniaturized bioreactor platforms for high-throughput analysis of growth and genomic data. *Appl. Microbiol. Biotechnol.* **2005**, *68*, 518-532.

Boccazzi, P., Zhang, Z., Kurosawa, K., Szita, N., Bhattacharya, S., Jensen, K.F., Sinskey, A.J. Differential gene expression profiles and real-time measurements of growth parameters in Saccharomyces cerevisiae grown in microliter-scale bioreactors equipped with internal stirring. *Biotech. Prog.* **2006**, *in press.*

Bodrossy, L., Sessitsch, A. Oligonucleotide microarrays in microbial diagnostics. *Curr. Opin. Microbiol.* **2004**, *7*, 245-254.

Chang, W.-J., Akin, D., Sedlak, M., Ladisch, M.R., Bashir, R. Poly(dimethylsiloxane) (PDMS) and silicon hybrid biochip for bacterial culture. *Biomed. Microdev.* **2003**, *5*, 281-290.

Choi, H.-G., Zhang, Z., Boccazzi, P., Laibinis, P.E., Sinskey, A J., Jensen, K.F. Poly(ethylene glycol) (PEG)- modified poly(dimethylsiloxane) (PDMS) for protein- and cell resistant surfaces in microbioreactor. *Proc. Micro Total Analysis 2003*, Transducers Research Foundation, Inc., **2003**, 1105-1108.

Curotto, E., Aros, F. Quantitative determination of chitosan and the percentage of free amino groups. *Anal. Biochem.* **1993**, *211*, 240-241.

Debouck, C., Goodfellow, P.N. DNA microarrays in drug discovery and development. *Nat. Genet.* **1999**, *21*, 48-50.

Doelle, H.W., Ewing, K.N., Hollywood, N.W. Regulation of glucose metabolism in bacterial systems. *Adv. Biochem. Eng.* **1982,** *23*, 1-35.

Draude, A., Franke, H., Lessard, R.A. Two-dimensional refractive index patterns with crystalline symmetry. *J. Phys. D: Appl. Phys.* **2005**, *38*, 974–980.

Duetz, W.A., Rüedi, L., Hermann, R., O'Connor, K., Büchs, J., Witholt, B. Methods for intense

aeration, growth, storage, and replication of bacterial strains in microtiter plates. *Appl. Env. Microbio.* **2000**, *66*, 2641-2646.

Duetz, W.A., Witholt, B. Effectiveness of orbital shaking for the aeration of suspended bacterial cultures in square-deepwell microtiter plates. *Biochem. Eng. J.* **2001**, *7*, 113-115.

Groisman, A., Lobo, C., Cho, H., Campbell, J.K., Dufour, Y.S., Stevens, A.M., Levchenko, A. A microfluidic chemostat for experiments with bacterial and yeast cells. *Nature Methods* **2005**, *2*, 685-689.

Gu, M.B., Gil, G.C., Kim, J.H. A two-stage minibioreactor system for continuous toxicity monitoring. *Biosensors and Bioelectronics* **1999**, *14*, 355-361.

Gu, M.B., Gil, G.C., Kim, J.H. A multi-channel continuous toxicity monitoring system using recombinant bioluminescent bacteria for classification of toxicity. *Biosensors and Bioelectronics* **2001**, 16, 661-666.

Gupta, A., Rao, G. A study of oxygen transfer in shake flasks using a non-invasive oxygen sensor. *Biotech. Bioeng.* **2003**, *84*, 351-358.

Han, K., Lim, H.C., Hong, J. Acetic acid formation in *E. coli* fermentation. *Biotech. Bioeng.* **1993**, *39*, 663-671.

Harms, P., Kostov, Y., Rao, G. Bioprocess monitoring. *Curr. Opinion. Biotech.* **2002**, *13*, 124-127.

Harvey, R.J. Metabolic Regulation in Glucose-Limited Chemostat Cultures of *Escherichia coli*. *J. Bacteriol.* **1970**, *104*, 698-706.

Herbert, D., Elsworth, R., Telling, R.C. Continuous culture of bacteria: a theoretical and experimental study. *J. Gen. Microbiol.* **1956**, *14*, 601-622.

Hermann, R., Lehmann, M., Büchs, J. Characterization of gas-liquid mass transfer phenomena in microtiter plates. *Biotech. Bioeng.* **2002**, *81*, 178-186.

Hittinger, C.T., Rokas, A., Carroll, S.B. Parallel inactivation of multiple GAL pathway genes and ecological diversification in yeasts. *Proc. Natl. Acad. Sci. USA* **2004**, *101*, 14144-14149.

Hood, L. Systems biology: integrating technology, biology, and computation. *Mech. Ageing Dev.* **2003**, *124*, 9-16.

Horvath, R., Lindvold, L.R., Larsen, N.B. Fabrication of all-polymer freestanding waveguides. *Micromech. Microeng.* **2003**, *13*, 419-424.

Ideker, T., Thorsson, V., Ranish, J.A., Christmas, R., Buhler, J., Eng, J.K., Bumgarner, R., Goodlett, D.R., Aebersold, R., Hood, L. Integrated genomic and proteomic analyses of a systematically perturbed metabolic network. *Science* **2001**, *292*, 929-934.

John, G.T., Klimant, I., Wittmann, C., Heinzle, E. Integrated optical sensing of dissolved oxygen in microtiter plates: a novel tool for microbial cultivation. *Biotech. Bioeng.* **2003**, *81*, 829-836.

John, G.T., Goelling, D., Klimant, I., Schneider, H., Heinzle, E. pH-sensing 96-well microtiter plates for the characterization of acid production by dairy starter cultures. *J. Dairy Res.* **2003**, *70*, 327-333.

Johnston, M. A model fungal gene regulatory mechanism: the GAL genes of *Saccharomyces cerevisiae*. *Microbiol. Rev.* **1987**, *51*, 458-476.

Johnston, W., Cord-Ruwisch, R., Cooney M.J. Industrial control of recombinant E. coli fed-batch culture: new prespectives on traditional controlled variables. *Bioprocess. Biosyst. Eng.* **2002**, *25*, 111-120.

Kamen, A., Garnier, A., Andre, G., Archambault, J., Chavarie, C. Determination of mass transfer parameters in surface aerated bioreactors with bubble entrainment. *Chem. Eng. J.* **1995**, *59*,

187-193.
Kawase, Y., Moo-Young, M. Mass transfer at a free surface in stirred tank bioreactors. *Trans. I. Chem. E.* **1990**, *68*, 189-194.
Kermis, H.R., Kostov, Y., Rao, G. Rapid method for the preparation of a robust optical pH sensor. Analysts **2003**, *128*, 1181-1186.
Kim, S.-Y. Microbial Production of Ethanol by Clostridum Thermosaccharolyticum. Master degree thesis, MIT, **1982**.
Kim, J.W., Lee, Y.H. Development of microfermenter Chip. *J. Korean Phys. Soc.* **1998**, *33*, S462-S466.
Korz, D.J., Rinas, U., Hellmuth, K., Sanders, E.A., Deckwer, W.-D. Simple fed-batch technique for high cell-density cultivation of *Escherichia coli*. *J. Biotech.* **1995**, *39*, 59-65.
Kostov, Y., Harms, P., Randers-Eichhorn, L., Rao, G. Low-cost microbioreactor for high-throughput bioprocessing. *Biotech. Bioeng.* **2001**, *72*, 346-352.
Kubitschek, H. E. *Introduction to research with continuous cultures.* Prentice-Hall, **1970**.
Kumar, S., Wittmann, C., Heinzle, E. Minibioreactors. *Biotech. Letters* **2004**, *26*, 1-10.
Lamping, S.R., Zhang, H., Allen, B., Shamlou, P.A. Design of a prototype miniature bioreactor for high throughput automated bioprocessing. *Chem. Eng. Sci.* **2003**, *58*, 747-758.
Larsen, D.H., Dimmick, R.L. Attachment and growth of bacteria on surfaces of continuous-culture vessels. *J. Bacteriol.* **1964**, *88*, 1380-1387.
Larsson, C., Nilsson, A., Blomberg, A., Gustafsson, L. Glycolytic flux is conditionally correlated with ATP concentration in *Saccharomyces cerevisiae*Saccharomyces cerevisiae: a chemostat study under carbon- or nitrogen-limiting conditions. *J. Bacteriol.* **1991**, *179*, 7243-7250.
Lohr, D., Venkov, P., Zlatanova, J. Transcriptional regulation in the yeast GAL gene family: a complex genetic network. *Faseb J.* **1995**, *9*, 777-787.
Maeda, K., Imae, Y., Shioi, J., Oosawa, F. Effect of temperature on motility and chemotaxis of *Escherichia coli*. *J. Bacteriology* **1976**, *127*, 1039-1046.
Maharbiz, M.M., Holtz, W.J., Sharifzadeh, S., Keasling, J.D., Howe, R.T. A microfabricated electrochemical oxygen generator for high-density cell culture arrays. *J. MicroElectroMechanical Sys.* **2003**, *12*, 590-599.
Maharbiz, M.M., Holtz, W.J., Howe, R.T., Keasling, J.D. Microbioreactor arrays with parametric control for high-throughput experimentation. *Biotech. Bioeng.* **2004**, *85*, 376-381.
Merkel, T., Bondar, V., Nagai, K., Freeman, B., Pinnau, I. Gas sorption, diffusion, and permeation in poly(dimethysiloxane). *J. Polym. Sci. Pt. B – Polym. Phys.* **2000**, *38*, :415-434.
Moeser, G. D., Roach, K.A., Green, W.H., Laibinis, P.E., Hatton, T.A. Water-based magnetic fluids as extractants for synthetic organic compounds. *Ind. Eng. Chem. Res.* **2002**, *41*, 4739-4749.
Moser, A. *Bioprocess Technology: Kinetics & Reactors.* Springer, **1988**.
Otterstedt, K., Larsson, C., Bill, R.M., Stahlberg, A., Boles, E., Hohmann, S., Gustafsson, L. Switching the mode of metabolism in the yeast *Saccharomyces cerevisiae*. *EMBO Rep.* **2004**, *5*, 532–537.
Parekh, S., Vinci, V.A., Strobel, R.J. Improvement of microbial strains and fermentation processes. *Appl. Microbio. Biotech.* **2000**, *54*, 287-301.
Perozziello, G., Jensen, M.F., Mc Cormack, J.E., Bundgaard, F., Geschke, O. Plug'n'pump fluidic interconnection. *Special Publication - Royal Society of Chemistry* **2004**, *297*, 575-

577.
Perozziello, G., Snakenborg, D., Zhang, Z., Kutter, J.P., Geschke, O., Jensen, K.F. Optical connector plugs for multiplexed and simultaneous detection purposes in microfluidic systems, 2006, in submission to *J. Micromech. Microeng.*
Perozziello, G., Snakenborg, D., Zhang, Z., Kutter, J.P., Jensen, K.F., Geschke, O. A Fluidic Motherboard Including Fluidic and Optical Interconnections for multiplexed and Symultaneous Detection in Microfluidic Systems. **2006**, in submission to *Lab on a Chip.*
Perry, R., Green, D. *Perry's chemical engineering handbook.* R. R. Donnelley & Sons Company. **1984**.
Phillips, D.H., Johnson, M.J. Aeration in Fermentations. *J. Biochem. Microbiol. Tech. Eng.* **1961**, *3*, 277-309.
Pilyugin, S.S., Waltman, The simple chemostat with wall growth. P. *SIAM J. Appl. Mathematics,* **1999**, *59*, 1552-1572.
Puskeiler, R., Kaufmann, K., Weuster-Botz, D. Development, parallelization, and automation of a gas-inducing milliliter-scale bioreactor for high-throughput bioprocess design (HTBD). *Biotech. Bioeng.* **2005**, *89*, 512-523.
Rao, G. Bioreactor and bioprocessing technique. **2002:** US patent US 2002/0025547 A1.
Shigley, J.E., Mischke C.R. *Mechanical Engineering Design*, **2001**. McGraw-Hill.
Shuler, M.L., Kargi, F. *Bioprocess Engineering: Basic Concepts*. **2001**, Prentice Hall.
Skoog, D.A., West, D.M., Holler, F.J. *Fundamentals of analytical chemistry*. **1992**, Sauders College Publishing.
Stahl, G., Ben Salem, S.N., Chen, L., Zhao, B., Farabaugh, P.J. Translational accuracy during exponential, post-diauxic and stationary growth phases in *Saccharomyces cerevisiae*. *Eukaryotic Cell* **2004**, *3*, 331-338.
Stanbury, P.F., Whitaker, A., Hall, S.J. *Principles of Fermentation Technology*. **1995**. Elsevier Science Ltd.
Szita, N., Boccazzi, P., Zhang, Z., Boyle, P., Sinskey, A.J., Jensen, K.F. Development of a multiplexed microbioreactor system for high-throughput bioprocessing. *Lab on a Chip* **2005**, *5*, 819-826.
Tolosa, L., Kostov, Y., Harms, P., Rao, G. Noninvasive measurement of dissolved oxygen in shake flasks. *Biotech. Bioeng.* **2002**, *80*, 594-597.
Topiwala, H.H., Hamer, G. Effect of wall growth in steady state continuous culture. *Biotech. Bioeng.* **1971**, *13*, 919-922.
van der Weide, D.W., Blattner, F.R. Microfabricated microbial growth assay method and apparatus. **2002;** US patent US 2002/0197709 A1.
Vuppu, A.K., Garcia, A.A., Saha, S.K., Phelan, P.E., Hayes, M.A., Calhoun, R. Modeling microflow and stirring around a microrotor in creeping flow using a quasi-steady-state analysis. *Lab on a Chip* **2004**, *4*, 201-208.
Walther, I., van der Schoot, B.H., Jeanneret, S., Arquint, P., de Rooij, N.F., Gass, V., Bechler, B., Lorenzi, G., Cogoli, A. Development of a miniature bioreactor for continuous culture in a space laboratory. *J. Biotech.* **1994**, *30*, 21-32.
Walther, I., van der Schoot, B.H., Boillat, M., Cogoli, A. Microtechnology in space bioreactors. *Chimia* **1999**, *53*, 75-80.
Walther, I., van der Schoot, B.H., Boillat, M., Cogoli, A. Performance of a miniaturized bioreactor in space flight: microtechnology at the service of space Biology. *Enz. Microbial. Tech.* **2000**, *27*, 778-783.

Weiss, S., John, G.T., Klimant, I., Heinzle, E. Modeling of mixing in 96-well microplates observed with fluorescence indicators. *Biotech. Prog.* **2002**, *18*, 821-830.

Weuster-Botz, D., Altenbach-Rehm, J., Aenold, M. Parallel substrate feeding and pH-control in shaking-flasks. *Biochem. Eng. J.* **2001**, *7*, 163-170.

Weuster-Botz, D., Stevens, S., Hawrylenko, A. Parallel-operated stirred-columns for microbial process development. *Biochem. Eng. J.* **2002**, *11*, 69-72.

Whiffin, V.S., Cooney, M.J., Cord-Ruwisch, R. Online detection of feed demand in high cell density cultures of *Escherichia coli* by measurement of changes in dissolved oxygen transients in complex media. *Biotech. Bioeng.* **2004**, *85*, 422-433.

Wikepedia coordination, website of http://en.wikipedia.org.

Wittmann, C., Kim, H.M., John, G., Heinzle, E. Characterization and application of an optical sensor for quantification of dissolved O_2 in shake-flasks. *Biotech. Letters* **2003**, *25*, 377-380.

Zanzotto, A., Szita, N., Boccazzi, P., Lessard, P., Sinskey, A.J., Jensen, K.F. A membrane-aerated microbioreactor for high-throughput bioprocessing. *Biotech. Bioeng.* **2004**, *85*, 376-381.

Zhang, Z., Boccazzi, P., Choi, H.-G., Szita, N., Sinskey, A.J., Jensen K.F. A microchemostat – continuous cell culture in microbioreactors. *Special Publication - Royal Society of Chemistry* **2004**, *297*, 231-233.

Zhang, Z., Szita, N., Boccazzi, P., Sinskey, A.J., Jensen, K.F. A well-mixed, polymer-based microbioreactor with integrated optical measurements. *Biotechnol Bioeng.* **2006**, *93*, 286-96.

Zhang, Z., Boccazzi, P., Choi, H.-G., Perozziello, G., Sinskey, A.J., Jensen, K.F. Microchemostat – microbial continuous culture in a polymer-based, instrumented microbioreactor. *Lab on a Chip* **2006**, *in press*.

APPENDIX A. Fabrication of Microbioreactor Devices

The fabrication procedures for the microbioreactor devices are presented in this appendix.

A.1. Fabrication of PMMA Device using CNC Milling Machine

Building material, PMMA sheets were purchased from MSC Industrial Supply, Co. and Goodfellow Corp. Sheets were cut using a table saw into chips (4"×1.4"), and Bridgeport CNC milling machines in Edgerton Machine Shop (MIT) were used for the fabrication of PMMA devices.

As the first step, a large piece of polycarbonate was clamped and fixed on the CNC machine as a milling base. A fly cutter with cutting diameter of 2 inches was used to cut a shadow groove into the polycarbonate base and to define the flat bottom and sharp side edge (Y-dimension) for PMMA chips. Double-side tape (3M, MN, USA) was used to fix PMMA chips in the shadow groove. By carefully selecting chips with uniform thickness, this setup procedure kept the PMMA chip horizontal. Edges (in X- and Y-dimensions) of PMMA chips were defined by an edge-finder and a cornor of the chip is set as (0, 0) in coordinates. The Z coordinate was defined by step-feeding rotating endmill in vertical direction until it touches the top surface of the chip. Alternatively, PMMA chips could be fixed directly onto machine bench by threaded bolts, if more permanent setup were allowed.

During milling, the machine bench moved in three-axis (X, Y, and Z), together with rotating endmill, allowing material to be removed and formation of a 3-dimensional structure. Endmill rotational speed of 3000 rpm, which was the fastest limit for this CNC machine, was applied when small endmills (less than 3mm in diameter) were used. Water-based coolant was applied during milling to prvent PMMA devices from melting. Cutting with higher speed is preferred for

fast fabrication and smooth finish surface. However, a high-speed CNC motor and air-cooling system was not available.

The device shown in Figure 3.1 (the middle layer) is used here to demonstrate the fabrication process. The whole process takes 7 steps, as illustrated in Figure A-1.

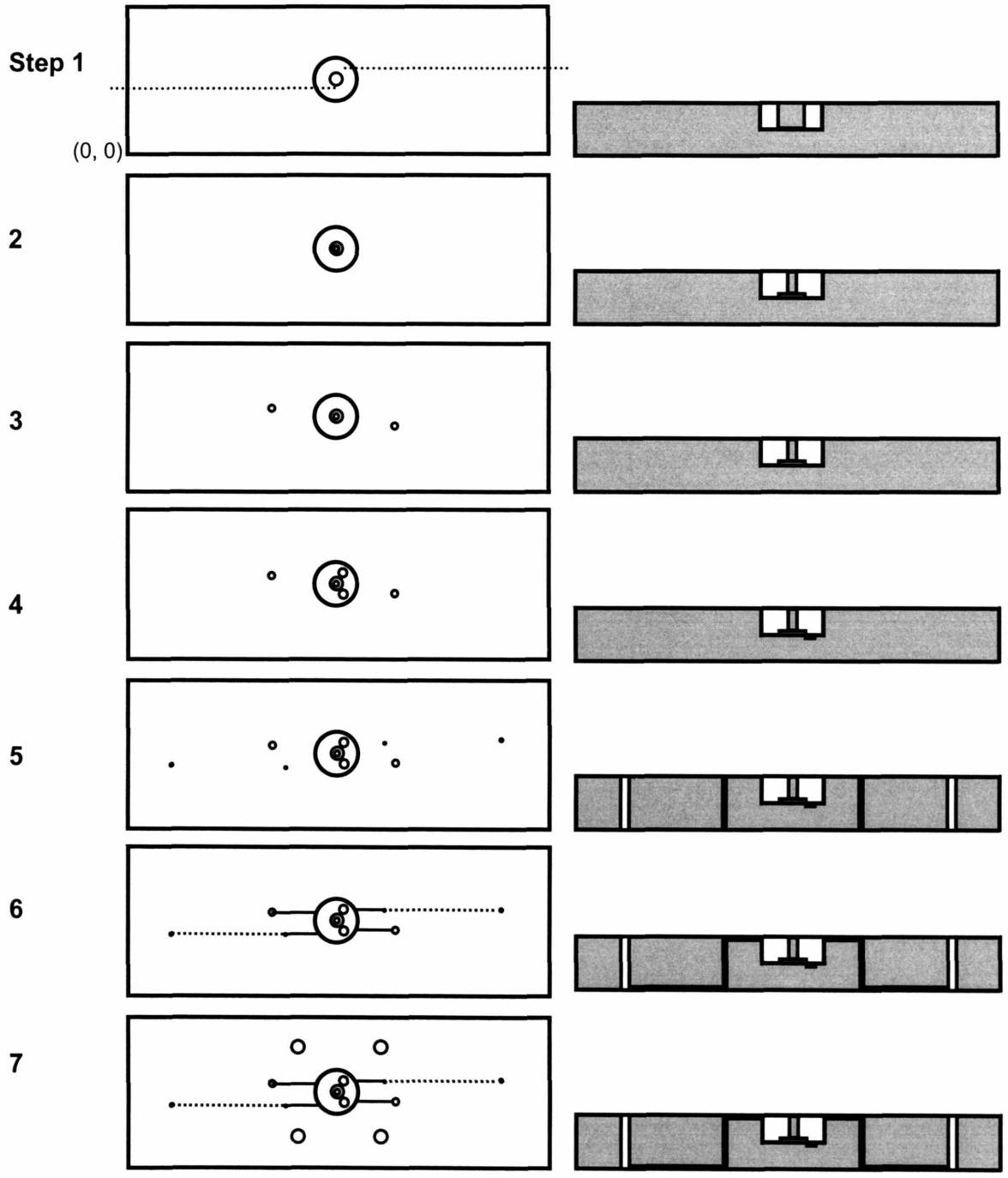

Figure A-1. Fabrication steps for PMMA device, top view and crosssection.

Note the dimensions in the crossscection figures are not to scale.

Step 1 and 2 in Figure A-1 shows the fabrication of reactor chamber. A four-flute, 5/32"-diameter endmill was used to cut a 1 mm-deep circular pocket in the chip. A PMMA post was formed by a second circular cut in Step 2. Program prarmeters for in Step 1 and 2 are listed as following (all length units are in inches):

	Step 1	Step 2
Cutting mode	1	0
Diameter of endmill	0.1562	0.1562
X Center	2	2
Y Center	0.7	0.7
Z Clearance	0.01	0.01
Z Cut (second round)	0.05	0.046
Z Cut (first round)	0.046	0.04
Cutting radius	0.207	0.0263
Clearance	0.005	0.005
Feed spead (first round, in/min)	5	5
Feed spead (second round, in/min)	0.2	1

In Step 3 a four-flute, 1/16"-diameter endmill was used to cut 0.4 mm-deep pockets in the chip. Bench movements in this step were controlled manually by using a "Jog" function. Recesses to accommodate pH and DO sensors were machined in Step 4 with the following program prarmeters:

	Step 4(1)	Step 4(2)
Cutting mode	1	1

Diameter of endmill	0.0625	0.1562
X Center	1.947	1.947
Y Center	0.792	0.608
Z Clearance	0.01	0.01
Z Cut (second round)	0.062	0.062
Z Cut (first round)	0.058	0.058
Cutting radius	0.04	0.04
Clearance	0.04	0.04
Feed spead (first round, in/min)	1	1
Feed spead (second round, in/min)	0.05	0.05

In Step 5, through holes with diameters of 0.024" and 0.0135" were machined by small drills (#73 and #80, respectively) using a manual operated microchuck. 0.024" holes were used to accommondate stainless steel fluidic connectors, as explained in Chapter Three. 0.0135" holes were used to connect microchannels on the other side of the chip.

In Step 6, a small endmill with 0.01" in diameter was used to fabricate microchannels with dimensions of 250μm×250μm. Program prarmeters are listed as following. Notice the chip needs to be detached from the base and the setup procedure needs to be repeated before machining the other side of the chip.

Step 6	(1)	(2)	(3)	(4)	(5)	(6)
Diameter of endmill	0.01	0.01	0.01	0.01	0.01	0.01
X Center	1.5	1.6	2.5	2.4	0.5	3.5
Y Center	0.78	0.62	0.62	0.78	0.62	0.78
Z Clearance	0.01	0.01	0.01	0.01	0.01	0.01

Z Cut (second round)	0.02	0.02	0.02	0.02	0.02	0.02
Z Cut (first round)	0.016	0.016	0.016	0.016	0.016	0.016
Cutting distance	0.335	0.235	0.335	0.235	1.13	1.13
Clearance	0.005	0.005	0.005	0.005	0.005	0.005
Cutting angle	0	0	180	180	0	180
Feed spead (in/min)	1.5	1.5	1.5	1.5	1.5	1.5

In Step 7, through holes with 1/8" diameter are drilled using manual "Jog" functions.

PMMA chips are detached and cleaned using hexane.

A.2. Thermal Bonding of PMMA Device

Thermal bonding of PMMA devices was performed in a home-made mechanical press, as shown in Figure A-2. In this press, PMMA chips were placed between two pieces of glass (1" in thickness, 5" in diameter) in an aluminum chamber to obtain a clean and transparent surface after bonding and to distribute pressure evenly across chips. The press used one pair (or more pairs) of Belleville disc springs (diameter: 119.0 mm; thickness: 1.25 mm; height: 2.80 mm. MSC Industry Supplier) to control pressue. Belleville spring with this specific height/thickness ratio has a remarable feature of allowing large extend of deflection with a load of 50 lb force (Shigley and Mischke, 2001). This feature is especially useful for thermal bonding applications, in which thermal expansion, retraction, and volume deformation occurs during heating, cooling, and bonding processes under constant pressure (100 lb force or proportionally higher), respectively. After the press chamber was sealed by six bolts on the edge, force was exerted by screwing in a large bolt in the center. The large bolt was locked at the bottom by a nut and an inside-threaded housing, and it transforms the screw force into compression force, which was uniformly distributed by a thrust-ball-grooved bearing (MSC).

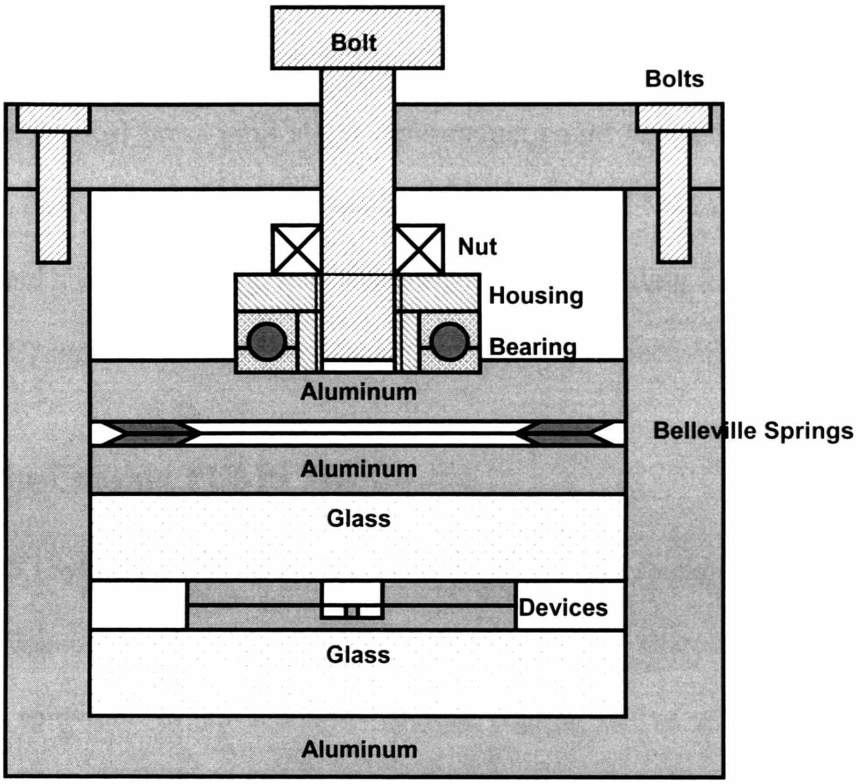

(a)

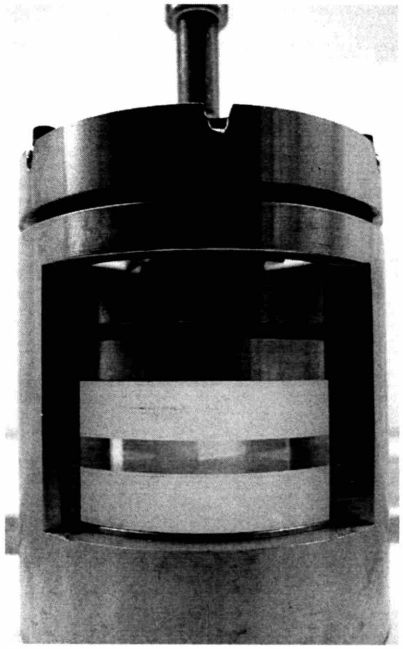

(b)

Figure A-2. (a) Cross-section and (b) picture of home-made mechanical press for thermal bonding of polymer devices.

Fabricated PMMA chips for bonding were first rinsed with ethanol and dried by nitrogen gas. Chips of different layers were carefully aligned by 3/32"-diameter pins and compressed together by the mechanical press until slight deformation could be seen in the Belleville springs. The press was then placed in the oven and heated for 1 hour. PMMA sheets purchased from different surplies and had different Tg, thus requiring different bonding temperatures of 120°C (purchased from MSC) and 140°C (purchased from Goodfellow), respectively.

A.3. Spin-Coating PDMS Membrane

PDMS (Sylgard 184, Dow) membrane with 100 μm thickness was spin-coated (WS-400B, Laurell Technologies Corporation, North Whales, PA) on silicon wafers with spin speed of 1250 rpm and spin time of 25 seconds. Before coating native silicon wafers were silanized by tridecafluoro-1,1,2,2-tetrahydrooctyl-1-triethoxysilane (CAS# 51851-37-7, United Chemical Technologies, Inc., Bristol, PA) to prevent the permanent bonding of silicon oxide surface to PDMS. PDMS were mixed with 10:1 ratio and de-gased in vaccum for 30 minutes before coating. Bulk PDMS were cut and placed onto the partially cured PDMS thin films to form a native bonding. Post-coating bake took 2 hours at 70°C.

APPENDIX B. Dimensions of Microbioreactor Device

The details of the microbioreactor device discussed in Appendix A are presented in this appendix. Note the numbers are inches.

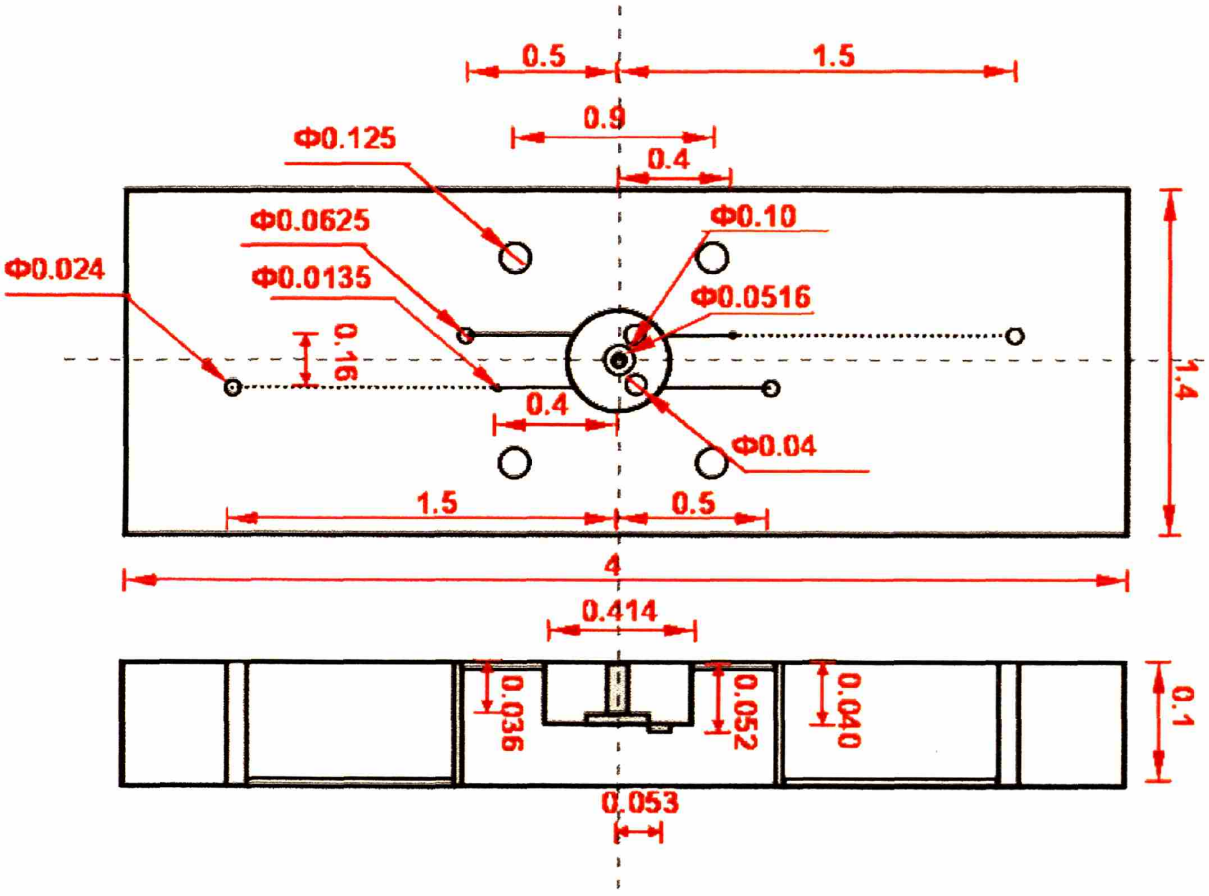

Figure B-1. Dimensions of the microbioreactor device discussed in Appendix A.